AN ABSTRACT OF THE DISSERTATION OF

Erin L. Bredeweg for the degree of Doctor of Philosophy in Molecular and Cellular Biology presented on January 21, 2014

Title: Transcriptional Networks Controlled by the Fatty Acid Regulators, FAR-1 and FAR-2

Abstract approved:

Michael Freitag

Fungi are capable of growth on a wide variety of carbon sources, both living and dead. They can produce an arsenal of enzymes and transporters for harvesting sugars, polysaccharides, amino acids, lipids and micronutrients from their environments [1]. Within the nucleus of a cell, transcription factors (TF) control whether genes will be transcribed, after which the transcripts can be translated into functional protein. TF contact with DNA can be influenced by nucleosomal occupancy, DNA binding affinity, and competition with other DNA binding proteins [2], [3]. Sequence specific DNA binding transcription factors associate with promoter sequences in order to tune core metabolic pathways in response to nutrient availability, for example *N. crassa*'s major nitrogen regulator NIT-2, [4], or in response to oxidative stress, the alternative oxidase regulator, AOD-2 [5]. Change in the relative abundance of proteins within the cell or "proteome" can have broad effects from redirection of metabolic flux via carbon and nitrogen use, production of enzymes for detoxification, and altered growth and development from the examples above. A survey of transcription factor binding influenced by light is underway in *Neurospora crassa* as part of the Neurospora Functional Genomics and Systems Biology (NcFGSB) program project funded by the NIH

(P01GM). This work began by testing the link of FAR-1, or Fatty Acid Regulator -1 (NCU08000) to light regulation, but has continued toward investigation of how both FAR-1 and a second TF, Fatty Acid Regulator-2, or FAR-2 (NCU03643) influence central metabolism, oxidative stress response, and development.

Transcription factor networks consist of describing TFs that bind to multiple genes and individual genes controlled by multiple regulators. Further, the "regulation of regulators" describes how the transcription of transcription factor genes is controlled. Chromatin immunoprecipitation, or 'ChIP' experiments show that a variety of factors are enriched at the same promoter region as can be seen by comparing multiple datasets [6], [7]. Transcriptional regulators may promote or inhibit one another from binding DNA, leading to a total regulation as the sum of TF activity. This complexity cannot be explained by single genetic experiments and study of a limited number of loci. Even in the event of TF association with specific promoter DNA as analyzed by ChIP, proximal binding of a transcriptional activator does not directly mean that transcript levels will increase, as we have seen with the identification of WC-2 binding sites [7].

I used a reverse genetics approach, assaying deletion mutants of selected loci, to determine the cellular effects of FAR-1 and FAR-2 transcriptional activity in different carbon sources. The tools of high throughput sequencing, and bioinformatics data analyses were combined with experiments to characterize phenotypes observed. Here I report (1) a collection of binding sites found in the *Neurospora* genome for FAR-1 and FAR-2 in sucrose, butyrate, and oleate, (2) changes in transcription as a result of the loss of FAR-1 and/or FAR-2 function, and (3) how the combination of binding sites and transcriptional activities are reflected in phenotypes. This work has developed and utilized methods for combining genome-scale ChIP- and RNA-sequencing data to describe direct and indirect transcriptional regulation, and has added to the definition of transcription factor networks in *N. crassa.*

©Copyright by Erin L. Bredeweg

January 21, 2014

All Rights Reserved

Transcriptional Networks Controlled by the Fatty Acid Regulators, FAR-1 and FAR-2

by

Erin L. Bredeweg

A DISSERTATION

submitted to

Oregon State University

in partial fulfillment of
the requirements for the
degree of

Doctor of Philosophy

Presented January 21, 2014

Commencement June 2014

Doctor of Philosophy dissertation of Erin L. Bredeweg, presented on January 21, 2014.

APPROVED:

Major Professor, representing Molecular and Cellular Biology

Director of the Molecular and Cellular Biology Program

Dean of the Graduate School

I understand that my dissertation will become part of the permanent collection of Oregon State University libraries. My signature below authorizes release of my dissertation to any reader upon request.

Erin L. Bredeweg, Author

ACKNOWLEDGEMENTS

I would like to thank my advisor Dr. Michael Freitag for his flexibility in letting me pursue a topic outside of the focus of the lab. He has provided a lab environment that has furthered my appreciation for fungal genetics and cell biology. His patience with me the last six and a half years, has allowed me to focus my scientific thinking, and gain teaching experience, which I have enjoyed greatly. I would also like to thank the many people I have had the privilege of working with through Freitag collaborations including Meritxell Riquelme, Frank Nargang, Buck Wilcox, Deborah Bell-Pedersen and Rigzin Dekhang.

I would like to thank my committee members, Dr. Barbara Taylor, Dr. John Fowler, Dr. Claudia Maier, and Dr. Christine Kelly for their time and input during the process of finding my scientific footing. I would also like to thank Dr. Gary Merrill, Dr. Barbara Taylor, and Dr. Robert Mason for the opportunities to gain experience teaching, as well as financial support. I would also like to thank Dr. Juliet Greenwood, and Dr. Marc Curtis, and especially Dr. Indira Rajagopal for working with me as a teaching assistant, providing examples of lecture styles, and caring interactions with students I hope to emulate.

I would like to thank the current and past lab members Lanelle Connolly, Jonathan Galazka, Kristina Smith, Pallavi Phatale, Steven Friedman, and the many undergraduate, visiting and rotation rotation students for their help, discussion, and shared scientific enthusiasm. I would like to thank Jason Cumbie for help with all things computer. I would like to especially thank Kyle Pomraning and Brett Mellbye for both testing and strengthening my mental fortitude, for their companionship, and for many good times.

Most strongly, I would like to thank my family for their support. I would like to thank my brother Evan and sister Megan and most of all, my parents Sally and Hollis for their inspiration and encouragement.

TABLE OF CONTENTS

TABLE OF CONTENTS (Continued)

Page

TABLE OF CONTENTS (Continued)

Page

TABLE OF CONTENTS (Continued)

LIST OF FIGURES

LIST OF FIGURES (Continued)

LIST OF TABLES

Chapter 1: Introduction: Transcription Factor Networks and Lipid Metabolism

Cells are able to gather information about the world outside their plasma membranes by using specific properties of sensor proteins, such as attached light absorptive molecules, or the ability to alter their activity in response to ligands. As signals are integrated from multiple sources and relayed, they change overall gene expression, called the "transcriptome"[8], most often gauged by differential mRNA populations, as a sum of production and degradation. Modulated by environmental signals, DNA-binding transcription factor (TF) proteins each affect a subset of all the genes in the genome to respond to the changing circumstances of a cell's environment. Binding of a TF in *cis* or *trans* to a eukaryotic promoter increases or decreases how often RNA polymerase and the general transcription factors assemble to produce a transcript [9], [10]. Stimulatory signals for a TF to bind DNA may include the presence of other transcription factors, an activating ligand, or post-translational modifications, e.g. phosphorylation by a kinase. The specific sequence bound by a transcription factor is dictated by electrostatic interactions between the nucleotides and the amino acids exposed on the DNA binding motif of the protein [11]. Multiple transcription factors may bind neighboring sequence elements or compete to bind the same sequence; their interaction with the basal transcriptional complex, chromatin remodeling enzymes, and co-activators and co-repressors alters the transcriptome, and subsequently, the proteome [10]. The sequence and location of DNA binding sites, and TF protein binding partners also may be under evolutionary flux, varying between organisms as they diverge [12]. These malleable TF networks control diverse processes e.g. primary growth, development, differentiation, in the short term, but also change on an evolutionary time scale.

Beyond the simple presence or absence of a transcription factor on DNA, binding dynamics also play an important role in transcription regulation. The DNA sequences where a protein interacts with DNA can be assayed by a method called "ChIP", or

chromatin immunoprecipitation [13]. Formaldehyde reversibly crosslinks DNA-protein, and protein-protein associations after which the protein of interest is recognized and physically removed from whole cell extract by use of protein-specific antibodies. DNA physically associated with the protein of interest is purified. The resulting DNA can be analyzed by three techniques: relative enrichment by polymerase chain reaction (PCR) assays, array hybridization, or high throughput sequencing. The first method uses a PCR product ratio to compare the presence of a control segment of DNA for comparison to an experimental segment, and can be qualitative, semi-quantitative multiplex or assessed by quantitative realtime PCR, all referred to as 'region-specific ChIP-PCR'. 'ChIP on chip' microarrays involve hybridization of ChIP-derived DNA conjugated to fluorescent tags against different types of DNA arrays with probes spaced throughout the genome [14]. Lastly, high throughput ChIP-sequencing, or 'ChIP-seq', is the most comprehensive, and provides information about protein-DNA interaction across the whole genome, including regions that are not well characterized and for which there are no arrays.

Using ChIP-seq, protein-DNA contacts are visualized by mapping sequenced fragments of DNA generated by the sequencer ('reads') to a reference genome. Areas of enrichment can be reliably quantified using analysis packages such as BWA [15] or Bowtie [16]. It is important to remember that ChIP results in information at only one point in time, and is the average found among a population of cells. Thus, the detection of DNA-protein interaction by ChIP may not capture the difference between a sustained interaction vs. 'treadmilling' behavior of continual protein loss and replacement at a DNA sequence [17]. Several approaches can address residence time and TF interactions. One method used an inducible TF distinguishable from the TF at the endogenous locus, and measured enrichment (i.e. protein-DNA contact) with and without induction [17]. Mechanistically, residence time on DNA can play a role in whether transcriptional regulators cause an increase or decrease in transcript levels [17]. Work on the glucocorticoid receptor, which specifically binds a response element on the order of

seconds, suggests that TFs can bind to the same sequence specific motif, in a non-competitive, cooperative manner, where the binding of each TF is specifically regulated by a different ligand [18]. By ChIP, and FISH, these two TF show cooperativity, where the binding of one TF increases the transient contact of another TF on the DNA. This type of TF cooperativity and potential competition of overlapping binding sites may have effects on the transcriptional output downstream of TF network analysis, as has been seen in data from the *Drosophila* ModEncode project [19]. A combination of ChIP- and cDNA-sequencing ('RNA-seq') assays can be used to describe transcription factor contact on DNA and effects on nearby genes. Sequence specific localization and condition specific transcriptome changes in strains mutant for transcription factors can reveal secondary effects of TF binding. In this way, we collect information about how cells respond to stimuli at the DNA and mRNA level, and decipher potential pathways or networks for each stimulus and response.

How do signals reach TFs and DNA in the first place? Molecular sensors monitor environments both inside and outside of the cell, where they transduce signals to proteins that respond to physical and chemical stimuli. A *Neurospora* protein, Vivid, contains a LOV (Light-Oxygen-Voltage) domain, and helps to calibrate the circadian clock transcription factors (described below) to different light levels [20]. Downstream of a sensor histidine kinase relay, the yeast kinase HOG1 controls TFs SKO1, MSN2, and HOT1 which respond to oxidative stress, reviewed in [21]. The broad effects of transcription factors (TF) and their roles as 'master regulators' or 'switches' make them interesting targets for understanding basic cell biology. TFs can be direct or indirect targets of molecular sensors in the production of new proteins or perpetuation of signals. As an example of a direct TF-linked sensor, the *Neurospora crassa* WHITE COLLAR-1 (WC-1) TF contains a LOV domain linked to a small molecule, flavin adenine dinucleotide (FAD), generating a light sensing flavin-cysteinyl adduct, which alters its structure when light is perceived [22]. An overview of Neurospora's circadian clock and related TF networks follows to detail our entry into these studies.

The *Neurospora crassa* circadian clock and the white collar complex (WCC)

Neurospora crassa is a filamentous ascomycete originally isolated as orange bread mold, and named following the discovery of its sexual fruiting bodies, called perithecia [23]. It is a heterothallic fungus, meaning that it requires another individual of a different mating type in order to sexually reproduce. *Neurospora* contains single copies of many genes due to genome defense mechanisms: pre-meiotic recombination [24], and repeat-induced point mutation (RIP), which mutates repeated DNA [25]. Many phenotypic mutants mapped by recombination and genetic tractability have made *N. crassa* an excellent organism for genetic studies [26].

Neurospora produces asexual conidia in a light-sensitive manner and in a periodic fashion linked to the circadian clock [27], [28]. It was recognized early on that this feature, particularly obvious in strains deficient in *ras* (previously called *timex* and then *bd* for the pronounced banding pattern), can be used to monitor the circadian clock of *Neurospora* [27], [29]. The conidiation cycle is approximately 22.5 hours long when the clock is 'free-running', meaning grown in the dark without environmental input, or 'zeitgeber' [30], [31]. Partly because of groundbreaking work in *Neurospora* it is now well understood that the ability to vary growth and development patterns, as well as metabolism over a daily time scale is directed by the circadian clock [32]. Circadian clocks are sets of proteins in positive and negative feedback loops that oscillate on a 24 hours time scale, persist in the absence of an input, and remain relatively constant at different temperatures [33]. The molecular output of the clock aligns the functions of core cellular processes to protect it from damage, such as controlling the cell cycle in cell types during light exposure [32]. For example, the rhythmically expressed *N. crassa prd-4* gene halts cell cycle progression into mitosis after DNA damage, like its ortholog mammalian checkpoint kinase 2 [34]. In *N. crassa*, the positive elements of the clock are WHITE COLLAR-1 and -2 (WC-1, WC-2), while the negative elements are FREQUENCY (FRQ) and a FRQ-interacting RNA helicase (FRH)

(Figure 1.1). FRQ is progressively phosphorylated by casein kinase 2 (CK2), and dephosphorylated by PPA2 [35]. Together, FRQ and FRH repress the transcriptional activity of the WCC, while phosphorylation and degradation of FRQ allow WCC-driven transcription. These proteins form the core FRQ oscillator [22], [33], [36]. There are modulators that increase light sensitivity, for example VIVID (VVD, mentioned above) and TFs that mediate repression or activation of the immediate clock components at specific times of day, such as CONIDIAL SEPARATION-1 (CSP-1) [6]. Because of its advanced molecular genetics, biochemistry and convenient conidiation and more increasingly engineered reporter assays (e.g. luciferase, [6], [37]) , *Neurospora* has become a robust and preferred system for studying the circadian clock.

Previous studies have shown that both components of the WCC have DNA binding motifs [38], [39]. In order to investigate genes that are directly regulated by binding by the WCC, we performed ChIP with WC-1 and WC-2 [7]. Corroborating previous results, WC-1 seemed to be less efficiently binding DNA, and we only reported data obtained with WC-2. We confirmed all previously known five binding sites near the *frq*, *vvd* , *fluffy* (*fl*), *submerged protoperithecia-1* (*sub-1*) and *albino-1 (al-1*) genes and found more than 300 additional WC-2 binding sites [7], [22], [40]–[42]. Several of the newly identified sites were confirmed by qRT-PCR (31 out of 36). Among the genes with WC-2 enrichment in their promoters, there were 28 known or predicted transcription factors, 21 of which responded to light dependent upon WC-2, and the remaining 3 of which require WC-2 for wild type expression levels [7]. All 24 TFs and a number of other light responsive kinases and chromatin modifiers are currently under intensive study by a multi-laboratory collaboration whose aim is to uncover the light-responsive gene regulatory network of *Neurospora* (Table 1.1). Several publications from this work are in preparation (see Appendix). While I have participated in all of these studies and will be co-author on several of these papers, I will not mention specific results and outcome from these studies unless required for an understanding of my work on two of the 28 TFs, the FATTY ACID REGULATORS of *Neurospora*, FAR-1 and FAR-2.

Many laboratories study light regulation and the circadian clock. I became interested in TFs that did not fit the pattern of a typical light- and WCC-regulated TF. Based on our ChIP assays, the *far-1* promoter was predicted to bind WC-2 but its transcript levels did not show any significant sensitivity to the absence of WC-2 [7]. The *far-2* promoter, however, did not have WC-2 binding sites that were detectable by ChIP, but transcript levels were regulated by light in microarray experiments [41]. The *vad-3* gene also displayed light responsiveness without detection of a WC-2 ChIP peak. Both *vad-3* and *far-2* do have a WC-2 binding site that may be bound under conditions not addressed by our experiment. These results suggested that WC-2 was not only involved in mediating regulation by light and the central circadian clock components but possibly additional pathways. In addition to the well-studied clock-controlled genes (*ccg*; [43]–[46]) and blue-light inducible genes (*bli*; [41]), we thus predicted the existence of additional white collar inducible genes (*wig*) and white collar associated genes (*wag*). A number of these ccgs are linked to central metabolism such as ccg-7, encoding glyceraldehyde-3-phosphate dehydrogenase [6], [46].

Four categories of WC-2-controlled genes are defined as: (1) wigs: white collar induced genes which are direct targets of the WCC after light induction [7]; (2) wags: white collar associated genes, which are bound by WC-2 or WC-1 but may be conditionally responsive [7]; (3) ccgs: clock controlled genes which are part of the molecular output of the clock, varying over the circadian period [43], [47]; (4) blue light inducible genes, which are controlled by blue light detection by photosensors, but are not necessarily output of the clock [41]. These categories are not exclusive of one another, and some genes fall into more than one. Some contributions to these differences could include variations in histone modifications [48], or a difference in protein levels or stability of the WCC components [36]. WC-2 localization by ChIP [7] has provided data to question models developed by circadian researchers of exclusively activating modes of action by the WCC, which may be investigated further by probing downstream TF networks and other growth conditions.

To test the hypothesis of the existence of *wigs* and *wags*, I chose to study the regulation of the two *far* genes and the ties of light signaling to fatty acid metabolism. The complex relationship of responses to light, salt stress, and reactive oxygen species (ROS) via the WCC is one example of ties between signals from outside cells to response and metabolism inside. The presence of reactive oxygen species (ROS) provided by menadione, hydrogen peroxide, or in a *sod-1* mutant (superoxide dismutase) caused an advance in the phase of the clock [49]. The ROS levels of *N. crassa* oscillate over a 24 hour period, and regions of conidiation correspond to troughs of ROS presence [50]. Metabolic patterns that generate ROS as well as the enzymes that detoxify them have in part been shown to vary over a circadian period [29]. Taken together, this suggests that metabolic changes that alter ROS levels may be part of the output of the clock, and may also feedback into clock signaling under normal conditions (Figure 1.1), though the mechanism for feedback is unclear. To date, ROS generation (H_2O_2) mediated by beta-oxidation via long chain fatty alcohol oxidase, or peroxisomal enzymes detoxifying oxidative nitrogen species have not been implicated in altering the clock [51], [52].

In addition to circadian conidiation correlating with ROS levels, the clock is able to directly modulate ROS levels through the osmotic sensitive (OS) kinase cascade (Figure 1.2). Catalases, which detoxify ROS by reducing H_2O_2 to water, are partially regulated through a kinase cascade responsive to high salt via a phosphorelay, OS-2 (a MAPK, for 'mitogen activated protein kinase' and *S. cerevisiae* Hog1 homologue), and OS-4 (a MAPKKK) [50], [53]. The *os-2* promoter is bound by the WCC [7], and is instrumental in up-regulating the glycerol synthesis pathway, *cat-1*, and other components of the osmotic stress response [53]. OS-4 is directly regulated by the WCC, and is a positive regulator of OS-2 activity [54]. There has been limited investigation of the direct targets of these kinases [53]–[56]. However, the collection of genes responsive to ROS stress have been described in more detail, notably among them FAR-2, which is one focus of this study [57].

Transcription factor networks

Transcription factor network refers to description of (1) TF binding to the promoters of individual genes and (2) individual genes controlled by multiple TFs [58]. Some analyses extend this analysis to compare TF binding sites of an ortholog across species [12], [59]. Early work on sea urchin development regulatory networks pioneered description of the effects DNA binding proteins can have on one another, and on transcription of genes [60]. High throughput sequencing technologies have increased our knowledge about specific genes, genomic structures, and transcriptional regulators in different genomes through bioinformatics and genetic resources such as the 1000 Fungal Genomes Project [61]. Integration of multiple data types may be employed to find biological patterns such as histone modification sensitive TFs [19], or TF binding as a driving codon bias evolution [62]. One classification of network modeling presents 4 types of networks: (1) parts list (2) topological networks (3) network control logic models (4) dynamic models, or how networks change in over time [63]. High throughput sequence data of genomes has enriched parts lists, and the wealth of ChIP-Seq and ChIP-chip experimental data has also contributed to the topology of histone-DNA and TF-DNA interactions [62], [64], [65]. However, more experimental work is necessary to make inroads on deciphering the control and dynamics of biological systems networks.

Transcription factor networks have the potential to describe complex systems. A recent survey of TFs in *S. cerevisiae* identified ~209 TF that bind DNA in a sequence specific manner [58]. In *N. crassa*, 178 predicted TF are expected to bind DNA, though their sequence specificity is unknown [66]. This large group is representative of 6 families of DNA binding domains including Zn_2Cys_6 fungal binuclear cluster, C2H2 zinc finger, GATA, bHLH, bZIP, Myb, as well as miscellaneous others [1]. Of the 178, 98 show expression under vegetative growth [66]. A survey of transcriptional profiles for seven available mutants of nine bZIP TFs assayed transcriptional differences during vegetative growth of early and late colony tissue [1]. Another approach to network analysis has

been to use electronic and literature curated data to populate *in silico* models, such as seen in the metabolic reconstruction done for *Neurospora crassa* [51]. One concern for comprehensive TF description is that standard lab conditions may not encompass the signals and stressors for activity of many TFs [58], [66]. Some potential pitfalls include concern over data quality and replicate quality [58]. Misleading or incomplete information may confound assessment of regulatory targets and co-localizing DNA binding proteins.

Construction of the FAR TF network contriubtes elements to basic cell biology, regulation of central metabolism and has potential applications for a greater understanding of other ascomycete fungi. The results of this dissertation include parts lists, bioinformatics, and elements of dynamics and logic control of FAR TFs derived from changing carbon sources and TF mutants in combination. Additionally, transcription factors controlled by the WCC are under investigation by several *Neurospora* laboratories, as mentioned above (Table 1.1). Unraveling the primary metabolism under the control of multiple TF will be crucial to understanding how transcription factors affect one another. TF network analysis of both the FARs and other TFs done in a model filamentous fungus may inform our understanding of agricultural and medical pathogens [67], and develop tools for industrial utilization of enzymes [68], antibiotics [69], and biofuels [70]–[72].

Regulators of carbon source availability: simple sugars

Filamentous fungi take up nutrients from the environment surrounding them as they grow in an exploratory fashion [73]. Individual sugar units or multimers may also be enzymatically broken from complex carbohydrates during degradation of plant cell walls. For this purpose, fungi secrete enzymes such as cellulases and β-glucosidases [72], [74]. Sugars are transported across the plasma membrane by a wide variety of sugar transporter proteins, using ATP-driven pumps and chemiosmotic ion gradients to power solute movement [75]. Once inside the cell, the sugars can be 'repurposed' for

incorporation into building fungal cell walls, or broken down by glycolysis and the TCA cycle for energy.

Which carbon sources are available depend upon a cell producing the requisite machinery for transport and breakdown. The eukaryotic 'switch' between utilization of different sugar sources has been described in detail for the *S. cerevisiae* Snf1 kinase regulon, named for its phenotype 'sucrose non-fermentable' and a transcriptional repressor that it controls, Mig1, 'multi-copy inhibitor of galactose genes'. Carbon catabolite repression (CCR) is mediated by the DNA binding protein Mig1. The functional homologs of Mig1 are often named for their catabolite repressor function, such as *Aspergillus nidulans* CreA and *Neurospora* CRE-1 from the filamentous fungi. CCR stops the transcription of enzyme or transporter mRNAs necessary for use of other sugars, until preferred sugars are no longer available [72], [76]. This repression has been a problem in the biofuels industry, for example, because as cellulases free sugars from plant biomass, cellulose production is stopped by CCR [72]. The yeast CCR system represses gene expression by Mig1 activity. Phosphorylation of Mig1 by Snf1 kinase excludes the Mig1 repressor from the nucleus [77], indicative of cellular starvation, and a need for access to other sugar types (Figure 1.3). The absence of Mig1 and release of CCR allows transcription and translation of the TF gene *CAT8*, and subsequent upregulation of gluconeogenic genes [78]. Additional transcriptional regulators (Adr1, Ert1, Oaf1, Pip2) upregulate genes for alternative carbon metabolism and respiration, reviewed elsewhere [78]–[80]. Snf1 is regulated by phosphorylation at conserved residue Thr210 [81] and interacts with Snf4 to remove self-inhibition and one of Sip1, Sip2, or Gal83 for localization [82]. The protein phosphatase 1 subunit Glc7, and redundant kinases Sak1, Elm1, Tos3, all modify Thr210, though it is still unclear precisely what intracellular signal or metabolite triggers Snf1 activation [82]. Downstream Snf1 activity is responsive to the levels of ADP, making it an intercellular monitor of energy levels [82]–[85]. Indeed, the mammalian homolog of Snf1, AMPK, serves as a direct indicator of ADP/ATP ratios, as it was found to be resistant to dephosphorylation in the

presence of ADP. Interestingly, AMPK also allosterically binds fatty acids, which suggests that it serves as a more comprehensive sensor and regulator of carbon flux including sugar and lipid anabolism and catabolism in mammalian cells [86]. Energy stores in the form of glycogen in a yeast cell are monitored by SNF1 directly binding glycogen [86]. In this way, Snf1 and Mig1 minimize transcriptional waste when sugars are available.

The *Neurospora* homolog of Mig1/CreA, CRE-1 (NCU08807), xylan degradation regulator XLR-1 (NCU06971), and cellulose degradation regulators CLR-1 (NCU07705) and CLR-2 (NCU08042) are four of many TFs that participate in regulation of cellulose degradation enzymes [70], [71], [87]. Both *cre-1* and *clr-1* have potential WCC binding sites, but their relationship to light signaling remains unclear [7], [70]. It is clear that *Neurospora* has several systems for keeping a variety of carbon sources available, and we are only now beginning to piece together how the regulons of these TFs overlap. The complexity of how these TFs interact with one another, and respond together to different environmental signals needs further research. In the absence of sugar, fungi may turn to long chain carbon molecules, such as fatty acids, for gluconeogenesis and fuel for the TCA cycle, but there is as yet no defined sensor which aides in this switch. The switch mechanisms in other systems for fatty acid anabolism and catabolism provide a starting point in defining a model regulatory structure and they are introduced in the following sections.

Regulators of carbon source availability: fatty acids

Beta-oxidation can be regulated by direct or indirect means, from direct binding of fatty acids in bacteria [88], to a cascade of regulator activation and fatty acid synthesis inhibition by AMPK in mammalian cells [89]. In mammalian systems, PPARs (’peroxisome proliferator activating receptors’, there are alpha, beta and gamma variants) are fatty acid ligand-binding TFs that regulate a variety of functions in different tissues [90]–[93]. Broadly, the alpha variant regulates enzymes involved in beta-

oxidation, while the gamma variant mediates carbon storage in adipose tissues, and beta is known to regulate acetyl-CoA synthetase, and has functions in both glucose metabolism and beta-oxidation. Differences between human and mouse functions for these proteins may have developed due to regulatory changes in evolving promoter regions resulting in independent regulation of catalase, acetyl-CoA oxidase, and cyclooxygenase 2 [94], [95]. These enzymes are involved in detoxification of reactive oxygen species generated by fatty acid breakdown. All three PPAR variant proteins may modulate their transcriptional regulator activity by detection of fatty acids ligands, some of which are shared between the isotypes [90], [96]. PPAR-alpha can also heterodimerize with the orphan nuclear receptor RXR-alpha, which binds retinoic acid or interacts with a fatty acid binding protein; protein levels of these cytosolic shuttles of fatty acids to the nucleus are proportional to PPAR transactivation which is required for full transcription factor activity [97], [98]. Though the PPAR activators are not similar in sequence to TFs found in filamentous fungi, the structure and regulation of the PPAR/RXR heterodimer is close to that of the well characterized yeast TF heterodimer Oaf1/Pip2 that activates genes in response to fatty acids [96]. However, given the large differences, it is impossible to tell whether the similarity has arisen through homology or convergent evolution.

Though yeast is a sugar specialist, it is responsive to oleate and can grow on it as a sole carbon source by upregulating machinery for beta-oxidation, peroxisome proliferation, detoxification, and lipid transport [97]. Oleate induction in yeast is a feature that has since long been used to study peroxisome biogenesis and import [99]–[102]. OAF1 and PIP2 can act together, and have been shown to bind a consensus sequence by EMSA (electrophoretic mobility shift assay) even in glucose-grown cells [97]. This suggests that a ligand is unnecessary for DNA binding. Alternatively, OAF1 homodimers, and another TF, ADR1 (alcohol dehydrogenase regulator), have been found to regulate some of the same genes involved in gluconeogenesis and non-fermentive carbon metabolism [78]. The OAF1/PIP2 system is unique to a subset of the

Saccharyomycotina, while other hemiascomycetes, and true ascomycetes utilize separate fatty acid regulators [103]–[105]. Some yeasts display a hybrid set of proteins, containing a homologue of *Neurospora crassa* FAR-1 and all or part of the OAF1/PIP2 heterodimer, such as the oleaginous yeast *Yarrowia lipolytica* [104], and the human pathogens *Candida albicans* [105], and *Debaryomyces hansenii* (Figure 1.4).

In organisms more closely related to my model, ascomycete filamentous fungi share the FAR-1 and FAR-2 regulators, for example *A. nidulans* FarA and FarB [106] or *Nectria haematococca* CTF1α and -β (cutinase transcription factor-1) [107], [108]. Though implicated in pathogenicity [105], [109], fungi with FAR orthologs range widely in lifestyle (Figure 1.5), from saprophytic soil dwellers to plant and insect pathogens. Searching by sequence similarity has indicated the FAR proteins originated within ascomycetes, while the closest resemblance to metazoan, plant, or bacterial proteins is within the less structured C-terminal amino acid sequence of FAR-1 [106], [110]). Ascomycete fungi show documented differences in metabolic pathway regulation, such as the structure of basic metabolic pathways and possession of degradation enzymes across a range of species [59]. In aspergilli, FarB has been shown to be specific for the utilization of short chain fatty acids, while FarA is required for metabolism of chains over ten carbons long [106]. Biochemical investigations by EMSA in *A. nidulans* identified a DNA binding site, common between FarA and FarB, which consistent with promoter DNA motifs upstream of cutinase genes in *Nectria haematococca* (also called *Fusarium solani pisi*) [106], [107]. By northern blot analysis, FarA and FarB together coordinate expression of genes for the glyoxylate shunt enzymes, proteins for the carnitine shuttle of acetyl units, and PEX11 - a peroxisomal biogenesis protein [106]. Similar regulation of several beta-oxidation enzymes and PEX5 has been found in *Y. lipolytica,* suggesting that this role is conserved [104]. *Neurospora* to have similar activities, singly or together. Different regulation may show lifestyle specific differences between *N. crassa* and *A. nidulans*. My comprehensive analyses of FAR-1 and FAR-2 binding and transcriptional regulation address the diversity of responses they mediate, including genes of

peroxisomal proteins and carbon flux machinery, as well as the potential for integrated regulation of TF responsive to nitrogen, oxygen, or other micronutrient levels.

In summary, evolutionarily divergent organisms have developed different systems for fatty acid metabolism regulation. However, comprehensive genomic surveys of binding by a FAR homolog have not been done for any fungus, excepting the work presented in this dissertation. Many agricultural pathogens share regulators with the same protein structure as FAR-1 and FAR-2 (Figure 1.4, Figure 1.5) making *Neurospora* a model for complicated regulation in the genome-expanded fusaria or related ascomycetes in which molecular tools are still lagging behind. The phylogenetic trees generaged based on protein sequence indicate presence of a FAR-1 homolog in both true ascomycetes and hemiascomycetes, while FAR-2 is found only in true ascomycetes (Figure 1.4) suggestive of a duplication or development following divergence from the yeasts. FAR-1 homologs are distrubted through ascomycetes of diverse lifestyles (Figure 1.5) showing that FAR function is not limited to a specialized growth habit. Though the FAR proteins bind DNA, it remains unclear what physical or chemical mechanism directs the transcriptional regulator role of these proteins.

How fungi metabolize lipids: pathways downstream of the regulators

The chitinous fungal cell wall is largely made up of assembled chains of chitin and glucans, a variable family of polysaccharides, and requires a steady supply of cytosolic nucleotide-activated sugars, for wall or hyphal growth [111]. When sugars are in low supply in the environment, fungi are capable of building sugar from other carbon sources, such as lipids [112]. Just as when accessing different sugars from polysaccharides and cellulose, fungi secrete enzymes for partial breakdown of lipids into the space around them, and into the plasmalemma between the cell wall and plasma membrane. Lipases can be key for pathogenic fungi in human infection [113]. Lipase enzymes are on a continuum with cutinases and esterases, and act at a lipid-aqueous interface to emulsify lipids for access by fungal cellular transport [114]. They act upon

triacylglycerol to release free fatty acids. Lipases and cutinases are co-regulated by FAR-1/CTF1α in the plant pathogen *N. haematococca* [108]. The expression of several secreted cutinase and lipase genes was decreased by loss of the CTF1α TF, however pathogenicity of tomato roots by *Fusarium oxysporum* was unaffected [114]. However, in *Fusarium graminearum,* disruption of a lipase gene decreased virulence [115], [116]. suggesting these genes have additional regulators, or other degradation enzymes contribute to pathogenicity in this organism. Cutinases and lipases are important for pathogenicity in other fungi such as during immune interactions of *Cryptococcus neoformans* [105], [117]. Fungi take up hydrocarbons through several barriers, namely the cell wall and the plasma membrane [118], [119]. To reach areas for carbon utilization, fatty acids and neutral hydrocarbons must pass through the cell wall and through pores and channels of the plasma membrane due to their bulky size [120].

As part of transport, hydrocarbons are activated by linkage to the thiol group of a coenzyme A molecule to form an acyl-CoA [120], [121]. An acyl-CoA may then be processed in either glyoxysomes, or mitochondria. While in the cytosol, the hydrophobic hydrocarbon chains are chaperoned by lipid binding proteins, and moved into the appropriate compartment [122]. Based upon carbon labeling studies, it is clear that fungi will use an external source of C16 or 18 fatty acids for making membrane phospholipids, and/or forming di- or tri-acyl glycerol for energy stores [123]. Carbon labeling studies in mycorrhizal fungi suggest that they can extend or elongate provided lipids, but not synthesize new ones and that fatty acid synthase activity was linked to areas of plant association [124]. Genetic experiments in *Neurospora* identified a *cel* mutant, defective in fatty acid chain elongation, which displays a perturbed rhythm in the presence of unsaturated lipids (such as linoleic 18:2), and requires 16:0 or other unsaturated lipids for a normal conidiation rhythm [125], [126]. Data from *A. nidulans* shows that peroxisomal beta-oxidation is needed for shortening of very long chain fatty acids such as C22, but is not essential on short (C4-C6) fatty acids breakdown [127]

indicating that the mitochondrial beta-oxidation pathway may be sufficient for short chain carbon catabolism if it is intact.

Beta-oxidation breaks down fatty acids from their carboxyl end into two carbon units (targeting the β carbon, second from the carboxyl group) that can be used for energy by re-entering the TCA cycle, as prosthetic groups for enzymes, or building materials [128], [129]. The resulting acetyl-CoA units must be taken to the mitochondrion, or trafficked to the enzymes that build sugars during gluconeogenesis [128]. The acetyl group is swapped from coenzyme A to carnitine in some cases, or cleaved directly to acetate for transport into the cytosol, and into the mitochondrion. Fungi and plants avoid the loss of CO_2 during the TCA cycle by employing a variant pathway: group of enzymes in the glyoxysome, called the glyoxylate bypass [130]. TCA intermediates shuttled to the glyoxysome generate glyoxylate and succinate, which are later converted to malate through the action of the two primary bypass enzymes, isocitrate lyase and malate synthase. Malate and oxaloacetate can be converted into phosphoenolpyruvate by phosphoenolpyruvate carboxykinase, the first enzyme in gluconeogenesis, [128], [130]. Thus, we have a source of ATP as generated by the TCA cycle as well as a source of carbon for gluconeogenesis and lipid synthesis.

If the acetyl units will be used for lipid biosynthesis, they may be taken to the endoplasmic reticulum, cytosol, or mitochondrion, where lipid synthesis occurs in eukaryotes [131]. Similar to the shuttle required for the TCA cycle, enzymes for sterol synthesis may be distributed between lipid bodies and the ER, or the mitochondrion [123]. Some fungi, such as *Y. lipolytica* and other oleaginous yeasts, show intracellular aggregation of hydrocarbons especially under conditions of high carbon:nitrogen ratios [123] while others, such as the pathogenic yeast *Candida tropicalis* produce a fatty acid complex which induces uptake of hydrocarbons when grown in the presence of alkanes [132]. Additional uses for carbon may include biosynthesis of small molecules with specialized functions, including heme rings and siderophores, which trap iron in a biologically available state [133]–[136]. The importance of oxidative and reductive

enzymes which contain heme-bound iron co-factors to beta-oxidation may also necessitate the production and regeneration of the reductive tri-peptide glutathione, used to reduce toxins, disulfide bonds, and reactive oxygen species [57]. Lipid-based carbon flux is thus dependent upon iron, suggesting regulatory targets may be subject to signal integration by multiple transcriptional regulators. Nutrient inducible carbon storage is an area of developing research for use in the biological oil production [137], [138].

Beta-oxidation and peroxisomes are affected by fatty acid regulators

Beta-oxidation in eukaryotes is a degradative process that happens largely in mitochondria, but also in other specialized microbodies like peroxisomes and glyoxysomes. The reactions consist of four steps carried out by three enzymes to generate two-carbon units, carried as acetyl-CoA, for fuel or building materials in gluconeogenesis, as mentioned previously. The diversity of microbody contents and function has been reviewed [139], [140]. For our purposes, it should be noted that *Neurospora* catalases do not localize to microbodies, making this organelle family largely similar to glyoxysomes, defined by the presence of the enzymes of the glyoxylate shunt or bypase [141]. However, other detoxification enzymes are present, such as nitropropane dioxygenases (*npd-1* and *npd-2*, NCU04803 and NCU09931, respectively), and peroxiredoxins (NCU06031) which detoxify H_2O_2 and then use thioredoxin to return to its reduced state [57], [142]. For beta-oxidation to occur efficiently, the proteins that catalyze these basic steps must be trafficked to the appropriate compartment. This requires proteins that identify peroxisome targeting signals (PTS1 and PTS2) and provide passage across the organelle membrane. These functions are associated with peroxins ('Pex'), proteins originally identified *in S. cerevisiae, Hansenula polymorpha and Pichia pastoris* by screening for peroxisome dysfunction phenotype mutants [101], [143], [144]. Pex proteins involved in protein sorting and trans-membrane delivery to peroxisomes or glyoxysomes were characterized. A complete listing [139] was used to find the

Neurospora homologs by BLAST homology searches (Table 1.2). If an increase in beta oxidation activity is required, glyoxysomes must be expanded in volume and undergo division by fission in a manner similar to mitochondria or chloroplasts [145]. New proteins entering peroxisomes or glyoxysomes are threaded across the membrane as unfolded polypeptides, but may also pass as folded proteins or as oligomers during population of organellar space for enzymatic reactions [140]. Pex26, a protein important for peroxisome import is enriched in the subpopulation of peroxisomes that mature into Woronin bodies [140].

A number of Pex proteins have been previously identified as regulatory targets of FAR TFs in *A. nidulans* [106] and *C. albicans* [104]. The *pexK* gene, a predicted PEX11 homolog, is not upregulated to the same extent in either *farA* or *farB* mutant. The *A. nidulans* homologs for *pex3*, *pex1*, *pex5* and *pex6,* encoding peroxisome biogenesis and peroxisome import machinery proteins, contain the FAR recognition motif 5'-CCTCGG-3' in their promoters [106] though their expression and response to the FARs is unknown. *PEX5* transcripts similarly fall short of wild type levels by northern blot in a *farA* homologue, called *por1*, knockout [104]. It should be noted that *Neurospora* FAR TF mutants had no developmental difficulties on medium with various fatty acids as sole carbon source, unlike the *pex* mutants. This suggests that the FARs are responsible for induction, but are not the sole transcriptional activators of certain beta-oxidation enzymes and the peroxisomal machinery.

We have a fairly comprehensive understanding of how carbon flows into cells, and how it is trafficked to the celluar components. These processes differ slightly, and in an evolutionarily trackable manner, between organisms [59], [129], [146]. We also have evidence for differential regulation of lipases, cutinases [108] and cellulases, and integration of light, stress, and nutritional signaling [147]. What we still lack is a clear picture of how the TFs doing the regulation are controlled, and how they relate to other nutrient regulators. In the absence of a TF, the balance between activation and repression may be perturbed, and other regulators may step in with redundancy. In

order to broadly define a picture of a relationship between integration of environmental signals and transcriptional regulation and its metabolic consequences, we carried out experiments in *N. crassa*.

Hypotheses and aims of this thesis

I chose to do ChIP experiments to identify all FAR-1 and FAR-2 binding sites in the *Neurospora* genome under different growth conditions. These studies will be detailed in section 1. Phenotypic assays on *far-1* and *far-2* single and double deletion strains test the functional relevance of the results identified by ChIP-seq (see section 2). RNA-Seq was used to determine which transcripts were changing as a result of single or double FAR loss on different carbon sources (section 3).

Genomic scale sequencing can be used to address experimental questions, but the resulting datasets can also be analyzed systematically to form new hypotheses about function and related regulation. My original hypothesis that FAR-1 binds DNA in a light dependent manner proved false, which eliminates one possibility of how FAR-1 is regulated. In order to test another possibility, I asked whether FAR-1 binds DNA dependent upon carbon source. Aim 1 of this thesis is to characterize the binding behavior of FAR-1 under different nutrient conditions. In parallel, the TF FAR-2 was tested for binding behavior given the same three nutrients. I will discuss some background and bioinformatics of fatty acid regulators. Aim 2 extensively describes which transcripts alter or fail to alter their transcript levels between wild type and a FAR mutant in order to identify the consequences of these missing regulators. Aim 3 of this thesis was to identify phenotypes which differ between the wild type and FAR mutants. This was done to test hypothesized functions of FAR regulation based upon ChIP targets. This characterization includes primary targets of the FARs as indicated by ChIP, as well as secondary targets which may be affected by perturbed TF levels. Together, we have vastly improved the detailed knowledge of the FAR transcriptional network.

Table 1.1: Transcription factor genes near white collar complex binding sites
Transcription factor (TF) genes near which the White Collar Complex (WCC) binds, based on ChIP-seq with WC-2 [7]. Where appropriate gene names are listed (with synonyms in parentheses) and for all genes the unique Neurospora locus ID is listed. For some of the TFs papers have been published but many of them are still under investigation by the consortium of laboratories that constitute the Neurospora Functional Genomics and Systems Biology (NcFGSB) program project funded by the NIH (P01GM).

TF	Locus	Reference
CLR-1	NCU07705	Coradetti, 2012
CSP-1	NCU02713	Sancar, 2011
VOS-1	NCU05964	NcFGSB
ADV-1	NCU07392	NcFGSB
TF	NCU07846	NcFGSB
TAH-3	NCU03686	NcFGSB
SAH-1	NCU04179	NcFGSB
SAH-2 (SREBP)	NCU04731	NcFGSB
KAL-1	NCU03593	NcFGSB
GHH-1 (CSP-2)	NCU06095	NcFGSB
FAR-1	NCU08000	this work
FAR-2	NCU03643	this work
WC-1	NCU02356	Smith, 2010
TF	NCU04295	NcFGSB
TF	NCU09615	NcFGSB
NIT-2	NCU09068	NcFGSB
TF	NCU09829	NcFGSB
MIT-4	NCU01243	NcFGSB
TF	NCU01871	NcFGSB
HSF-2	NCU08480	NcFGSB
CRE-1	NCU08807	NcFGSB
BEK-1	NCU00097	NcFGSB
SUB-1	NCU01154	NcFGSB
TF	NCU06534	NcFGSB
SRE-1	NCU07728	NcFGSB
TF	NCU00275	NcFGSB
VAD-2	NCU02094	NcFGSB
TF	NCU05994	NcFGSB
TF	NCU03273	NcFGSB
TF	NCU03184	NcFGSB

Table 1.2: Peroxin homologs of *Neurospora crassa*
N. crassa unique locus numbers (NCU) of genes encoding proteins the most similar to the listed peroxin in *S. cerevisiae* [139]. In some cases, the encoded protein shows domain or sequence characteristics of several proteins, noted by a (/).

Function	Pex homologs	NCU
PTS1 and PTS2 import		
docking complex (matrix)	*PEX8*	NCU00032
docking complex	*PEX13*	NCU02618
docking complex	*PEX14*	NCU03901
docking complex	*PEX33/23*	NCU01535
PTS1 and PTS2 import into peroxisomes	*PEX20*	NCU04062
PTS1 and PTS2 import into peroxisomes	*PEX5*	NCU02960
PTS2 import into peroxisomes	*PEX7*	NCU07662
Organelle biogenesis		
organelle biogenesis	*PEX11*	NCU04802
farnesylated protein contributing to biogenesis	*PEX19*	NCU04301
targeting to membrane	*PEX3*	NCU06175
negative regulator of peroxisome size	*PEX31*	NCU05564
Ubiquitin conjugation for receptor recycling		
UBC enzyme	*PEX4/22*	NCU02636
RING finger peroxin and UBC enzyme complex	*PEX12*	NCU05245
RING finger peroxin and UBC enzyme complex	*PEX10*	NCU03277
receptor for docking at UBC	*PEX2*	NCU02070
AAA ATPase complex for receptor recycling		
ATPase; recycle pex5 receptor to cytosol	*PEX6*	NCU08373
ATPase; recycle pex5 receptor to cytosol	*PEX1*	NCU08118
anchor of pex6 ATPase	*PEX26*	NCU00347
chaperone and import for peroxisomal proteins	*PEX19*	NCU04301
Miscellaneous/putative		
peroxisomal membrane protein	*PEX16*	NCU01850
peroxisomal membrane protein	*PEX24*	NCU06637
putative ATPase subunit	*PEX1/6*	NCU05160

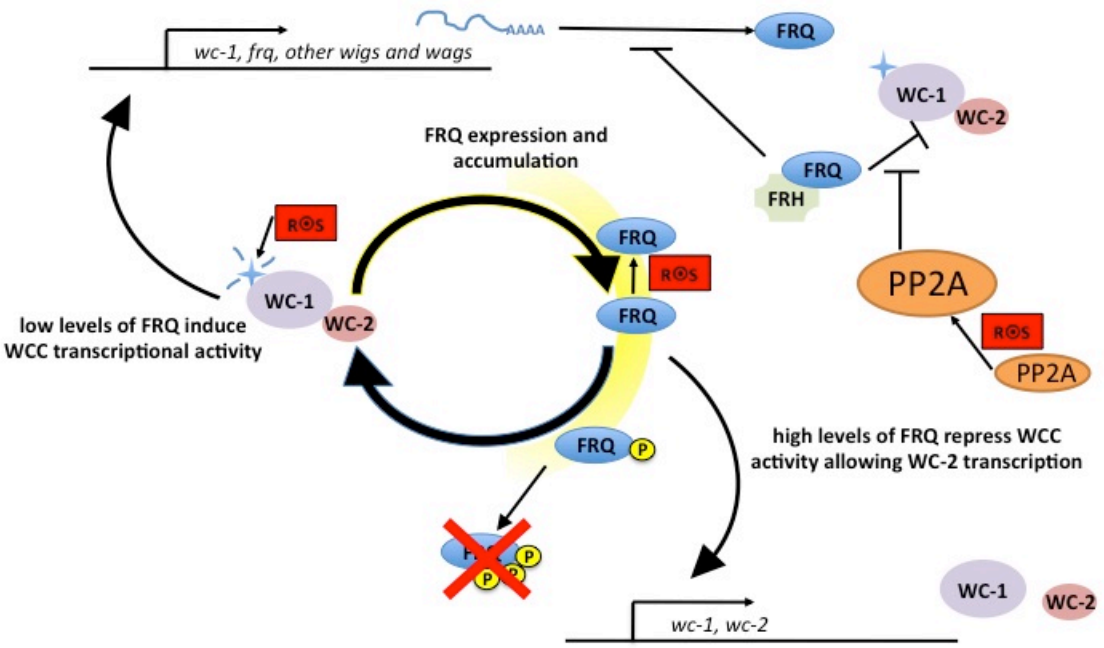

Figure 1.1: Model of the core *N. crassa* circadian oscillator
WHITE COLLAR-1 (WC-1) and -2 (WC-2), FREQUENCY (FRQ), FRQ-interacting RNA helicase (FRH) and some of the proteins that contribute to changes in activity or protein level of the clock components are shown. Reactive oxygen species (ROS) affect clock signaling at several places. WCC binds at frq and upregulates transcript production. Upon translation and transport into the nucleus, FRQ is phosphorylated in stepwise fashion by several kinases (Casein Kinase I, Casein Kinase II, Calmodulin-dependent protein Kinase I) [33]. Yellow fade shows FRQ accumulation and degradation. A dimer of FRQ and FRH specifically interact with the White Collar Complex (WCC), both inhibiting its activity, and preventing WCC degradation [148]. FRQ-FRH also decreases *frq* transcript levels. Exposure to hyper-oxidative environments prevented WCC dimerization, while hypo-oxidative states may inhibit the function of the WCC [50]. ROS levels elevated compared to cell conditions showed an alteration in WC-1 structure similar to those in light absorption even in darkness. PP2A is protein phosphatase 2A which works to remove phosphate groups from WCC increase its transcriptional activity [49]. FRQ levels were higher earlier in strains treated with ROS [49]. “Wigs” are white-collar induced genes, “wags” are white collar associated genes.

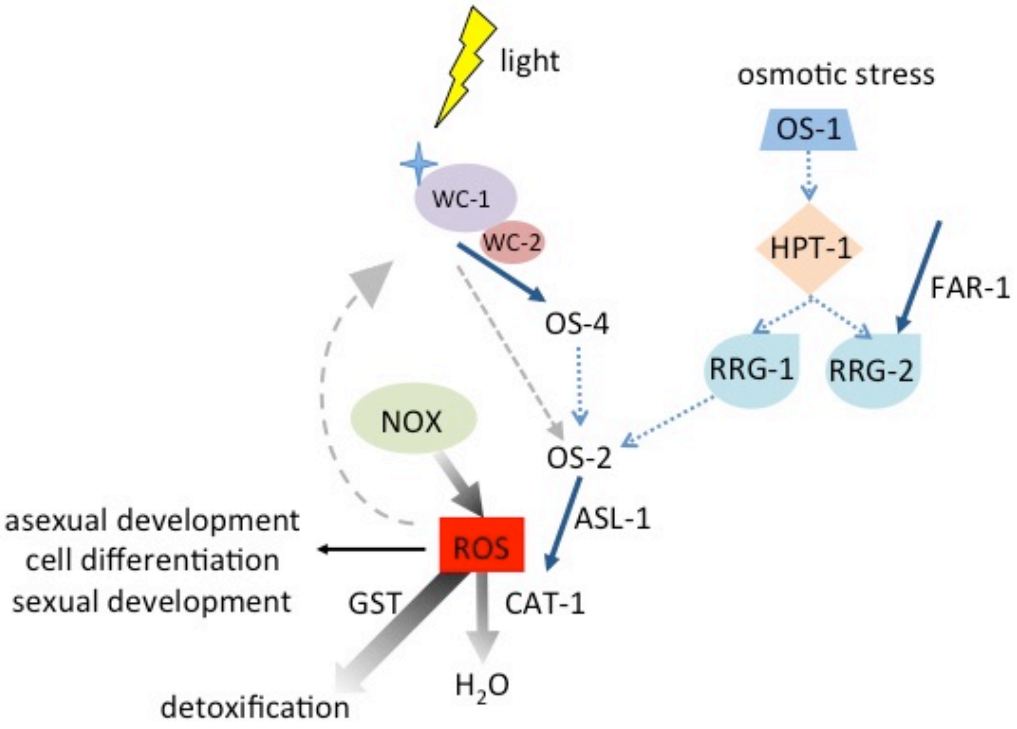

Figure 1.2: The canonical osmotic stress signaling pathway
Osmotic stress signaling begins with histidine kinase OS-1, which signals (with 10 other histidine kinases) through the histidine phosphotransfer protein HPT-1. HPT-1 mediates signals through response regulator kinases RRG-1, and RRG-2. RRG-1 affects OS-2 kinase activity [55]. The mitogen activated protein kinase or MAPK OS-2 affect the cellular proteome by controlling the transcription factor ASL-1. Glutathione-S transferase (GST) activity is a non-enzymatic scavenger and detoxifier of a variety of products, which can act on reactive oxygen species, while catalase-1 is the only detoxifier of ROS, 'reactive oxygen species' that is light induced [53]. NOX, NADPH oxidases (nox-1 and nox-2) are ROS generators [50]. Fading arrows show changing abundance, with light color being less, while dark is more. Solid arrows indicate affects on transcription; dotted arrows signaling pathways, while dashes are potential interactions such as feedback within the clock.

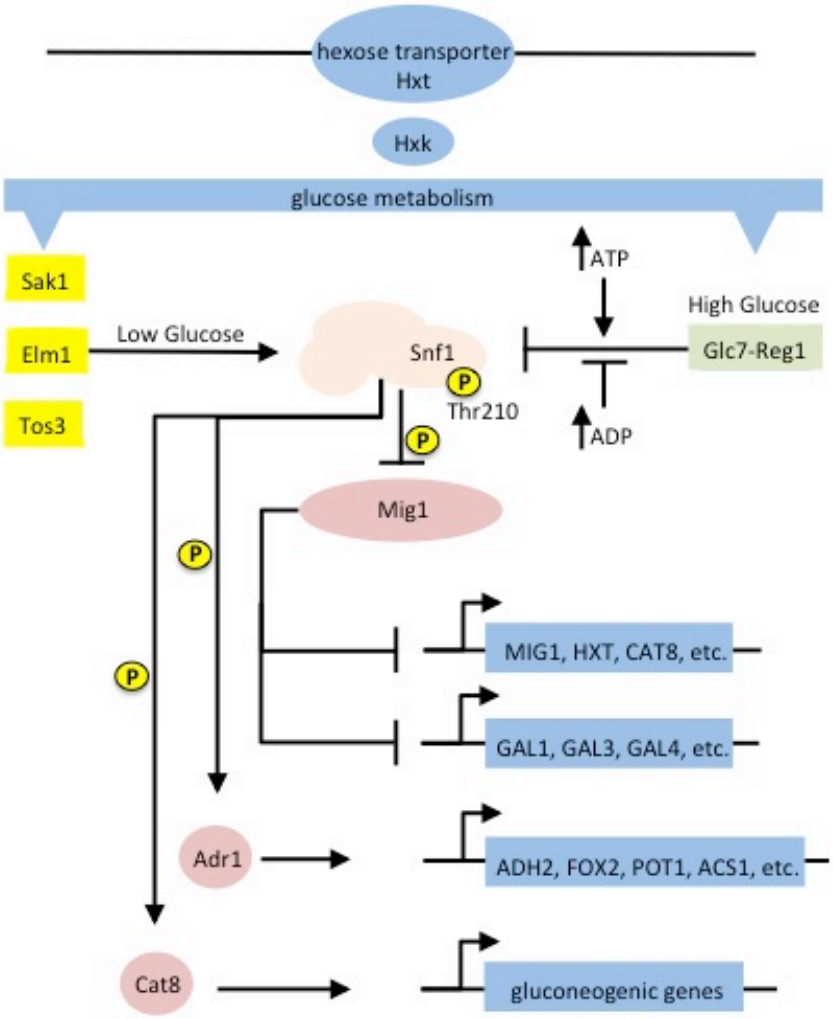

Figure 1.3: The Snf1 kinase regulatory pathway
The Snf1 kinase complex activation is regulated by the phosphorylation state of Threonine 210. It is turned on by the activity of kinases Sak1, Elm1, or Tos3, and dephosphorylated by Protein phosphatase 1 subunit Glc7. Snf1 phosphorylation of Mig1 transports it out of the nucleus, removing its transcriptional repression. When active, it represses transcription of itself, a number of GAL genes, hexose transporters, and other TFs including CAT8 which control the cellular machinery to utilize other carbon sources. Snf1 also phosphorylates and activates transcriptional activators Cat8 and Adr1 which are responsible for upregulating transcription of gluconeogenic genes and a number of genes involved in ethanol, glycerol and lactate utilization respectively. The activation state of Snf1 is sensitive to ADP/ATP levels which control the phosphatase activity of Glc7 [78], [82].

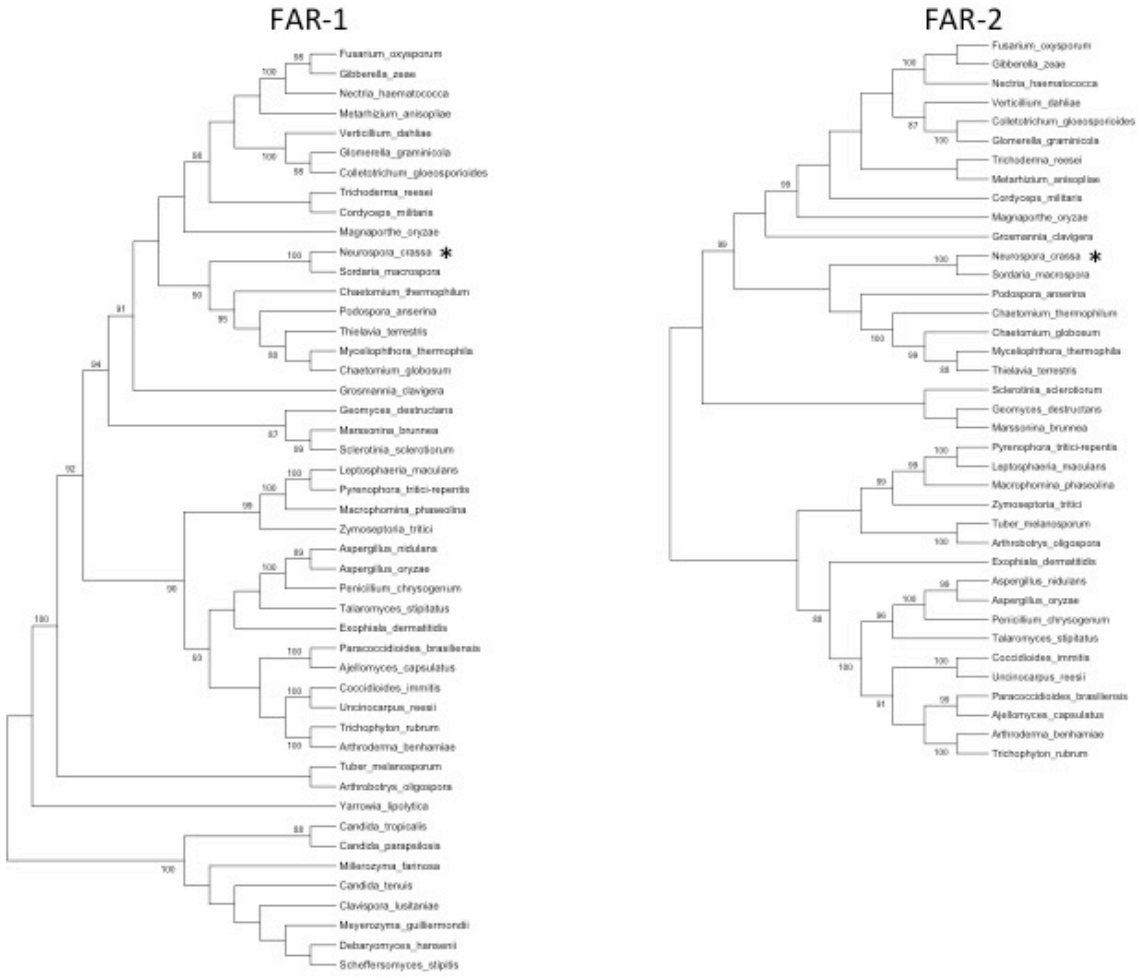

Figure 1.4: Phylogenetic trees for FAR-1 and FAR-2 based on protein sequence.
For the FAR-1 tree, 47 species are represented, while due to the restriction of FAR-2 to the true ascomycetes, FAR-2 is represented by 38 species. FAR-1 homologues are distributed among true ascomycetes and some hemiascomycetes. Saccharomycetales do not produce proteins with homology to FAR-2. *Neurospora crassa* proteins are marked with an asterisk. Trees generally follow the order of species divergence found by other means [103].

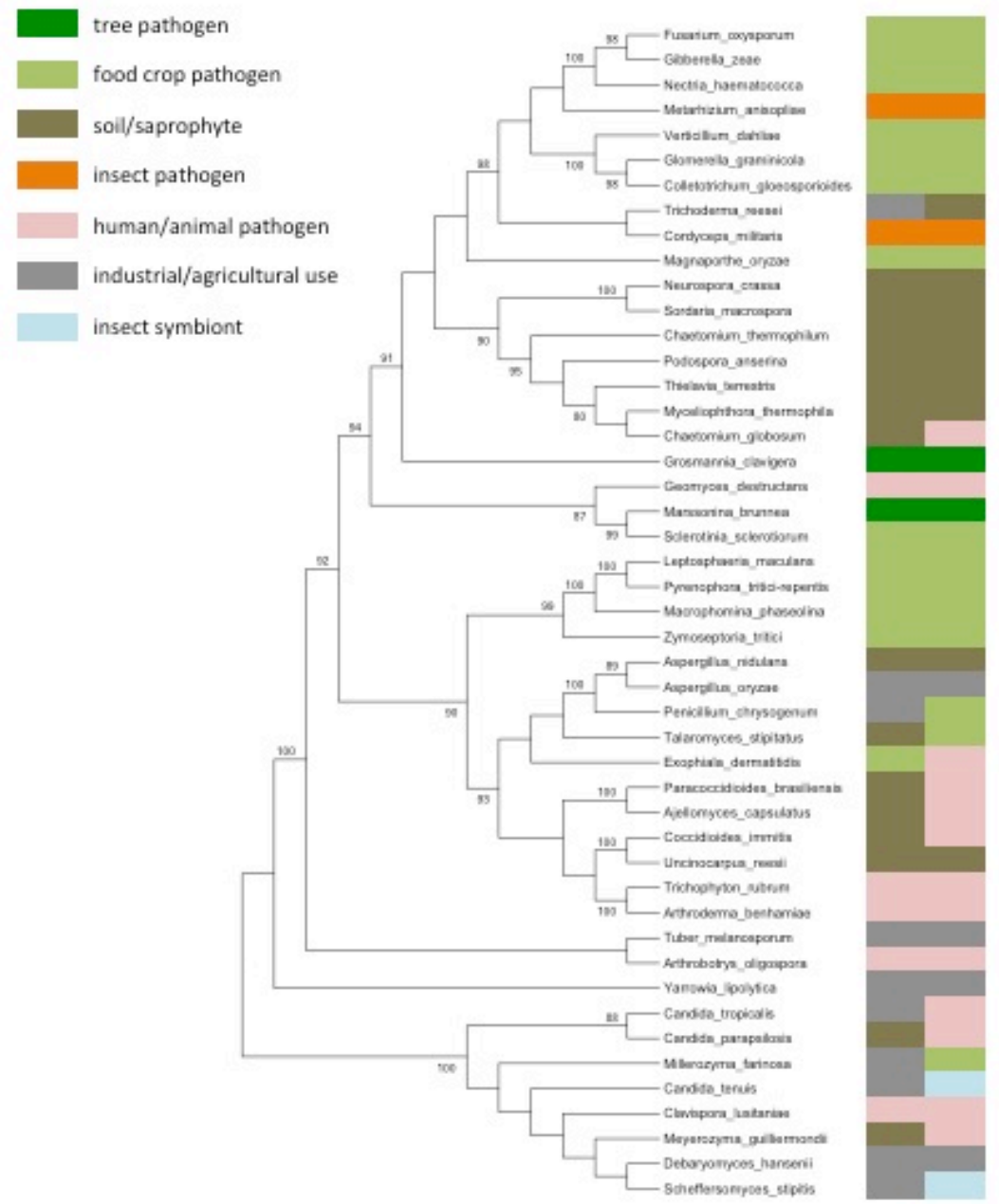

Figure 1.5: Phylogenetic tree of FAR-1 amino acid sequences with lifestyle categories
Image generated in MEGA [149] after 500 repetitions of bootstrapping a neighbor joining tree ("Neighbor Joining method [150], evolutionary distances based on the Poisson correction method [151]"). Bootstrap values above 80 are shown. Represented are all species included in phylogenetic trees in this document. For comparative species groupings, see Lutzoni et al or Schoch et al. [103], [152].

Chapter 2: Materials and Methods: Transcriptional Networks Controlled by the Fatty Acid Regulators, FAR-1 and FAR-2

Strains and growth conditions

Strains are part of the FGSC collection, or were generated by crossing transformant heterokaryons to wild type (FGSC2489, 74-OR23-1V A; Table 2.1). Strains were grown and maintained as described [153]. Crosses were performed on 0.3% sucrose synthetic crossing media [154] (Russo, modified) in 100 mm sterile plates. Ascospores were collected from plate lids using sterile water after a few weeks. Strains were confirmed by a combination of Southern blots and PCR (Figure 2.1).

NMF261 was used for the sequencing of the *N. crassa* reference genome. NMF 263 (FGSC 9718) and NMF264 (FGSC 9719), used for transformations, are mutants in *mus-51* and *mus-52*, homologs of the ku-70 and ku-80 proteins that are involved in non-homologous end joining repair. Deletion of *mus-51* and *mus-52* decreases recovery of ectopic integration of DNA fragments when targeting genes to a specific locus in the genome under selection [155].

All strains were cultured from freezer stocks on 25 mL Vogel's minimal medium (VMM) with 1.5% sucrose and 1.5% agar in 125 mL Erlenmeyer flasks or small glass tubes containing 1 mL of the same medium [156]. Strains were grown at 30° C for 1-2 days until conidia formed, and allowed to conidiate for 7 to 10 more days if strains were used for transformation experiments. Conidia collection from flasks was performed using 50 mL sterile distilled water poured into the flask with brief agitation, 5-10 minutes of settling, and centrifuging for 5 minutes in a table top centrifuge (Beckman CS-6R) at 2,000 rpm and 4° C. Floating hyphae and water were poured off, and pelleted conidia resuspended in 30-50 mL sterile water, followed by resuspension, and counting of spore density on a haemacytometer.

Epitope tagging at an endogenous gene

We designed constructs for tagging NCU08000 and NCU03643 endogenously by fusion PCR based on the plasmid pZero-GFP-loxP-hph-loxP as described previously [157], [158]. The 5' and 3' flanking regions of NCU08000 were amplified from the genomic DNA of NMF261 with primer pairs OMF 1597-OMF1598 and OMF1599 - OMF1600, respectively (Table 2.2). A fragment containing GFP or 3x FLAG and *hph* was amplified from pZero-GFP-loxP-hph-loxP or pZero-3xFLAG-loxP-hph-loxP with OMF83 and OMF84. The 5' split marker fragment was amplified by PCR to contain the 5' gene fragment and GFP with new stop codon along with a partial *hph* gene using OMF1817, while the 3' fragment made using OMF1816 contained an overlapping fragment of *hph* and the 3' flank downstream of the coding region (Figure 2.2). NCU03643 was tagged with 3xFLAG by the same scheme. Tagging with the V5 epitope was accomplished by using long overlapping primers and the same *hph* fragment amplified from the pZero plasmid. The 5' gene fragment located at the terminus of the gene was amplified by OMF 2304-OMF2305 for tagging with a FLAG epitope (from pZero-3xFLAG-loxP-hph-loxP) or using OMF 2304-OMF2308 for tagging with V5. The *hph* gene for selection on the antibiotic hygromycin B (Hyg) was amplified with OMF2309 – and OMF84, to contain the V5 tag followed by the *trpC* promoter and *hph* gene. Split marker fragments of *hph* were generated with OMF1817 and OMF1816, respectively. DNA constructs for GFP, FLAG and V5 tagging were transformed into NMF264 or NMF263 by electroporation [159]. Hyg^R colonies were selected and backcrossed to NMF261 or NMF 262 to obtain homokaryotic strains. Homokaryons were confirmed to have integration of the tag-*hph* construct by Southern blot and western blot using anti-GFP antibody (Santa Cruz, sc-9996) or anti-V5 antibody (Invitrogen, 46-0705).

Transcriptional start clarified by Sanger sequencing

The predicted 5' end of the NCU08000 gene was amplified using primers OMF2494 and OMF2499 by PCR from cDNA prepared by reverse transcription with a

Transcriptor First Strand cDNA Synthesis Kit (Roche, 04379012001). After PCR amplification using dynazyme (Finnzymes), PCR products were purified and submitted to the CGRB core labs with primer OMF2494 for sequencing across a potential transcriptional start. The new start codon identified was over 700 bp upstream of the annotated start in version 10 of the *Neurospora* genome (previously available from Broad Institute, http://www.broadinstitute.org/). Four introns in and around the Gal4 DNA binding domain motif contained the previously annotated start codon. The upstream transcriptional start and shifted intronic positions were used to design primers for cloning and expression of FAR-1 domains (Figure 2.3). Transcriptional start sites for *far-1* and *far-2* were further validated by RNA-sequencing during this project.

Cloning of *far-1* domains

Domains spanning portions of the *far-1* gene were amplified using primers for cloning (Figure 2.3) to be in frame based upon Sanger sequencing. Five sections, encoding different sections of the protein A: the DNA binding domain, B: the DNA binding domain and fungal TF domain, C: the fungal TF domain, and E: The C-terminal portion, were amplified from cDNA, and cloned into plasmid pE-SUMO (lifesensors) designed for fusion with a 6x-his tag and Smt3 for expression. Once confirmed by digestion, these plasmids were transformed into Rosetta *E.coli* cells. Chloramphenicol was added to terrific broth [160] to maintain the rare-codon plasmid used by the Rosetta cell line, and Kanamycin was used to select for pE-SUMO presence.

***E. coli* growth and induction of FAR-1 domain expression**

E.coli cultures of 5 mL grown overnight for 17 hours were used to inoculate 25 mL of terrific broth containing kanamycin and chloramphenicol. Cells were grown with shaking at 37°C to an OD of 0.6, and then IPTG was added to .4 mM for 4 hours. Cells were harvested by rapid chilling followed by pelleting in a 30 mL oakridge tube. Cells were initially induced at 37 °C, but after poor results, growth after IPTG addition was

done at room temperature, and then 16°C keep protein from precipitating or degrading. Pelleted cells were resuspended in 2 mL E. coli lysis buffer (50 mM Tris pH 8.0, 20 mM NaCl, 5% glycerol, 1mM PMSF (Sigma, 1 ul/mL each leupeptin (Roche), E-64 (Roche), and 3 uL/mL pepstatin (Roche). Cells were sonicated 3 times for 10 seconds, with 30 second intervals between burses. The resulting extract was centrifuged for 20 minutes at 4°C at 15K in a microcentrifuge before applying the supernatant to equilibrated Talon Cobalt Resin and 6mL wash buffer (50mM sodium phosphate, 300mM NaCl at pH 7.0, 20 mM imidazole, protease inhibitors as above). Samples were rocked on ice at 4°C for 1 hour. Resin was spun down for 5 minutes in a swinging bucket rotor centrifuge, and supernatant removed. Resin was transferred to 1.7 microcentrifuge tubes, to which 1 mL wash buffer was added, followed by a spin of 2 minutes at 5K. This wash was repeated a second time. For elution, 600 uL elution buffer (150mM imidazole, 50mM sodium phosphate, 300mM NaCl) was added, and samples were rotated 10 min at 4°C, spin 2 minutes at 5K at 4°C. Elution was repeated with buffer containing 500mM imidazole.

Western blot analysis

Protein samples were extracted from lyophilized mycelial mats that were grown for 1-2 days at 30°C on VMM containing 1.5% sucrose, or supplemented as indicated. Lyophilized tissue was ground by vortexing with a metal spatula. Urea-SDS loading buffer (1% SDS, 9 M urea, 25 mM Tris-HCl pH 6.8, 1 mM Na-EDTA pH 8.0, 10 mM β-mercaptoethanol (BME), 0.05% w/v bromophenol blue) was added to the tissue powder. Samples were heated to 100° C for 10 minutes, vortexed again, chilled briefly, and loaded on pre-poured SDS-PAGE gels (BioRad, Any kD, 456-9033). Proteins were separated by running at 190 volts for 35 minutes, and transferred to PVDF membranes in Towbin buffer [161] with 20% methanol for 1 hour at 100 volts. Membranes were blocked for 1 hour in TBST (50 mM Tris.HCl, pH 7.4, 150 mM NaCl [160] + 0.5% Tween20) and 5% nonfat dried milk powder. Primary antibody incubation was

overnight at a concentration of 1:1000 of anti-GFP antibody (Santa Cruz, SC-9996) in TBST containing 0.5% dried milk powder. Membranes were washed four times in 20 mL TBST at room temperature for 10 minutes. Secondary antibody (goat-anti-mouse; Invitrogen, 62-6520) was diluted 1:25,000 in TBST and 0.5% dried milk, and incubated for 1 hour at room temperature with rocking. After four additional washes with TBST, blots were developed after 5 min of incubation with 1 mL of each substrate from SuperSignal West Femto kits (Pierce, 34096) diluted into 23 mL TBST. Film exposure times were as noted in the figure legends.

Chromatin immunoprecipitation

Chromatin immunoprecipitation (ChIP) was performed according to published protocols [162] with slight modifications. For tissue growth, 1 x 10^6 conidia per mL were inoculated into 25 mL of VMM with 1.5% sucrose, and grown for 16 hours at 30 °C with shaking. Initial experiments with light induction were grown from agar plugs in the dark, followed by light exposure for 0 (DD or dark), 15 minutes (LL15), 60 minutes (LL60), or 120 minutes (LL120), fixation, and snap freezing for shipment (performed in the Dunlap laboratory at Dartmouth). Mycelia were filtered and washed with 1x PBS (137 mM NaCl, 2.7 mM KCl, 10 mM Na_2HPO_4, 1.8 mM KH_2PO_4, sterilized by autoclaving), followed by transfer into 25 mL of medium supplemented with 1.5% sucrose, 5 mM oleate (1.61 uL/mL), or 5 mM Na-butyrate. Tissue was grown for another 4 hours, after which tissue was fixed by the addition of 1 % formaldehyde (from 37% stocks or from 20% freshly dissolved paraformaldehyde) to the medium, and shaking at room temperature for 15 minutes. Fixation was quenched by addition of 2.5 M glycine to a final concentration of 0.12 M. Tissue was filtered on number 4 Whatman filters, and washed with PBS. A pea-sized portion of tissue was immediately placed into 0.5 mL of ChIP lysis buffer containing protease inhibitors (E-64, pepstatin, leupeptin, and 0.1 M PMSF) on ice. Tissue was sonicated (Branson Sonifer 450A Sonicator) for lysis at an output of 2, duty cycle 80, for 30 pulses. Chromatin was sheared by six rounds of

sonication for 20 pulses at output 1.2, interrupted by at least 3 minutes rest on ice after each sonication step. Antibodies used for ChIP were anti-GFP (Abcam, ab290) and anti-V5 (Invitrogen, 46-0705), which were captured using Protein-A (anti-rabbit; Invitrogen, 15918-014) or Protein G (anti-mouse; Invitrogen, 15920-010) agarose beads. Eluted samples were used to generate Illumina sequencing libraries.

Illumina library preparation and sequencing

Initial Illumina sequencing libraries were constructed by ligating single end sequencing adapters with barcodes to the sheared eluted DNA purified by ChIP, and amplified according to our published protocol [163]. Later libraries were prepared according to the low throughput protocol for TruSeq DNA sequencing (Illumina Sample Preparation Guide, version 2). Illumina adapters for genomic DNA sequencing (diluted 1:100 in water) or undiluted adapters for RNA-sequencing were attached to polished ChIP DNA with A overhangs during the ligation step to minimize adapter dimer formation during PCR amplification. ChIP libraries were amplified for 21 cycles using Phusion PCR mix (Finnzymes Oy) with the following program: 98°C for 30 sec, then repeated cycles of 98° C for 10 sec, 65° C for 30 sec, 72° C for 30 sec, and one final extension at 72° C for 5 min. Libraries were size-selected for 250-550 bp fragments on a 2% NuSieve gel, followed by removal of agarose using a QIAquick Gel Extraction Kit (Qiagen), washing twice with 750 uL of PE buffer before elution. After quantification by NanoDrop2000 spectrophotometer, DNA concentration was adjusted to 10 nM or 30 nM, and pooled with different barcodes before sequencing. Single-end reads were generated on the Illumina GAII or HiSeq2000 at the Center for Genome Research and Biocomputing (CGRB) at OSU.

ChIP-sequencing data processing and analysis

Illumina 51-nucleotide (nt) reads were trimmed of their barcodes using the IlluminaParser program (CGRB, Nathan Lai and Chris Sullivan). Alternatively, read files

parsed by the CASAVA1.8 Illumina software were mapped to version 12 of the Neurospora genome using bowtie [16] with removal of duplicate reads (Table 2.3).

Mapped reads were analyzed by MACS2 [164] which calls peaks for each sample independently. MACS2 output was used when only single replicates were done. (Figure 2.4) Where applicable, MACS2 output was analyzed by Irreproducible Discovery Rate (IDR) [165], an R program designed to do pairwise comparisons of peaks called in different samples. To get a consensus set of peaks for treatments with more than one replicate, several ChIP-seq data sets were mapped and taken through the following workflow. An analysis of 'pseudo-replicates' made by combining reads from all runs and calling peaks on a percentage of the reads (4 replicates of 15% were made by using the randsample function in MACS2), followed by consensus peak calling by comparing pseudoreplicates in IDR (Table 2.4). The true replicates that had a similar average peak number to the pseudoreplicates below an IDR of 0.01 (HTS 274 vs HTS 275) were then used as a beginning set. The same peaks from ChIP-seq replicates containing fewer reads (HTS 273 vs HTS 673) were kept if they overlapped with this peak set below 0.01 IDR. I wrote programs ("IDR_annotate.pl" and "annotate_MACS2.pl") to find genes in the Neurospora assembly near each identified peak. Gene ontology (GO) distribution was further queried for enriched groups of genes near binding sites using the functional categories (FunCat) database [166]. After ordering peaks by peak enrichment, the limited input size for FunCat web submission output created two tiers of genes enriched against total genes found in the genome (Tables S7-S10, available online). I generated a visual functional network using a combination of the FunCat database, updated Broad annotations (http://www.broadinstitute.org/) for the *Neurospora* genome in Cytoscape [167] with Map Enrichment [168]. Carbon source specific analysis of peak locations was accomplished using the join function in unix.

Luciferase reporter constructs

Promoter regions of 4 genes (NCU00275, NCU07666, NCU09534, NCU00552) identified as ChIP binding targets were amplified from Yeast recombination fragment DNA, a provided by collaborators (from the Dunlap laboratory at Dartmouth). As I was unable to amplify the entire csr interruption cassette from all yeast DNAs but one, primers were used (OMF2925 crs5F and OMF2926, csr3 to amplify only the promoter regions using, csrOL_F_NotI, OMF2927; csrOL_F_XmaI, OMF2928; csrOL_R_XmaI, OMF2929; csrOL_R_EcoRI, OMF 2930 in combination (Table 2.5). These fragments were then cloned into pBM60, after I constructed and confirmed cloning of codon optimized Luciferase [37], also from the Dunlap laboratory (Figure 2.5A). The promoters were designed to contain different numbers and combinations of FAR-1 and WC-2 binding sites to address the possibility of interaction between the regulators. This was to test the possibility that WC-2 may block interaction of DNA with FAR-1, given the protein similarity of WC-2 to the *N. haematococca* palindrome binding protein (PBP) (Figure 2.6). The fragments were ligated into a pBM60 backbone, a plasmid that targets the *his-3* locus. These fragments were integrated in Neurospora by electroporation and plated on minimal media without histidine supplement for selection. Experimental design to assay the effects of FAR-1 employed *his-3*$^{-}$ strains containing a wild type *far-1* or a *far-1* deletion (Table 2.6).

RNA preparation and cDNA synthesis

For growth of RNA cultures, 4 x 10^{6} conidia per mL were inoculated into 100 mL of VMM with 1.5% sucrose, and shaken for 16 hrs at 200 rpm and 30° C. Cultures were collected by vacuum filtration, washed briefly with 1 X PBS, and tissues placed in fresh 100 mL aliquots of VMM containing 1.5% sucrose, 5 mM butyrate, or 5 mM oleate. The cultures were grown for another 6 hours with shaking at 30° C. Tissue was collected by vacuum filtration, and washed with 1 X PBS. Samples were ground to a fine powder under liquid nitrogen, and stored at -80° C until RNA extraction. RNA was prepared as

described [169] with minor modifications. Acid phenol at pH 4.0 was used. RNA was precipitated in ethanol, DEPC, and sodium acetate for 5 hrs at -20° C before centrifugation.

RNA-sequencing analysis

Analysis and visualization of RNA-sequencing data was done using several programs including Bowtie for mapping, and Cuffdiff for differential expression analysis [16], [170]. cDNA reads were aligned to version 12 of the *N. crassa* genome (currently available from Broad Institute, http://www.broadinstitute.org/). Cuffdiff, a program within the RNA analysis suite CuffLinks, was used to analyze differential expression of transcripts, combining data from three biological replicates each of four strains (wild type, Δ*far-1*, Δ*far-2,* Δ*far-1;* Δ*far-2*) in three growth conditions (sucrose, butyrate, oleate). The R program 'pretty heatmaps' (pheatmaps) was used for visualization of data, with Euclidean clustering of the $\log_2$ (change in FPKM), where FPKM is "fragments per kilobase of the genome per million reads". Fold expression change was taken from cuffdiff output comparing the samples listed in each column of a heatmap [171]. Cytoscape [167] was used to generate regulatory network images.

Race tube assay

Glass tubes of 30-35 cm with curved ends (Ryan or "race" tubes) were sealed with cotton plugs, and autoclaved for sterilization. 15 mL of VMM with 1.5% agar and different carbon sources (5 mM oleate, 5 mM butyrate, 0.5% Tween-20, 3 mM (= 0.1% w/v) sucrose, or a combination of the different carbon sources) were added and allowed to solidify prior to inoculation. Tubes were inoculated at one end with a few microliters of conidia, marking progress of the leading edge of hyphae every 24 hours to assess rate of linear growth. Experiments were done in duplicate or triplicate and averaged, with standard deviations included to show variance. Each growth condition was repeated three times.

Reactive oxygen species sensitivity

60 mm plates containing 8 mL of agar were poured mixed with 1 mM, 10 mM, 20 mM, or 30 mM of hydrogen peroxide taken from a 10 M stock solution stored at 4° C. Strains including NMF261 (wild type), NMF641 (*Δfar-1*), NMF643 (*Δfar-2*), and NMF640 ("ΔΔ", *Δfar-1 Δfar-2*) were grown initially on SC agar containing 0.3% sucrose for 48 hours. Plugs made with a size three cork borer were transferred from the inoculated plate to those containing hydrogen peroxide. This removes perturbation of germination and differentiation genes expressed in conidial anastomosis tube formation in the presence of hydrogen peroxide [172] as well as equalizing inocula. Plates were grown for 72 hours at 32° C before imaging.

CAS agar assay for siderophore secretion

Plates with chromeazurol S (CAS) agar were made by transferring one half of a plate with solidified dye-containing agar to an empty plate. The remaining space was filled with VMM agar lacking iron, with either sucrose or 5 mM oleate as a carbon source. For CAS dye, 30.25 mg chromeazurol S (Fluka) was dissolved in 25 mL sterile distilled H_2O, and 5 mL of 1 mM $FeCl_3$ x $6H_2O$ (in 10 mM HCl) added. I then dissolved 36.45 mg hexa-decyl-trimethyl-ammonium bromide (HDTMA, Fluka) in 20 ml sterile distilled H_2O, which was slowly added to the CAS-$FeCl_3$ mixture. The resulting dye was autoclaved, then added in a ratio of 1:10 to VMM agar made with salts lacking iron. Strains were inoculated from agar plugs, and grown for 7 days, to assay for color change from purple (unbound) to orange (bound by secreted siderophores) before images were taken.

Perithecial development assay

Plates containing 20 mL synthetic crossing media containing 3 mM sucrose, 5 mM oleate, or 5 mM butyrate, were inoculated with the recipient ("female") strains and

grown for 48 hours before fertilization with 2 x 10^6 conidia of the donor ("male") *mat A Δfar-1; Δfar-2* mutant (NMF640) in one drop in the center of the plate. Plates were sealed with parafilm and placed in the dark at room temperature for 14 days, after which the image was taken.

Nuclear isolation and FLAG precipitation for mass spectrometry

Strains containing 3xFLAG-epitope tagged FAR-1 or FAR-2 proteins were grown in flasks for 7-10 days, and then inoculated into 500 mL of VMM with 1.5% sucrose with 1.75*10^6 conidia/mL in a Fernbach flask. Conidia were grown overnight with shaking for 16 hours at 30° C, with shaking at 150 rpm. Tissue was harvested by vacuum filtration, followed by a wash of the mycelial mat with 250 mL 10 mM Tris-HCl pH 7.5 at room temperature. Pad was then snap frozen in liquid nitrogen and then a -80° C until nuclei prep. Pad was ground into a fine powder with mortar and pestle under liquid nitrogen, and then transferred into a 50 mL conical, and placed at -80° C until the liquid nitrogen evaporated. To this powder, 40 mL of ice cold buffer A (1 M Sorbitol, 7% Ficoll, type 400, 20% glycerol, 5 mM Mg acetate, 3 mM $CaCl_2$ 5 mM EDTA, 50 mM Tris-HCl pH 7.5 at 4°C with 0.5 mM DTT and protease inhibitors (E-64, pepstatin, leupeptin, and 0.1 M PMSF)) was added, and mixed to homogeneity with a sterile wooden stick. After transfer to a 250 mL Erlenmeyer flask on ice, 70 mL of ice-cold buffer B (10% glycerol, 5mM Mg acetate, 5mM EDTA, 25 mM Tris-HCl pH 7.5 at 4° C) containing DTT and protease inhibitors was added slowly. The resulting homogenate was filtered through cheesecloth to remove solids. The clarified cell extract was layered on top of 15 mL of a 1:1.7 mL buffer A:buffer B mixture in ice cold 40 mL oakridge tubes, 4 per sample. Tubes were centrifuged in a pre-chilled HB-4 swining rotor at 4,000 rpm (2,600 g) for 7 minutes. The top 20 mL of supernatant was collected from each tube, and transferred to a fresh 50 mL disposable conical containing 5 mL of ice cold buffer C (1 M sucrose, 10% glycerol, 25 mM Tris-HCl pH 7.5 at 4° C). Conicals were centrifuged at 6,200 rpm (7,500 g) for 16 minutes in an HS-4 rotor. A portion of the supernatant was kept as the

'cytosol' fraction, and the rest carefully decanted. The resulting pellets were resuspended in 500 uL of buffer D (10 mM HEPES-NaOH pH 7.5, 10 mM KCl, 1.5 mM $MgCl_2$) with protease inhibitors. Two tubes containing two resuspended pellets each were centrifuged in 2 mL tubes to pellet membrane debris, and the supernatant transferred to 1.7 mL microcentrifuge tubes for FLAG immunoprecipitation. A portion of this supernatant was kept as 'input'.

For each sample, 150 uL of ANTI-FLAG M2 affinity Gel (Sigma cat. No. A2220), 75 uL per 1.7 mL tube, was added to the sample and tumbled overnight at 4° C. The FLAG resin was pelleted by a spin at 1,000 g for 5 minutes and 4° C, and the cleared supernatant was discarded. Pellets were resuspended in 1 mL of wash buffer (250 mM NaCl, 50 mM HEPES-NaOH pH 7.5, 1mM Na-EDTA, 1 mM Na-EGTA). Resin was washed 6 times with wash buffer by resuspending the resin in 1 mL of wash buffer, tumbling for 5 minutes at 4° C, pelleting at 1,000g for 1 minute, and discarding supernatant. Bound proteins were eluted from the resin by tumbling with 300 mL of wash buffer containing 200 ug/mL 3XFLAG peptide for 5 minutes at 4° C, followed by pelleting at 1,000g for 5 minutes. Resin was eluted a second time for a total of 600 uL, of eluate split into two 1.7 mL tubes. Eluate was precipitated with 75 uL 100% TCA per 300 uL fraction by incubation for 1 hour on ice, followed by a 5 minute spin at 14,000 rpm at 4° C. Most of the was removed (250 uL), and the remaining pellet was washed 3 times with 200 uL ice-cold acetone, spun down each time at 14,000 rpm for 5 minutes at 4°C. Each pellet was dried for 10 minutes with the lid open on a 95° C heat block. Tubes were stored at -80 until evaluation by SDS-page and silver stain, western blot, or mass spectrometry analysis.

Table 2.1: *N. crassa* strains used for this study.
The table includes the lab-use NMF numbers from the Michael Freitag lab, strain numbers from the Fungal Genetics Stock Center, or experimental procedure used to generate them (XEB as a cross done by Erin Bredeweg, TEB as a transformation), and genotype.

strain	other name	genotype
NMF261	FGSC2489	74-OR23-1V A
NMF262	FGSC4200	74-ORs-6a
NMF263	FGSC9718	Δ*mus-51::bar*$^{+}$
NMF264	FGSC9719	Δ*mus-52::bar*$^{+}$
NMF637	XEB54.1	*far-1-GFP::hph*
NMF638	XEB104.1	*far-2-v5::hph*
NMF645	XEB53.4	*far-1-3xFL::hph*
NMF646	XEB105.1	*far-2-GFP::hph*
NMF639	XEB102.2	Δ*far-1::hph, Δfar-2::hph, mat a*
NMF640	XEB103.3	Δ*far-1::hph, Δfar-2::hph, mat A*
NMF644	FGSC11050	Δ*far-2::hph, mat A*
NMF643	FGSC11049	Δ*far-2::hph, mat a*
NMF642	FGSC11005	Δ*far-1::hph, mat A*
NMF641	FGSC11004	Δ*far-1::hph, mat a*
NMF658	TEB97.5	*far-2-3xFL:hph*
NMF659	TEB99.1	*hph*$^{+}$*::3xFL-N-far-1*
NMF660	TEB100.1	*hph*$^{+}$*::GFP-N-far-1*

Table 2.2: Oligonucleotides used for this study.
The table includes a list of primers including the lab-system OMF number, name and sequence.

primers	name	sequence
OMF83	10XGly-F	GGCGGAGGCGGCGGAGGCGGAGGCGGAGG
OMF84	loxP-R	CGAGCTCGGATCCATAACTTCGTATAGCA
OMF1597	08000_glyF	AACCAGCAACACCAGTACCAG
OMF1598	08000_glyR	CCTCCGCCTCCGCCTCCGCCGCCTCCGCCCAGCTGTCTCATCAGTTCCGG
OMF1599	08000_loxF	TGCTATACGAAGTTATGGATCCGAGCTCGTTGTATCGACCCCAGCCCATA
OMF1600	08000_loxR	TCTGTTCATGGGGCTCTACAA
OMF1816	hph_SM_F	AAAAAGCCTGAACTCACCGCGACG
OMF1817	hph_SM_R	TCGCCTCGCTCCAGTCAATGACC
OMF3337	JG_SM_HPH_F	GTGCTTTCAGCTTCGATGTAGG
OMF3338	JG_SM_HPH_R	AGAAGATGTTGGCGACCTCG
OMF2304	far2_glyF	TAGCTTGATTGCCCAGCAG
OMF2305	far2_glyR	CCTCCGCCTCCGCCTCCGCCGCCTCCGCCGCAAACAGCCGCGGGGACAACATT
OMF2306	far2_loxF	TGCTATACGAAGTTATGGATCCGAGCTCGGGGATTTTCCTTTTGTTCTTTCTT
OMF2307	far2_loxR	TGATGCAACTCCACCTCGT
OMF2308	far2_v5endR	CGTAGAATCGAGACCGAGGAGAGGGTTAGGGATAGGCTTACCGCAAACAGC CGCGGGGACAACATT
OMF2309	v5_hphF	GGTAAGCCTATCCCTAACCCTCTCCTCGGTCTCGATTCTACGTCGACAGAAGA TGATATTGAAGGAGC

Table 2.3: ChIP-Seq Samples

Samples used for ChIP-Sequencing of FAR-1 and FAR-2, listed by High Throughput Sequencing (HTS) number from laboratory records, including the number of mapped reads and percentage with respect to total reads. Samples used for IDR are indicated in the right-most column.

HTS#	Sample	reads	mapped reads	Bowtie % mapped	IDR
198	0m dark FAR-1	1,158,749	1,093,350	94.36%	N
199	60m light FAR-1	618,691	584,370	94.45%	N
272	DD dark NCU08000	6,019,402	5,508,629	91.51%	N
273	15m light NCU08000	8,002,584	7,184,130	89.77%	Y
274	60m light NCU08000	6,913,127	6,489,287	93.87%	Y
275	120m light NCU08000	7,967,373	7,362,882	92.41%	Y
438	sucrose FAR-1/gfp	10,911,303	8,822,810	80.86%	N
440	oleate FAR-1/gfp	14,347,475	10,770,462	75.07%	N
490	oleate FAR-2/V5	4,254,815	2,405,302	56.53%	na
491	butyrate FAR-2/V5	10,856,976	8,039,577	74.05%	Y
492	sucrose FAR-2/V5	13,390,581	10,619,514	79.31%	na
670	FAR-2/V5, VLM	17,844,180	12,503,466	70.07%	na
671	FAR-1/gfp, BUTR	23,653,262	14,137,682	59.77%	Y
672	FAR-1/gfp, OL	28,088,633	24,382,996	86.81%	Y
673	FAR-1/gfp, VLM	27,456,871	21,832,391	79.52%	Y
674	FAR-2/V5, BUTR	20,862,752	14,000,460	67.11%	Y
675	FAR-2/V5, OL	19,710,020	15,170,315	76.97%	na

Table 2.4: Generation of IDR "pseudoreplicate" samples and ChIP-seq samples selected for MACS2 significant peaks.

In order to choose the ChIP samples that best describe the average data output, IDR [165] uses a subsampling of pooled reads from all samples, represented in sections of 15% of the reads subsampled using a MACS2 [161] function (top panel). The number of peaks detected by MACS2 and IDR are shown for each of the pseudo-replicate comparisons at different significance thresholds (middle panel). Actual samples were then analyzed in the same way, and samples consistently showing similarity to the pseudo-replicates in peak number were selected. Four samples were analyzed (see Table 2.3). In bold are the two IDR comparisons encompassing the 4 samples passing the pseudo-replicate similarity threshold which were used to generate the significant peak list for ChIP enrichment of FAR-1 in sucrose.

far1-sucrose pooled	**reads mapped**	
pseudo1-15	6,413,396	
pseudo2-15	6,413,577	
pseudo3-15	6,413,613	
pseudo4-15	6,412,116	
comparisons-pseudo	**peaks at 0.01**	**peaks at 0.1**
1v2	1,171	1,940
1v3	1,218	1,853
1v4	1,231	1,929
2v3	1,174	1,908
2v4	1,198	1,857
3v4	1,207	1,937
comparisons-actual	**peaks at 0.01**	**peaks at 0.1**
HTS 198 vs. HTS 438	279	721
HTS 198 vs. HTS 273	569	1,097
HTS 198 vs. HTS 274	643	1,189
HTS 198 vs. HTS 275	582	1,113
HTS 198 vs. HTS 673	333	805
HTS 273 vs. HTS 274	1,022	1,652
HTS 273 vs. HTS 275	994	1,678
HTS 273 vs. HTS 438	484	998
HTS 273 vs. HTS 673	**572**	**1,239**
HTS 274 vs. HTS 275	**1,065**	**1,815**
HTS 274 vs. HTS 438	513	1,030
HTS 274 vs. HTS 673	559	1,161
HTS 275 vs. HTS 438	495	994
HTS 275 vs. HTS 673	585	1,215
HTS 438 vs. HTS 673	425	880

Table 2.5: Oligonucleotides used for *far-1* domain cloning and luciferase constructs
Primers for cloning the *far-1* domains contain restriction sites for putting into the plasmid pE-SUMO (lifesensors), which contains a 6xHis tag for purification and a portion of the Smt3 to enhance protein expression in a translational fusion. Primers for amplification of the luciferase constructs were designed to flanking regions of the csr-1 (cyclosporin resistance 1) NCU00726, common to the template DNAs containing promoters bound by FAR-1.

PrimerOMF	Primer name	Sequence
OMF2494	far1_sumoF1	GCTATTCTAGAATGTCTGCGACAACGCCAGC
OMF2555	far1_2sumoF1	CCCGGGATGTCTGCGACAACGCCAGC
OMF2495	far1_sumoF2	GCTATTCTAGAATGCTCACATCATGCCCGTT
OMF2556	far1_2sumoF3	CCCGGGATGTTGCTGCTGCAAGCCATGCTT
OMF2557	far1_2sumoF4	CCCGGGATGCCTGATGACTCGCCCTACCCA
OMF2554	far1_2sumoR1	GCTAGTTCGAATTAAGCCGGGAAGGTGTTGTTTGC
OMF2499	far1_sumoR2	GCTAGTTCGAATTAGTCGCTTGGGTTATCCG
OMF2500	far1_sumoR3	GCTAGTTCGAATTACAGCTGTCTCATCAGTTC
OMF2439	lucF_BamHI	GTAGAGGATCCATGGGCGGAGGCGGCGGAGGC
OMF2440	lucR_ecoRI	AGACTGAATTCTCAGAGCTTGGACTTGCC
OMF2441	HYR1proF-notI	GTAGAGCGGCCGCGGTTCCATTCCATCACGACAG
OMF2442	HYR1proRgly	GCCTCCGCCGCCTCCGCCCATGTTTTCCAGGTTTGAACG
OMF2443	al1proF-notI	GTAGAGCGGCCGCCAAATGCAGTTCGCAAGCGTAG
OMF2444	al1proRgly	GCCTCCGCCGCCTCCGCCCATTTTGTCTGTAAGTCTGGT
OMF2445	NCU8002proF-notI	GTAGAGCGGCCGCTCTTGGCTTTCTTTCCTGTTC
OMF2446	NCU8002proRgly	GCCTCCGCCGCCTCCGCCCATTACTCGATAACCACAGAC
OMF2459	lucF2_BamHI	GTAGAGGATCCATGCGAGGACGCCAAGAACATCAA
OMF2460	lucF	CGAGGACGCCAAGAACATCAA
OMF2925	csr_5f	GTAACGCCAGGGTTTTCCCAGTCACGACGCTGGAGAAGCTCATTCCAC
OMF2926	csr_3r	GCGGATAACAATTTCACACAGGAAACAGCCAACCGAGCACACCAACTAAC
OMF2927	csrOL_F_NotI	AGTCTGCGGCCGCTACGATTTAGGTGACTGCAGG
OMF2928	csrOL_F_XmaI	AGTCTCCCGGGTACGATTTAGGTGACTGCAGG
OMF2929	csrOL_R_XmaI	AGTCTCCCGGGCTATAGTGTCGGATCCTCTAG
OMF2930	csrOL_R_EcoRI	AGTCTGAATTCCTATAGTGTCGGATCCTCTAG
OMF2494	far1_sumoF1	GCTATTCTAGAATGTCTGCGACAACGCCAGC
OMF2555	far1_2sumoF1	CCCGGGATGTCTGCGACAACGCCAGC
OMF2495	far1_sumoF2	GCTATTCTAGAATGCTCACATCATGCCCGTT
OMF2556	far1_2sumoF3	CCCGGGATGTTGCTGCTGCAAGCCATGCTT

Table 2.6: Transformations for luciferase reporter assay
Neurospora strains and genotypes used to generate reporter constructs for FAR-1 transcriptional activity in conjunction with WC-2 binding sites. Linearized plasmids were targeted to the *his-3* locus by selection on minimal media.

TEB#	Parent Strain	Transforming DNA
TEB78	N2928 (Δ*mus-51*:*bar*+, *his-3*-, *mat A*)	pEB4:pMF272_luc
TEB79	N2928 (Δ*mus-51*:*bar*+, *his-3*-, *mat A*)	pEB9:NCU09534(HYR1)promLuc
TEB80	XEB101.8 (Δ*far-1*, *his-3*-)	pEB1:al-1promLuc
TEB81	XEB101.8 (Δ*far-1*, *his-3*-)	pEB2:NCU09535promLuc
TEB82	XEB101.8 (Δ*far-1*, *his-3*-)	pEB3:08002promLuc
TEB83	XEB101.8 (Δ*far-1*, *his-3*-)	pEB9:NCU09534(HYR1)promLuc
TEB87	N3011 (Δ*mus-51*:*bar*+, *his-3*-, *mat a*)	pBM60-00275promoter-luc
TEB88	N3011 (Δ*mus-51*:*bar*+, *his-3*-, *mat a*)	pBM60-00552promoter-luc
TEB89	N3011 (Δ*mus-51*:*bar*+, *his-3*-, *mat a*)	pBM60-07666promoter-luc
TEB90	N3011 (Δ*mus-51*:*bar*+, *his-3*-, *mat a*)	pBM60-08000promoter-luc
TEB91	XEB101.8 (Δ*far-1*, *his-3*-)	pBM60-00275promoter-luc
TEB92	XEB101.8 (Δ*far-1*, *his-3*-)	pBM60-00552promoter-luc
TEB93	XEB101.8 (Δ*far-1*, *his-3*-)	pBM60-07666promoter-luc

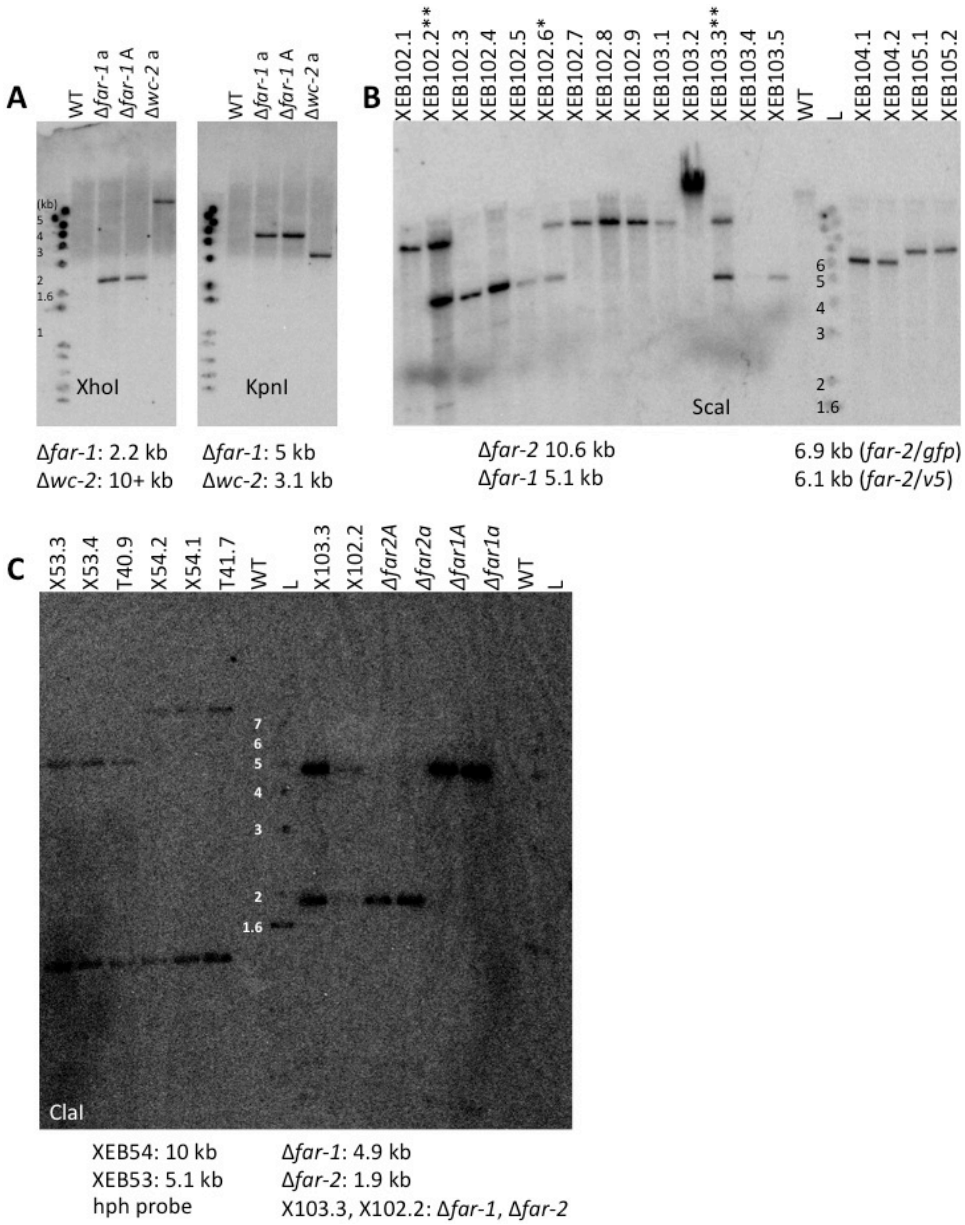

Figure 2.1: Southern blots to validate strains with tagged FAR proteins and far gene deletions

Southern blots confirming single incorporations of *hph* into the knockout strains of *far-1* and *wc-2* (A), and double knockout cross progeny of far-1 and far-2, XEB102 and XEB103, and tagged strains of FAR-2, XEB104: far-2-V5, XEB105: far-2-gfp (B). Progeny and parent strains for tagged strains of FAR-1 (C), XEB53: far-1-3xFLAG, XEB54: far-1-gfp, as well as a second confirmation of the double deletion strains XEB102.2 and XEB103.3. Sizes indicate homologous recombination was at the expected locus. Enzymes used as indicated. Blots were probed with part of the hygromycin resistance gene *hph* used for selection of recombination during transformation.

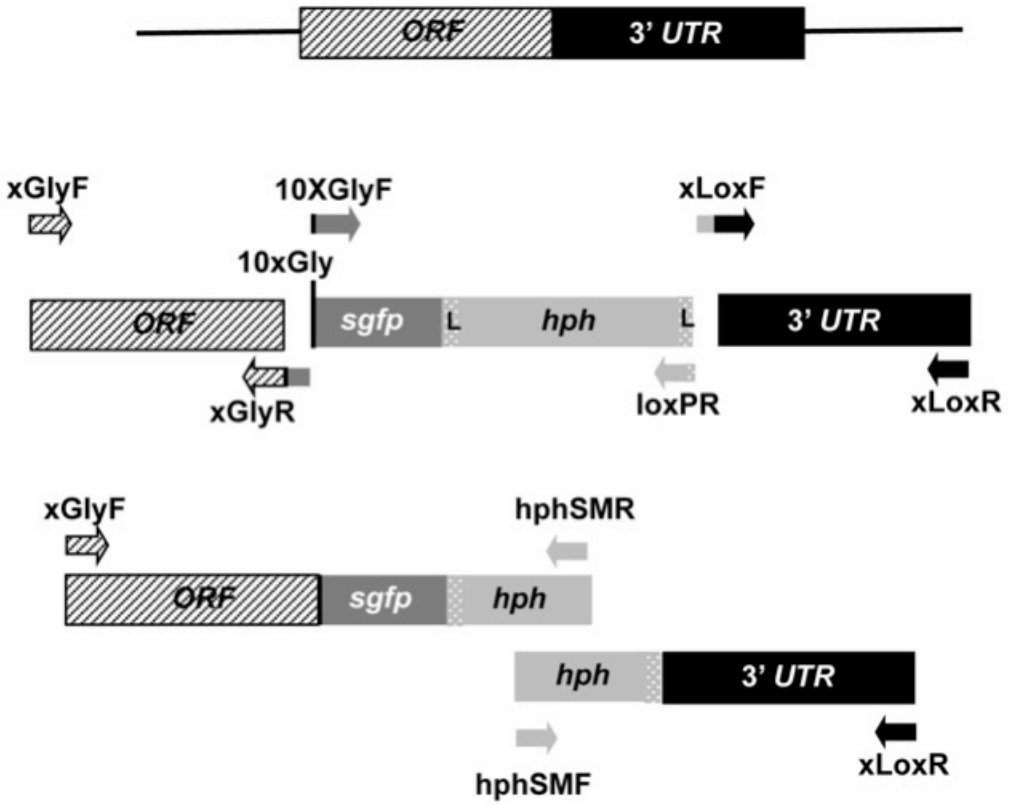

Figure 2.2: Split marker recombination of resistance genes for C-terminal tagging
DNA segments 1 kb upstream and downstream of the stop codon are amplified. Amplification primers contain extra sequence allowing secondary priming on a plasmid fragment during a second PCR reaction. The plasmid fragment contains a 10XGly linker, an epitope tag DNA sequence (such as GFP) and a promoter and resistance gene (hph). Resulting PCR fragments from the bottom panel are used for transformation.

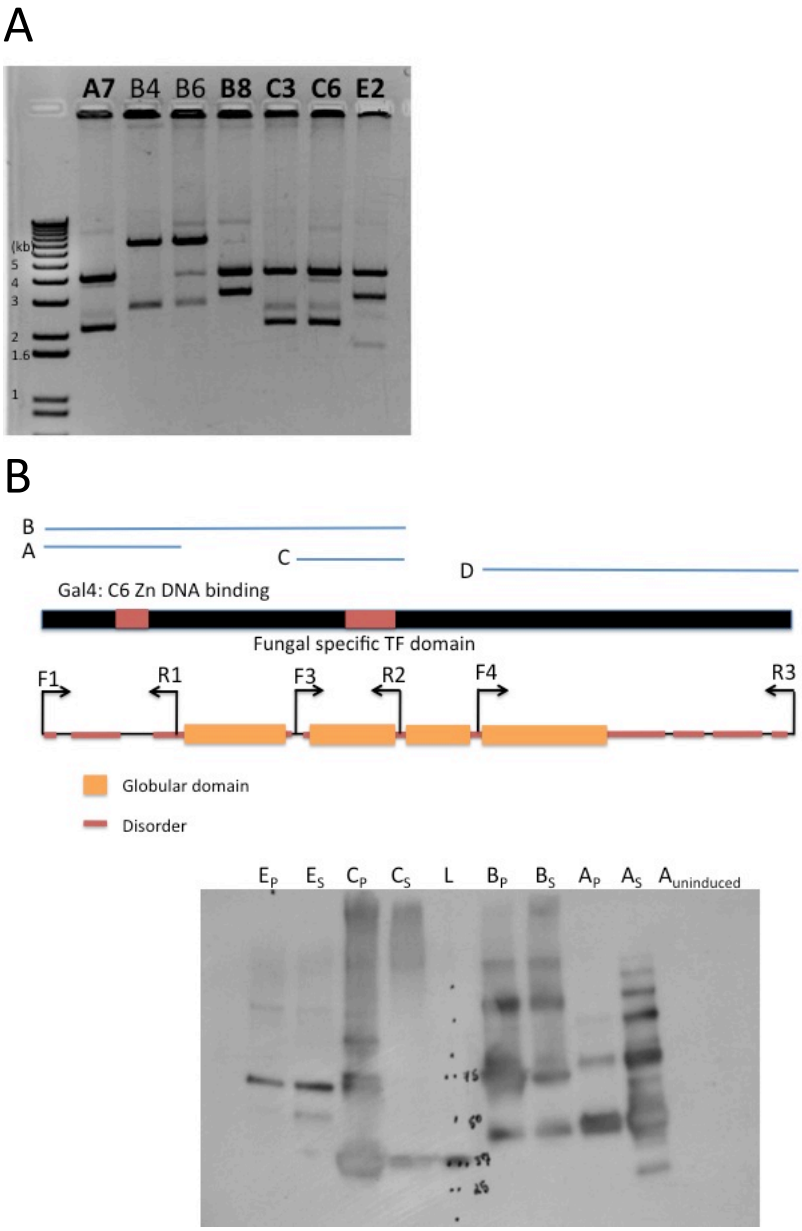

Figure 2.3: Cloning and expression of *far-1* domains.
(A) PstI digest of pE-SUMO constructs containing domains of FAR-1. Bolded plasmid numbers digested as expected. Expected band sizes: All should have the backbone piece at 4094 kb. Fragment sizes: A: 2185, B: 3121, C: 2104, E: 2953. (B) Model of cloned domains in FAR-1. Globular domains and disorder identified by ELM [110] and anti-6xHis western of induced extracts of FAR-1 recombinant protein domains. Expected sizes for these expressed proteins are: A 32.6 kDa, B 67.3 kDa, C 29.5 kDa, E 61.1 kDa. Laddering in A is expected to be from GAL4 domain dimerization behavior. Subscripts indicate different parts of the extraction: P: pellet, S: supernatant.

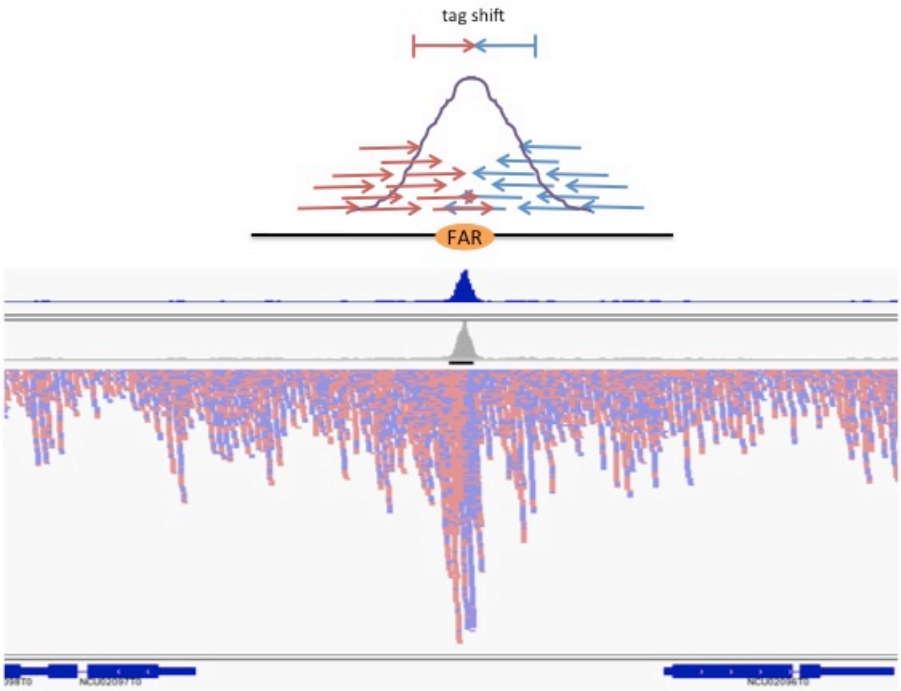

Figure 2.4: Binomial peaks are characteristic of sequence specific binding protein ChIP assays.
Binomial distribution of sequencing reads (51 nt from the Illumina Hi-Seq platform) is characteristic of DNA enriched by ChIP associated with a sequence-specific DNA-binding protein. MACS2 evaluates peak significance based upon sequencing read (referred to as 'tag') distribution to eliminate background noise from genomic sequencing or duplicated reads [164]. The tags are shifted to find overlapping peaks, i.e. binomial distributions, and assigned an enrichment value against local tag distribution. If the probability of finding a peak passes the significance threshold (based upon the mean and variance of the tags along the genome), the highest tag pileup is called as the 'summit'. Summit locations were used to place peaks relative to NCUs in the *N. crassa* genome by "IDR_annotate.pl" or "annotate_MACS2.pl".

A

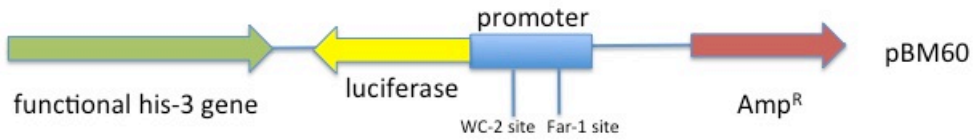

B

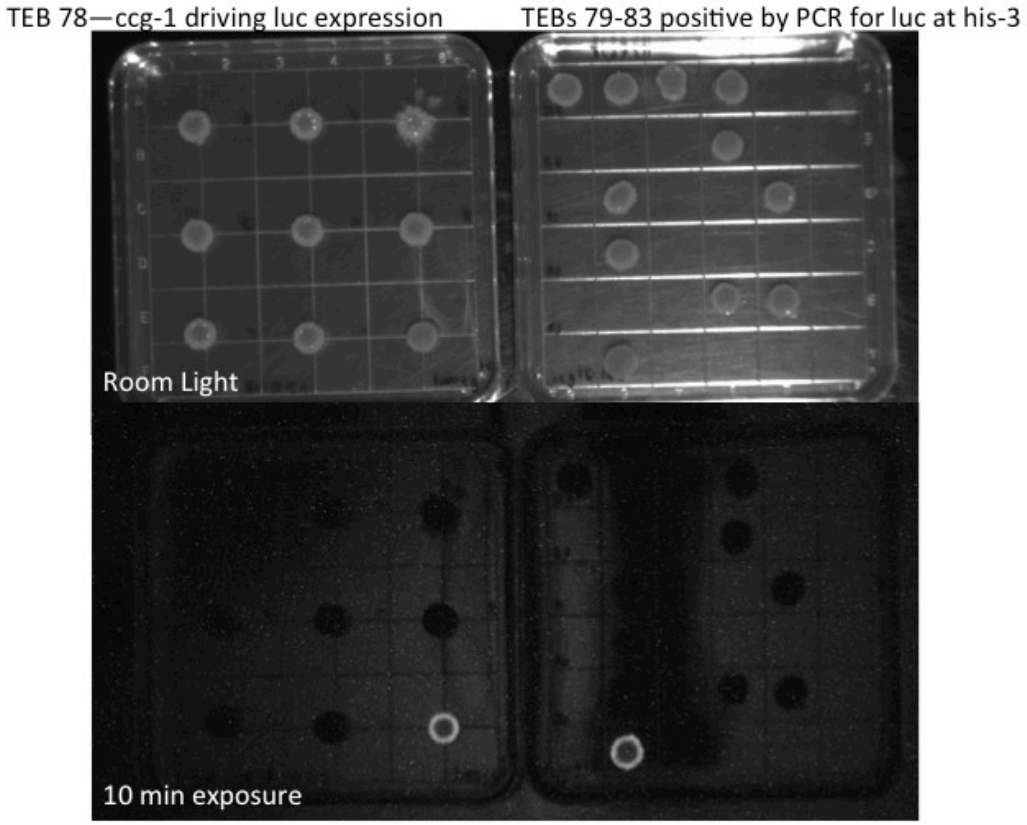

Figure 2.5: Luciferase activity of FAR-1 reporter construct transformants.
Promoter fragments were cloned into pBM60, which targets integration at the *his-3* locus. Plasmids were linearized and transformed into *N. crassa* strains containing either wild type *far-1* (N3011) or Δ*far-1* (XEB101.8). After confirmation by PCR of incorporation, transformants were spotted onto plates of FGS media, grown for 48 hours, and then imaged. Glowing spots after 10 minutes are the positive control, the codon optimized *luc* luciferase gene driven by the ccg-16 promoter (from the Bell-Pedersen lab of Texas A&M). See Table 2.6 for details of transformant strains. Left: TEB78:ccg-luc, Right, top to bottom in rows: TEB79:HCU09534(HYR1)promLuc, TEB80:al-1Luc, TEB81:NCU09535promLuc, TEB82:08002promLuc TEB83:NCU09534(HYR1)promLuc. Transformations and imaging were repeated in a strain wild type for far-1 with no signal detected.

A

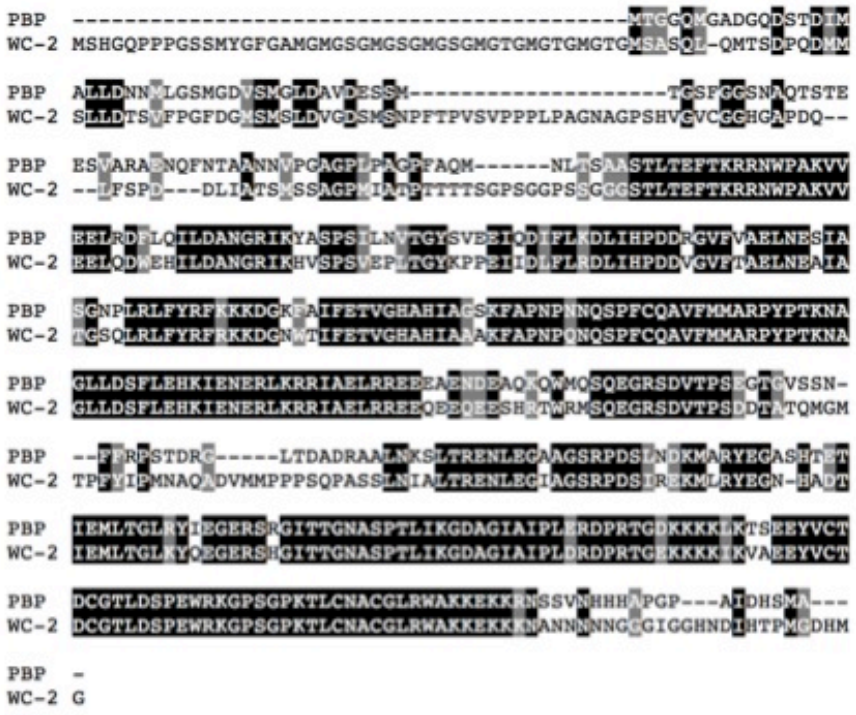

B

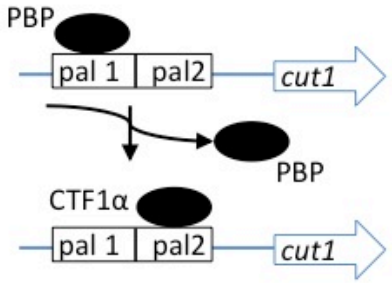

Figure 2.6: WC-2 of *N. crassa* is similar to the PBP of *N. haematococca*.
(A) The protein sequence of *Neurospora crassa* White Collar-2 (WC-2) aligned to the palindrome binding protein (PBP) of *Nectria haematococca*. Sequences aligned with Clustal Omega [173]. (B) Interaction model of the palindrome binding protein of *N. haematococca* competing for occupation at the promoter of the cutinase 1 gene for cutin-inducible expression (adapted from [108]). Palindrome pal1 contains the sequence 5'-GATCGC-3', which is very close to the consensus sequence for WC-2 binding 5'-GATCGA-3' [7]. The FAR-1 and FAR-2 consensus sequence 5'-CCGAGG-3' is found within pal2.

Chapter 3: Results: Transcriptional Networks Controlled by the Fatty Acid Regulators, FAR-1 and FAR-2

FAR protein structure

In comparison to other fungi, the FAR-1 and FAR-2 proteins have a similar structure, containing an N-terminal DNA binding domain of the GAL4 type, and a 'fungal specific transcription factor domain" in the middle of the amino acid sequence (Figure 3.1). The domains of the GAL4 type have a zinc binuclear cluster containing 6 cysteine residues [174] (Figure 3.1B). The DNA binding domain of FAR-1 spans amino acids 101-147 and the fungal specific transcription factor domain from 413 to 486 (sequence analysis by ELM [110]). An alignment of FAR-1 homologs reveals that some ascomycetes lack amino acid sequence similar to the *N. crassa* GAL4 domain (3.1B). FAR-2 has a DNA binding domain of the same type ranging from residues 67 to 113, and the fungal specific transcription factor domain from 401 to 474 (Figure 3.1A). The fungal specific transcription factor domain, also termed 'middle homology region' has a weakly conserved structure and is found in many transcription factors with the same DNA binding domain type [175].

FAR-1 and FAR-2 proteins bind DNA consensus sequence bound by homologs in other fungi

DNA motifs enriched for FAR-1 and FAR-2 binding sites were discovered using sequences corresponding to peak sites on Chromosome 1 (FAR-1: 111 peaks, FAR-2: 87 peaks) on several web-based submission sites: SCOPE[176], Weeder[177] and BioProspector[178]. Resulting position weight matricies of the most commonly found sequence were visualized using WebLogo3 [179]. The sequence 5'-CCTCGG-3' and its reverse complement 5'-CCGAGG-3' are equally represented in the logo 5'-CC T/G C/A GG-3' (Figure 3.2). This is identical to the DNA sequence bound by EMSA in *A. nidulans* [106]. Additionally, the ChIP dataset identifies how frequently other base identities are found within the consensus while being associated with ChIP enrichment, and provides

the context of surrounding base pairs for the consensus, genome-wide. For instance the 3rd position of 5'-CCTCGG-3' has been identified as a 'C' just over 10% of the times the motif is found in the peak regions surveyed for FAR-1, while FAR-2 shows a similar figure ranging between 7 and 13% at that position using BioProspector.

FAR-1 domain cloning

The initial goal in cloning these domains was to determine the necessity of different portions of the FAR-1 protein to binding the sequence specific consensus motif for FAR-1, shared by FAR-2. It was previously observed in other organisms by EMSA that FarA and CTF1α bind this consensus sequence [106], [108]. Adjustment of the induction temperature conditions resulted in expression of all 5 constructs, detected by coommassie stain and by western blot (Figure 2.3B). Despite success in cloning these regions into expression plasmids (Figure 2.3A), the combination of ChIP-sequencing data and previous binding data from *A. nidulans* suggested that the planned EMSA experiment would be redundant to what we know about the FARs. Additionally and importantly, *in vitro* biochemical studies remove the influence of additional potential ligands and modifications the protein may receive from an *in vivo* context. The ChIP-sequencing data for FAR-1 combined with RNA-sequencing data shows that many transcripts change expression level in a FAR-1 dependent manner, despite unaltered DNA association. This supports the hypothesis that FAR-1 transcriptional regulatory activity is controlled by post-translational modification. As these modifications would likely not be captured by an *in vitro* assay in bacteria, work on this experiment was not continued.

N-terminal tagging by homologous recombination to probe UTR regulation

Additional experiments were done to probe the possibility that the C-terminal tag interferes with binding or regulation of FAR-1 activity. An N-terminal construct was used to tag the protein in its endogenous locus, so that the selectable *hph* gene was

under the control of the endogenous FAR-1 promoter, while *far-1* expression was driven by *qa-2*, a quinic acid-inducible promoter [180]. After successful transformation, the marker and *qa-2* promoter can be removed by expression of Cre recombinase activity at flanking loxP sites [157]. A codon-optimized version of Cre recombinase was transformed into the *his-3* locus of the N-terminally tagged FAR-1 strains (NMF659, NMF660, Table 2.1), and tested for loss of hygromycin resistance by spotting on minimal and hyg^+ plates. Heterokaryon strains carrying the N-terminal FAR-1 and pS-Cre did not show *hph* loss. Additional mitoses accomplished by passing strains through a race tube also did not yield any loss of hygromycin resistance, even in the absence of selection. This suggests that *hph*-containing nuclei within the heterokaryon are maintained as well as hyg^- nuclei. Even though Cre has been previously described as a useful tool for Neurospora [157], my experience is similar to that of others in the Freitag laboratory (Phatale, Friedman and Freitag, unpublished data). Cre expression or activity appeared inadequate to remove the region of DNA flanked by loxP sites, which encompasses the *hph* gene, to place *far-1* back under control of the endogenous promoter. As non-native promoter expression levels of *far-1* may misrepresent FAR-1 binding activity, I chose to not take this line of investigation any further.

ChIP-sequencing identifies numerous binding sites of FAR-1 and FAR-2 in the *N. crassa* genome

The first ChIP-sequencing experiments with tagged FAR-1 protein tested for detection of altered enrichment of FAR-1 in the Neurospora genome at four different time points, i.e. 0, 15, 60, and 120 min of light induction. All tissues were grown on sucrose and showed no light-dependent changes in binding (Figure 3.3D). This was supported by lack of light responses measure by western blot (Figure 3.3B). Subsequent ChIP samples addressed the question of whether FAR-1 and FAR-2 bind DNA when Neurospora was grown on different carbon sources.

A summary of ChIP-seq data (Figure 3.4A) was analyzed in order to compare all samples. I determined which samples were the most consistent across sequencing platforms, quality and depth. The IDR method uses an R script to compare peaks called by MACS2 in a pairwise manner. 'Pseudoreplicates' were generated by subsampling from a pool containing all reads from the same condition, and the actual samples bearing the most resemblance to the subsampled files were chosen. I began the analysis by using multiple replicates of FAR-1 ChIP-seq all grown in sucrose. I saw close resemblance of four replicates to the subsampled 'pseudoreplicate' analysis. IDR analysis on these replicates revealed two sets of peaks (for a total of four samples, Table 2.3 and Table 2.4) by pairwise comparisons when using the most stringent significance within the program determined by *p* value. These sets were then combined to find common peaks. In this global survey of ChIP binding and transcript level change, I found that some peaks were associated with transcripts that were upregulated, some peaks were associated with transcripts that were downregulated, and some peaks were associated with transcripts that didn't change in the conditions tested. This multi-faceted behavior of the FARs suggests that there may be additional regulators contributing to transcript levels. Because our experimental approach of ChIP was not testing the activation or repression ability of individual binding sites, when the interval between two genes contained two or more peaks, they were reduced to a single representative peak in the annotation for subsequent comparison with RNA-seq data, resulting in 915 peaks for FAR-1 in sucrose (Figure 3.4A). Remaining conditions for FAR-1 were not analyzed by IDR due to either poor quality ChIP reads in one of two samples as in FAR-1-GFP strain grown in oleate, or containing a single replicate as for FAR-1-GFP in butyrate. Similarly, one of two samples of FAR-2-V5 ChIPs from strains grown in butyrate medium was of insufficient sequencing quality to be analyzed by IDR. Peaks called in poor quality samples were sorted by *p* value and validated by inspection with results from other replicates available.

In order to identify FAR-1 peaks that only occurred in one carbon source, i.e. peaks that occur in butyrate (Table S2) or oleate (Table S3) but not sucrose, I compared the peak lists between the different treatments, and extracted unique peaks by elimination of common elements (Figure 3.4) (Tables S1-S12 are available online: https://ir.library.oregonstate.edu/xmlui/handle/1957/44860). These loci were also validated by inspection for consistency in IGV, and checked for the presence of consensus binding motifs (Figure 3.2). FAR-1 butyrate- or oleate-specific peaks were eliminated if they overlapped with peaks found in the sucrose condition, even if the sucrose peak did not meet the very stringent requirements for a high IDR score and occurrence in all four sucrose replicates. Of the inspected peaks for FAR-1, only ~8% of all peaks (83 of 998 FAR-1 peaks total) were specific for butyrate, oleate or both (Figure 3.2). Extensive FAR-2 ChIP peaks were found only in butyrate conditions (Table S5). A small number of FAR-2 peaks were identified in the sucrose and oleate ChIPs showing a binomial pattern and presence of a consensus motif (Table S4 and Table S6). These peaks were validated by inspection, and all were found to coincide with peaks common between FAR-1 and FAR-2 on butyrate (Figure 3.4, Table S4 and S6). Genes near these peaks were analyzed RNA sequencing, and those found to be differentially expressed between two conditions were totaled to reflect direct FAR effects (Figure 3.4A, lower table). Some FAR-2 peaks co-occurred with peaks found only in FAR-1 butyrate or FAR-1 oleate samples and not FAR-1 sucrose (37 of 997 FAR-2 peaks, from 20 of 52 FAR-1 butyrate and 23 of 44 FAR-1 oleate). FAR-2 also showed unique binding sites not identified in FAR-1 ChIPs (525, from 997 total FAR-2 peaks, removing overlaps with FAR-1). About half the FAR-1 and FAR-2 binding sites (47%, 435 of 997) determined by ChIP were shared between the two proteins under the growth conditions investigated here.

Functional Category analysis of ChIP targets reveals new functions for FAR-1 and FAR-2

ChIP-seq analyses resulted in a list of enriched predicted protein functions sorted by category in the Functional Catalog (FunCat) database [166]. Genes near peaks

ordered by rank (here the top 1000 unique genes) were compared to genome-wide established functions to look for enriched gene ontologies (GO). As one would predict based on previous studies [104]–[106], among the highest scoring categories for FAR-1 were “fatty acid degradation” and “processing of carbon chains of various lengths”. Also enriched were “peroxisomal proteins”, and “proteins binding cofactors” such as heme (Table S7). Prominent categories for FAR-2 included “cation and heavy metal transport”, and “peroxisomal transport”, though peroxisomal proteins themselves were less enriched than for FAR-1 targets. Additionally, FAR-2 ChIP peaks occur near a number of genes involved in sexual and asexual development (Table S8). To determine whether any of these categories were linked to phenotypes, I tested wildtype and *far* mutant strains for visible characteristics related to enriched functions of oxidative stress reactivity, siderophore secretion and perithecium formation (see Phenotypes section). Many of the regulatory functions of the FARs I found were previously unknown.

The functional category grouping analysis was done again using genes filtered by a transcriptional change requirement under our experimental conditions (Table S9, Table S10). It is interesting to note that transcriptional control is an enriched function among FAR-1 targets. Indeed, FAR-1 and FAR-2 bind the regulatory sequences of a variety of other transcription factor genes, some of which were also bound by WC-2 (Figure 3.5A).

In order to capture the relative importance of these functional categories among all ChIP targets, I parsed the database files from the FunCat (Table S7, Table S8) and ran an analysis using Map Enrichment [168] through Cytoscape [167]. The result was a comprehensive visual representation of the overlapping functional categories shared between FAR-1 and FAR-2 binding targets (Figures 3.6 through 3.10). Large nodes include the category “chromosome interacting”, which is reflective of transcription factors, chromatin modification proteins and other DNA-binding proteins. Other nodes are (1) mitochondrial inner membrane space proteins, which include TCA cycle enzymes and TCA intermediate transporters, (2) co-factor binding proteins, including a large

number reliant upon heme and its associated iron to catalyze redox reactions, (3) heavy metal transport-associated proteins, (4) transport activities, and (5) protein and amino acid degradation. Among the genes for "Lipid, Fatty Acid, and Isoprenoid metabolism" are several lipase genes expressed at 2- to 50-times wild type levels in the double mutant (Figure 3.7B). This expression pattern is suggestive of a few scenarios: 1) FAR proteins are acting as repressors or 2) an additional transcriptional regulator is working to express these lipases in the absence of the FARs. Unique or uncharacterized regulators in *N. crassa* such as the aspergillus-specific *scfA* may be discovered in a screen for perturbation of lipase expression levels with these data established.

The generalized DAVID gene ontology database [181] was used to analyze the same dataset, which identified functions that were known or suspected (Figure 3.11). Using the FunCat-parsed data for simultaneous analysis of ChIP datasets for both FAR-1 and FAR-2 identified functional similarities and differences that may not have been obvious when the sets were analyzed separately by generalized GO analyses. Novel predicted functional categories identified here drove hypothesis formation and testing for the functionally partially redundant FARs. The majority of the genes I found in my analyses were related in function to already known targets, but they were not previously known to be regulated by FAR-1 and/or FAR-2. My results reflect a dynamic system responsive to different carbon sources and balancing transcript levels uniquely viewed by altering a set of transcriptional regulators rather than functional metabolic enzymes.

Luciferase reporter constructs yielded no signal by multiple assays

The goal of this experiment was to show whether the absence of a functional FAR-1 protein would directly affect a promoter region driving a reporter construct. Several promoter regions containing FAR-1 and WC-2 binding sites were cloned into *his-3* targeting plasmids, and transformed into *his-3*$^-$ strains containing a wild type *far-1* or a *far-1* deletion. The expectation was that a lack of functional FAR-1 would result in loss

of expression. Strains containing reporter constructs (Table 2.6) were assayed for luciferase activity in protein extract, conidial suspensions, and in vitro by a 10-minute exposure to a gel-imaging camera. All yielded little to no luciferase activity by the methods used for measurement, excepting the positive control, seen as a glowing spot growing on the plates next to the luc-contruct transformants (Figure 2.3B). Some potential issues with this work were low expression levels of some of the genes despite strong FAR-1 peaks for NCU00275 and NCU07666 and NCU00552. Though *HYR1* NCU09534 was expressed at potentially detectable levels by RNA-sequencing data, it is possible that mis-annotation of the transcriptional start site in both versions 10 and 12 of the *N. crassa* genome may have changed luciferase expression. The 5' UTR region annotated in both versions is longer than the transcriptional start site detected by RNA sequencing. A lack of the promoter region immediately 5' of the *HYR1* gene suggests that the luciferase construct may not have had sufficient sequence elements for general TF assembly and expression. Additionally, it was decided that genome-wide RNA-sequencing of *far* mutant strains would provide a comprehensive survey of expression levels. Global RNA-sequencing also was useful to capture elements of TF interaction in FAR-1 and FAR-2 binding overlap as well as FAR-dependent transcriptional effects that do not occur as as result of ChIP-detected binding. Due to luciferase expression and detection problems, and inclusion of global RNA-sequencing data, work on this experimental approach was not continued.

Summary of transcriptional changes in *far* mutants

The aim of these experiments was to determine which genes with binding sites determined by ChIP were also affected in transcription under the conditions tested, and were thus direct targets of FAR-1 or FAR-2. By ChIP, I found FAR-1 consistently enriched at potentially 95% of the same genomic sites across all carbon conditions tested, suggesting that alteration in transcriptional activity of target genes may be controlled by other means than presence or absence of FAR-1 DNA binding, e.g. posttranslational

modification of FAR-1 or assembly of an active complex by co-factor binding. Similarly, we see lower protein expression levels of FAR-2 in conditions other than butyrate, by western blot, and less binding, by ChIP signal (Figure 3.3A, Figure 3.4B, Figure 3.12B). Is FAR-2 regulatory activity confined to only butyrate, as suggested by the ChIP signal? To answer these questions, I performed RNA-sequencing on three replicate samples each of the wild type, Δ*far-1*, Δ*far-2*, and Δ*far-1;* Δ*far-2* strains grown overnight in sucrose, and then transferred to sucrose (1.5%), 5 mM oleate, or 5 mM butyrate. Selected target genes had previously been assayed by northern blot in other organisms, but the RNA-seq experiments are the first comprehensive genome-wide survey of the effects of FAR-1 and FAR-2 on transcript levels in any organism.

I calculated the total number of genes that were differentially expressed on various carbon sources relative to wild type in each mutant (Figure 3.13). These data highlight mis-regulation of many transcripts in oleate in absence of the FARs. Similarly, FAR-2 is important for growth on butyrate, supported by phenotypic assays I report below. Though not as many genes are differentially expressed as in oleate, butyrate does perturb expression in the Δ*far-1;* Δ*far-2* mutant compared to wild type. All deletion strains grown on butyrate showed the most similarity in their transcriptional profiles when compared to other carbon sources (282 of the same genes are differentially expressed in butyrate between wild type and all *far* mutant strains). Self-regulation and compensation by the FARs is suggested by the transcript levels of the TFs themselves in the single mutants, i.e. FAR-2 expression is above wild type levels in the Δ*far-1* strain and vice versa (Figure 3.12B). As a result of FAR expression compensation, any conclusions we draw about carbon-specific behavior for either FAR-1 or FAR-2 based on this data set will require further testing.

ChIP enrichment paired with RNA-sequencing data informs us about regulation at bidirectional promoters, and TF activity, whether activation or repression, at each promoter. Heatmaps are used to summarize transcript level changes in genes near binding sites identified for both FAR-1 and FAR-2 (Figure 3.13B). Warm to cool colors

represent changes in transcript levels (as log_2-fold change of FPKM) between a strain grown in sucrose and the same strain grown in butyrate or oleate (Figure 3.13B, right) showing that wild type and Δ*far-2* look similar on oleate (columns 5 and 7), as do Δ*far-1* and Δ*far-1*; Δ*far-2* (columns 6 and 8). A similar pattern can be seen for butyrate (columns 1 to 4). As demonstrated by both increasing and decreasing levels of expression of these genes relative to wild type (Figure 3.13B, right), FARs confer both transcriptional activation and repression. In order to more clearly define transcriptional changes and thus metabolic consequences mediated by the FARs, I analyzed all RNA-seq data available, in all strains and conditions I tested.

Influences of FARs on the *Neurospora crassa* transcription factor network

One goal of my analyses was to contribute to the growing TF network description available for *N. crassa.* Cuffdiff analysis for differential expression was used to compare the same strain in varying carbon sources, and to compare each carbon source between strains (Table S11). Complete data for all genes, all conditions, and all replicates is found in Table S12. For these analyses, RNA-seq data are presented as an overlay for ChIP localization targets to explore targets likely to be directly regulated. The FARs can act as repressors or activators, likely in combination with other regulators or TFs. In order to describe the network of transcription factor regulation, I generated a network identifying the ChIP binding and qRT-PCR data effects of WC-2, based on our previous study [7], and ChIP- and RNA-sequencing of FAR-1, and FAR-2 (Figure 3.5A). Within the overlap of ChIP and RNA data, we found a number of transcription factors that are themselves regulated by the FARs. Some TF genes display derepressed expression patterns (*aod-2*, *fl* in butyrate, *clr-1* in oleate, *PacC* in oleate) or patterns indicating a loss of activation (*msn-1* in oleate, *adv-1* in oleate) as a result of the *far* mutant background (Figure 3.5B). Some of the expression may be mediated by only one FAR rather than both, such as with *msn-1* in butyrate, which is less transcribed in the absence of FAR-1, and *csp-1* which shows a similar pattern. Both *msn-1* and *csp-1*

promoters contain a FAR consensus sequence and show binomial FAR-1 enrichment, but not FAR-2 enrichment. The *aod-2* promoter is doubly bound by FAR-1 and FAR-2, and shows an increase in expression in butyrate in either *far* mutant; AOD-2 is a TF controlling expression of an alternative oxidase bypassing part of the electron transport chain in the mitochondria [5]. A mutant *fluffy, 'fl'* gene, also called *acon* for 'aconidiate', results in a strain that does not produce conidia, suggesting that this transcription factor may contribute to altered levels of conidiation in the Δ*far-1* and Δ*far-2* mutants (Figure 3.14, Figure 3.12D). A number of additional TFs that have changed expression in the *far* mutants have been investigated for their function in aiding breakdown of biomass for biofuels such as CLR-1, CLR-2, and VIB-1 [70], [182] (Figure 3.5B).

Ergosterol biosynthesis pathway

Another example of a pathway affected by carbon source changes and the presence of the FARs is ergosterol biosynthesis (Figure 3.15). This pathway contributes to membrane fluidity, and its disruption may partially contribute to the slow growth phenotype on Tween-20 medium. Though it was previously known that other transcription factors affect the regulation of the *erg* genes, such as CSP-1 (conidial separation-1) [6], it was not known which or if additional regulators may influence the expression of these genes. Enzymes within the ergosterol pathway of *N. crassa* are intimately linked to carbon source availability, as are many other biological molecules that are built from acetyl-CoA precursors. Genes in this pathway (NCU03633, *erg-7, erg-9, erg-1, erg-10*) show loss of expression in butyrate as a result of *far* deletion, in both the single and double mutants (Figure 3.15). Also of note is that expression of these genes is much higher when *N. crassa* is grown in sucrose. As these genes are also targets of FAR-1 and/or FAR-2 by ChIP (noted to the left of each bar graph, Figure 3.15), I conclude that CSP-1 is not the only regulator of ergosterol biosynthesis.

Loci regulated by both FAR-1 and FAR-2

Analysis of the Δ*far-1;* Δ*far-2* double mutant reveals targets that are regulated by both factors but which would not be revealed by RNA-sequencing in either single *far* mutant. To this end, expression data for ChIP targets found for both FAR-1 and FAR-2 (Tables S1 to S4) were analyzed for redundantly regulated genes. Redundancy was defined as the subset of genes whose transcript levels change in the Δ*far-1;* Δ*far-2* mutant but not in either of the single mutants (Figure 3.16). Several of these nuclear genes encode proteins found in the mitochondrion or peroxisome/glyoxysome. Glycosyl transferases and hydrolases (denoted as *gt* and *gh*) function by juggling polysaccharide sugars for energy storage and cell wall structure. The prominence of these sugar-manipulating enzymes highlights how controlling catabolism and anabolism of both sugars and lipids underlies all relationships between FAR-controlled genes. Genes involved in cytokinesis (*Myo2, ro-4*), nucleotide manipulation (*dnr-3, dnr-8, dnp-1*, adk-1, DNA replication helicase *Cdc47*) show a possible link to the cell cycle. A total of eleven genes involved in secondary metabolism were also a notable functional grouping (gt1-1 00130, chi-1 01902, cyp45-25 09419, cys-9 08352, 03295, 01704, 08199 6-hydroxy-D-nicodine oxidase, oxidoreductase 03693, 04817, 08167 iucB, 08291 ferrocheletase). NCU08291 along with NCU04817 both function in biosynthesis of porphyrins, also associated with heme, a function recalled by the ChIP GO analysis (Tables S7 to S10) and phenotype of siderophore production (Figure 3.27). The majority of redundant misregulation seems to have occurred when the double mutant was grown in oleate.

What we learn from RNA-seq is that there is a wide variety of TF action by the FARs, ranging from carbon-specific regulation by FAR-1 (Figure 3.4), to transcript levels affected individually by the presence of FAR-2 or the presence of FAR-1 (Figure 3.5, *fl*).

FAR-1 mediates changes in expression of genes for peroxisomal proteins, glyoxylate cycle enzymes, and other proteins involved in fatty acid metabolism

Peroxisomal proteins

Neurospora crassa has many of the peroxisomal proteins found by mutagenesis and morphological analysis of peroxisomes in yeast, collectively designated PEX proteins [139]. The majority of them function in establishing peroxisome structure, and populating it with proteins, by import of prefolded peptides that contain peroxisome targeting signals [183]. As mentioned in the introductory chapter, *N. crassa* microbodies—small spherical organelles encompassing peroxisomes, glycosomes, glyoxosomes and Woronin bodies—are known as glyoxysomes [141]. A 'glyoxysome' contains enzymes of the glyoxylate bypass, and may also describe peroxisomes. However the identification of an organelle as a 'peroxisome' is dependent upon the presence of a catalase enzyme, which detoxifies reactive oxygen species [184] Examples of PEX proteins include the peroxisome/glyoxysome biogenesis proteins PEX-3, PEX-11, and PEX-19. PEX-5, PEX-7 and PEX-20 receptor proteins contain domains that recognize two types of amino acid peroxisome targeting sequences, PTS1 and PTS2 [185]. Peroxisome-bound proteins plus receptor pass through a possible pore, made up of PEX-13, PEX-14, and PEX-33, which imports the complex into the lumen of the glyoxysome [183]. A homolog of Pex17, which is normally paired with Pex13 and Pex14 in yeast is not found [140]. Once inside the microbody, it is thought that PEX-8 directs empty PTS1 and PTS2 receptors to be mono-ubiquitinated by the UBC complex (PEX-2, -10, -12, and -4). Once modified, the receptor is passed back to the cytosol by the ATPase complex, PEX-6 and PEX-1, anchored by PEX-26, after which the ubiquitin is removed for another round of import [140] (Figure 3.17).

Peroxisomal proteins are a prominent feature of the functional category enrichment particularly for FAR-1 (Table S7). Given glyoxysomal importance to tasks so immediate to fatty acid metabolism, I chose to summarize the expression of the PEX proteins (Figure 3.17, heatmaps shown are detailed in Table 3.1). FAR-1 ChIP peaks are

found for nearly the entire list of peroxins in *N. crassa* (Table 1.2). The two exceptions include a putative homolog of *Pex1* or *Pex6*, NCU05160, which resembles the sequence of an ATPase gene involved in recycling receptors for peroxisome localization back to the cytosol. Additionally, the *pex-24* gene lacks a FAR-1 ChIP peak. A homolog of *pex-24* has only been found in a few yeast species; in *Yarrowia lipolytica* its function seems to be related to controlling the rate of peroxisomal fission [139], [185]. A ChIP peak for *pex-10* was not annotated within the cutoff for this analysis, but validation by inspection shows a binomial peak for the FAR-1 grown on butyrate, and a consensus binding sequence near the 5' end of the gene. Under the conditions we tested for transcriptional change, several of the *pex* transcripts did not change significantly relative to wild type, even though there were FAR binding sites present. These included the peroxisome biogenesis regulators *pex-3* and *pex-19,* RING-complex subunits *pex-10* and *pex-12,* PTS1 receptor *pex-5*, and peroxisomal membrane protein (PMP), *pex-24* (Table 3.1).

I used change in transcript levels (expressed as the $\log_2$-fold change in FPKM) between wild type and each of the *far* mutants to survey *pex* expression (Figure 3.17). The right-most panel (delineated by vertical black bars) of many of the gene-specific heatmaps shows a loss of transcript level in the *far-1* and double mutant. This suggests that FAR-1 is important for normal transcript levels of *pex* genes, particularly when grown on oleate as a sole carbon source. Table 3.1 also shows details of the Cuffdiff analysis, and whether the transcript was differentially expressed between these strains. Consistently, the largest, most significant ChIP peak found for FAR-1 under all conditions was one upstream of *pex-1* (Table S1). Though *pex-1* was also identified in the FAR-2 ChIP, it showed less enrichment than FAR-1, closer to 'middle of the pack'. Analysis of *pex* transcript levels also served to confirm that ChIP enrichment, indicative of strong binding, does not equal transcriptional regulator activity. This is suggestive of FAR-1 regulation by other mechanisms, e.g. post-translational modification or cofactor binding.

The transcript for *hex-1*, involved in plugging septal pores, showed more loss of expression in a double Δ*far-1*; Δ*far-2* mutant in oleate than in sucrose. In peroxisomal biogenesis, both *pex-3* and *pex-11* decrease in transcript levels without FAR-1 (Figure 3.17, Table 3.1). Of the PTS receptor genes, the *pex-20* transcript was the most affected in *far* mutants in oleate. The translocator complex gene *pex-14*, and *pex-33*, but not *pex-13* were expressed at significantly lower levels than wild type in the double knockout in oleate (Table 3.1). With FAR-mediated effects on the PEX import machinery established I now turn to consequences of FAR function for beta-oxidation, and the TCA and glyoxylate cycles, as sufficient levels of the *PEX* proteins are required to localize substrates, and enzymes to the glyoxysomal lumen.

Peroxisomal and mitochondrial transport proteins

The ABC half transporters NCU01751 and NCU08382, protein channels of entry for fatty acids, are expressed in similar patterns, however, only NCU08382 shows significant differential expression in *far* mutants when grown in oleate (Figure 3.19, Table 3.3). The homolog of pmp47, mic-14 (NCU03556) is similarly perturbed in *far* mutants grown in oleate relative to wild type. Entry of enzyme substrates into and out of compartments is a point of control addressed by FAR regulation.

Both mitochondrial transporters and acetyl-carnitine transferases found in the peroxisome change significantly in their expression in *far* mutants (Figure 3.18, Table 3.2; e.g. *mic-31* NCU08561, *mic-22* NCU07263, NCU01611, NCU08002). For all of these transporters, I found up-regulation relative to wild type for Δ*far-1* in butyrate. This butyrate-dependent up-regulation is likely dependent upon FAR-2 activity, as this effect is dramatically lost in the Δ*far-2* and Δ*far-1;* Δ*far-2* strains. On oleate, the effect is reversed with transcripts showing much lower expression levels relative to wild type in a Δ*far-1* strain, with full or partial recovery of expression levels in the Δ*far-2* and Δ*far-1;* Δ*far-2* strains. Interestingly, the double mutant did not show as much change on oleate,

suggesting that transcript levels were recovered by the action of some other regulator, or that the FARs may in some cases act with opposite effects.

Lipid modifying enzymes

In addition to transporters, proteins that interact with carbon metabolism intermediates are potential regulatory targets to carbon regulators. Sterol carriers (NCU06643 and NCU03372) and proteins which act by adding and removing CoA groups by forming and breaking thioester bonds like NCU00580, and ACU-8 (Figure 3.17), all co-enzyme interacting proteins, seem to be FAR-1-dependent, particularly in oleate, while ACU-8, named for its involvement in acetate metabolism [186], is more induced by FAR-2. Just like enzymes handling carbon intermediates and coenzyme A, I expected enzymes involved in fatty acid synthesis to be tightly regulated by the FARs. Both *cel-1* and *cel-2*, named 'chain elongation', displayed very similar expression patterns. The CEL-1 protein has been experimentally localized to the glyoxysomal lumen [141], while *cel-2* has a FAR-2 ChIP peak on its 3' end. The formation of double bonds along a phospholipid hydrocarbon chain contributes to membrane fluidity, as mentioned in the presentation of the race tube experiments. Double bond formation can be done by desaturases, which showed FAR-dependent expression. NCU02408, NCU09497, *ods* (NC02209), and NCU05259 all have reduced transcript levels when grown on butyrate, and particularly in strains without FAR-2. Analysis of membrane lipid saturation in *far* mutant strains, and using different carbon sources should be used in future experiments to unravel transcriptional control from other signals dictating desaturase activity.

General observations of beta oxidation and glyoxylate bypass enzymes

Expression of the multiple copies of central metabolism genes (e.g. citrate synthases *tca-1* and *tca-2*, Figure 3.18) can be tentatively divided into patterns for the glyoxysome and mitochondrion based on evidence obtained through microbody and organelle localization studies [141], [187]. This can clearly be seen in the *acs* (acetyl-CoA

synthetase) genes, whose gene products have been localized to different cellular compartments [133] (Figure 3.19). ACS-1 (NCU01654) localizes to the glyoxysome, as does ACS-5 (NCU06063), which is thought to function in siderophore biosynthesis (Figure 3.19). ACS-7 (NCU08935) also localizes to the glyoxysome, and has also been found in proteomics studies [141] but its function is unknown. Additionally, it shows minimal regulatory changes in the absence of the FARs, suggesting FAR-independent regulation (Figure 3.19). Acetyl-CoA dehydrogenases (ACD-1 NCU02287, ACD-2 NCU08924, ACD-3 NCU01181), the FOX-2 multifunctional enzyme and 3-ketoacyl-CoA enzymes (NCU04796, NCU09646, Figure 3.19) round out the necessary enzymes for beta-oxidation in the glyoxysome. For the majority of these genes, the Δ*far-1* mutant grown in oleate displays a drop in expression. In contrast, mitochondrial proteins that perform the same functions in beta-oxidation are expressed closer to wild type levels in the conditions tested. This trend suggests that enzymes of beta-oxidation that were found more frequently in the glyoxysome are also more drastically affected by a lack of the FARs [141].

Cataloging the expression patterns of beta-oxidation, TCA cycle and glyoxylate bypass enzymes by affecting transcriptional control rather than making mutants gave insight as to how the enzymes are interdependent. Specifically, we observed the effects of carbon source and FAR mutants on the transcripts of the enzymes of beta-oxidation and the glyoxylate cycle, and how they vary by organelle (Figure 3.18, Figure 3.19). In general, we saw a similar expression pattern for many of the TCA cycle enzymes, featuring an up-down-down butyrate pattern for Δ*far-1,* Δ*far-2,* and Δ*far-1;* Δ*far-2* respectively. This was true of the citrate synthase genes (*tca-1* and *tca-2*), 2-methylaconitate (NCU00680) of the 2-methylcitrate cycle, malate dehydrogenase subunits *tca-15* and *tca-16,* and the glyoxylate bypass genes *acu-3*, and *acu-9* (Figure 3.18). Other TCA cycle transcripts echoed this pattern but with lower amplitude.

Detoxification proteins

Though catalase was not localized in the glyoxysomes of *Neurospora*, glyoxysomes harbor other detoxification enzymes such as NPD-1 and NPD-2, which act on alkyl nitronates [141], [188] (Figure 3.17). Several other antioxidant proteins were FAR-regulated, such as peroxiredoxins (Figure 3.17), and proteins that produce, recharge, or utilize the tripeptide glutathione for its ability to reduce unstable lipid and oxygen species. *HYR1* NCU09534, a glutathione peroxidase, and *rhd* NCU06031, a peroxiredoxin, are two examples of genes that encode proteins with antioxidant function. RHD localizes to the glyoxysomal lumen where the protein can directly reduce hydrogen peroxide to water [141]. HYR1 may be elsewhere in the cell, and is responsible for reducing ROS via glutathione. The expression pattern of *rhd* echoed that of other glyoxysomal detoxification enzymes, with a promoter bound by FAR-2 (Table 3.1). The *HYR1* promoter was bound by both FAR-1 in all carbon sources, and FAR-2 in butyrate, which supported its variable, FAR-dependent regulation.

Visualization of FAR targets by clustering

Another approach to understanding control of gene expression is by cataloging patterns which may correspond to different gene clusters found by k-means clustering [189]. There are representatives of transporter genes, pex genes, and detoxification genes that are affected by the FARs as mentioned in the prior sections, but the functional categories do not describe the specific conditions or consequences of FAR loss. I have categorized the 680 genes depicted in the summary of the RNA sequencing data (Figure 3.14) into 5 different classes that describe different average expression patterns. These patterns provide insight into the needs of the fungus with respect to these genes.

Cluster A includes genes dependent on the FARs for normal expression in butyrate

Expression levels in butyrate as mediated by the FARs suggest these transcripts are important for handling short fatty acids or adjusting metabolism accordingly (Figure 3.21). Cluster A features invertase NCU04265 and beta-glucosidease (NCU09733) for processing of sugars, and a number of phosphatases which may be involved in signaling or signal termination (*pht-2* NCU03255, NCU03333, NCU08995). Genes for processing fats in either beta-oxidation or biosynthesis include *erg-1* (NCU04156, an acetyl-CoA desaturase (NCU05259), and another desaturase *ods* (NCU02209). Enzymes which are part of the core glycolysis/gluconeogenesis pathway are phosphoglycerate kinase or pgk (NCU07914) and glyceraldehyde-3-phosphate dehydrogenase or gpd-1 (NCU01528). Cluster A degradative enzymes that breakdown lipids and proteins include aspartyl proteases *apr-2* (NCU00994) and *apr-10* (NCU08739), and triacylglycerol lipase or *tgl-2* (NCU01901). A number of amino acid biosynthetic enzymes feature in cluster A, which may be an instance of secondary regulation. The transcription factor gene for cross pathway control *cpc-1* NCU04050, is responsible for balancing amino acid populations in response to starvation and controlling amino acid biosynthetic enzymes [190]. RNA-sequencing data shows that FAR mutants have consistently low expression levels of *cpc-1* compared to wild type. The gene *pdx-1* (NCU06550) is early in the pathway for thiamine biosynthesis and is also a CPC-1 target [190]. Other genes in the thiamine pathway include *nmt-1* (NCU09345) and a thiazole biosynthesis protein (NCU06110). Additional amino acid biosynthetic enzymes showing the Cluster A expression profile are *am* (NCU01195) and *arg-1* (NCU2639).

Cluster B genes are under-expressed without FAR-1 in oleate

When reliant upon oleate for carbon and energy, FAR-1 mediates transcription of genes to help the breakdown of fatty acids, and the preservation of carbon during respiration via the glyoxylate bypass for use in building carbon-rich fungal cell walls (Figure 3.23). Within cluster B are several genes for pex proteins, which aid in building

the glyoxysomes where beta-oxidation takes place, *pex-11* (NCU04802) and *pex-3* (NCU06175). The ATPase gene *pex-1* facilitates transport of proteins to function in the matrix of the glyoxysome. Numerous enzymes of beta-oxidation and the glyoxylate bypass are regulated by FAR-1 in oleate (Figure 3.23). Cluster B also features transporter genes of several types including nucleotide transporters *mic-1* (NCU00316) and *mic-26* INCU07578), long chain fatty acid transporters *acs-6* (NCU06032) and *mic-14* (NCU03556), mic-22 (NCU7263), and a sterol carrier (NCU3372).

Cluster C genes are over-expressed in a Δ*far-1*; Δ*far-2* mutant in oleate

In the absence of a TF to up-regulate beta-oxidation and fatty acid mobility and utilization, a growing fungal hyphae must attempt to acquire other nutrient sources [86], [190]. Cluster C consists of FAR ChIP targets which are expressed at higher than wild type levels in the FAR mutants, most notably in the Δ*far-1*; Δ*far-2* mutant in oleate (Figure 3.24). Without reporter studies it will be unclear whether these effects are directly as a result of FAR de-repression, mediated by a second regulator, or a combination of signals. Genes in cluster C that are overexpressed in oleate include seven TF, namely NCU02142, alternative oxidase regulator *aod-2* or NCU00730, NCU10080, glycogen responsive TF NCU04851, NCU03352, NCU10258, and *pacc-1* or NCU00090. Movement of small molecules via MFS transporters becomes a cellular priority, with 6 proteins of that class with this expression pattern. Calcium transporter *ena-1* (NCU05046) and magnesium transporters (NCU04457 and NCU06218) as well as an ABC-type transporter *abc-1* (NCU08056) are also overexpressed. Glycosyl hydrolases for segmenting carbohydrates also respond to FAR absence, with representatives from three families, *gh3-3* (NCU08755), *gh13-10* (NCU08132), and *gh43-6* (NCU07326). Cluster C also contains a collection of genes for heme-containing and redox proteins consistent with reactive oxygen species detoxification seen in other experiments as a FAR function. Two fatty acid biosynthetic proteins, fatty acid elongase NCU08976, and triacyl-glycerol biosynthesis protein NCU07741 are overexpressed in the double mutant

in oleate. Genes encoding succinate (NCU02505), pentose phosphate metabolism protein *ppm-2* (NCU03100) and pyruvate dehydrogenase *ace*-4 (NCU06218) in this cluster underscore the altered regulation of carbon metabolism resources caused by FAR mutation. These expression patterns suggest possible perturbation of normal expression levels, or over-compensation by another regulator that shares in the regulation of some FAR targets.

Cluster D genes are over-expressed in butyrate without the FARs, and are FAR-1 dependent in oleate

Cluster D genes combines some of the characteristics seen in clusters B and C with FAR-1 loss corresponding to under-expression in oleate or sucrose, and a loss of the FARs resulting in higher expression levels than wild type in butyrate (Figure 3.24). Also similar to cluster B, there are representatives of pex genes such as PTS carriers *pex-7* (NCU07662) and *pex-5* (NCU02960), membrane protein gene *pex-26* (NCU00347), and ring finger complex member *pex-12* (NCU05245). Genes encoding enzymes of beta-oxidation are also present with *acd-1* (NCU02287), *acd-2* (NCU08924), and *fox-2* (NCU08828). Like cluster C, cluster D contains transcription factors, MFS transporters, and metal transporters, and representatives of glycosyl hydrolase families. Unique gene groups of this expression pattern are DNA repair genes *apn-2* (NCU01961), *dnt-3* (NCU00081), and *dnr-8* (NCU10776), and genes encoding proteins involved in cell wall structure *acw-5* (NCU07776) and *acw-4* (NCU09263). Cluster D contains genes involved in signal perpetuation kinases *nik-2* (NCU01833), *dcc-1* (NCU00939), and *camk-3* (NCU06177) and phospholipase C *plc-2* (NCU01266), and is also linked to clock output genes *ccg-1* (NCU03753) and *ccg-13* (NCU08907). Glycolysis enzyme phosphoglycerate mutase (NCU11201) and reactive oxygen detoxification enzyme *cat-2* (NCU05770) Lastly, cluster D contains a number of genes involved in biosynthesis of siderophores: *iucB* (NCU06062), carotene pigments: *al-1* (NCU00552), fatty acids: *FAS1* (NCU02579), and pantothenic acid: *pan-2* (NCU10048).

<u>Phenotypes reveal specific functions for FAR-1 and FAR-2</u>

FAR-1 is required for normal linear growth on Tween 20

The ChIP-seq datasets for FAR-1 and FAR-2 served to generate hypotheses about new possible functions these regulators may have. In order to compare *N. crassa* FAR function to work done in *A. nidulans* and to characterize the ability of *N. crassa* to grow on different substrates, I chose to determine linear growth rates in race tubes. Tergitol has been found to cause colonial growth in Neurospora on VMM, and has been exploited for the inhibition of hyphae in contact with tergitol media without inhibition of aerial hyphal formation and conidiation [192]. This was confirmed here after testing growth conditions used for *A. nidulans,* which include Tergitol (NP-40) added to between 0.5 to 1% to increase fatty acid dispersion in growth media. Agar containing NP-40 resulted in very little lateral hyphal growth of *N. crassa* from areas of conidial inoculation, thus medium containing NP-40 were unsuitable for assaying transcription factor mutant phenotypes. After testing several non-ionic detergents as fatty acid dispersants, Tween 20 was the most effective while disturbing growth in liquid media the least.

Hyphal linear growth rate of *N. crassa* was quantified on different carbon sources (Figure 3.25). Given what had been found when growing other fungi on long chain fatty acids [106], [114], I expected inhibition of growth of the Δ*far-1* strain on oleate. Initial experiments were done on oleate with using Tween 20 as a dispersant for oleate for wild type, Δ*far-1, Δfar-2, and Δfar-1;Δfar-2.* Growth rates on oleate + Tween 20 showed a pattern consistent with Δ*far-1* based inhibition (Figure 3.26). However, when I examined Tween 20 and oleate components of the medium as individual carbon sources, I found that Tween 20 alone was responsible for causing the slow growth rate, rather than a general inability to metabolize oleate (Figure 3.25). The Δ*far-1* and Δ*far-1; Δfar-2* mutants and wild type grew at very similar rates on oleate alone (Figure 3.25A). When grown on butyrate, Δ*far-2* and Δ*far-1; Δfar-2* grew slightly slower than wild type

but were not significantly inhibited (Figure 3.25B). This finding is unlike what had been previously found with *A. nidulans*, i.e. minimal growth on long chain fatty acids for *farA* or on short chain fatty acids for *farB* [106]. The 0.5 to 1% NP-40 detergent included in the *A. nidulans* medium did not inhibit growth. Examining how fatty acids were dispersed evenly in the *A. nidulans* media may also yield more insight into FarA function relative to FAR-1.

When a Δ*far-1* strain is grown on identical carbon sources with and without Tween 20, I found that growth medium with Tween 20 caused an additional phenotype of slow growth. The Tween 20 detergent growth was reminiscent of colonial growth seen on NP-40 (Figure 3.25A and C). Interestingly, Tween 80 added to oleate did not slow Δ*far-1* growth, suggesting that a shorter length side chain of the non-ionic detergent contributes to the slow growth phenotype (Figure 3.26). Slow growth on Tween 20 is unique to Δ*far-1,* as the Δ*far-2* strain grows at a rate equal to wild type (Figure 3.26). Growth on Tween 20 also emphasizes the rhythmic appearance of a conidiation band, which is not seen on most other carbon sources (Figure 3.12D). Banding is also characteristic of the *bd* ("band") mutant (NCU08823), a gene encoding a ras-type small GTPase [27]. One strain with a *bd* allele has been used widely in studies on circadian rhythms [28] and *bd* is implicated in regulation of responses to reactive oxygen species [50].

In order to test whether the Tween 20-dependent phenotype was related to membrane dynamics which might be altered at elevated temperatures, we tested growth with and without Tween 20 on sucrose at room temperature and at 37° C. Rather than emphasizing the growth defect cause by Tween 20 at the elevated temperature, the linear growth rate of the Δ*far-1* mutant, and double Δ*far-1;* Δ*far-2* mutant was much closer to that of wild type at 37° C (Figure 3.25C). This suggests that metabolic or physiological differences seen at 25° C were resolved or at least compensated for at higher temperatures. The Δ*far-2* growth rate on Tween 20 equals that of wild type, while the double mutant shows a compounded phenotype of

extremely slow growth. Taken together, these data suggest that the Tween 20 growth defect may have a basis in FAR-1-dependent regulation. Regulation may be compensated for by yet another TF at higher temperatures, but remains to be tested.

Oxidative stress elicited by hydrogen peroxide causes decreased conidiation and linear growth defects in Δ*far-1*

To test a link between detoxification of reactive oxygen species (ROS) and potentially regulated FAR-1 ChIP target genes, we tested susceptibility of *far* mutants to hydrogen peroxide stress (Figure 3.14). The beta-oxidation of fatty acids generates oxidized lipid species, with hydrogen peroxide as a byproduct, and may occur in glyoxysomes or mitochondria in *N. crassa* (Figure 3.19, top) [129]. ROS are also heavily implicated in conidial germination and hyphal fusion by anastomosis [193]. To minimize growth issues, small, colonized agar plugs taken from a plate of SC medium containing 0.1% of sucrose were used as inoculum. Phenotypes of Δ*far-1* strains included poor growth and poor conidiation on hydrogen peroxide with 5 mM oleate compared to wild type (Figure 3.14A). The Δ*far-1;* Δ*far-2* double mutant also exhibited these phenotypes but to a more extreme degree. At higher concentrations of ROS in the agar, Neurospora grew more slowly or not at all. Using sucrose as a carbon source showed that poor conidiation and poor growth were not restricted by carbon source (Figure 3.14B). The latter experiment tested a link between the FARs and maintenance of oxygen species homeostasis and detoxification. We showed that poor outgrowth and poor conidiation result from a lack of FAR-1, but not simply because metabolic processes like beta-oxidation of oleate are disturbed.

Deletion of *far-1* affects secreted siderophore production

Enriched functional categories of genes, such as isoprenoid metabolism (FAR-1, FAR-2), iron transport (FAR-2), heme and iron cofactor binding (FAR-1, FAR-2), and siderophore ion transport (FAR-2) among ChIP targets suggested iron-sequestration was

affected by the FARs (Table S7, Table S8). Siderophores are small molecules constructed from isoprene subunits, and they sequester iron in a biologically available oxidation state [135]. Fungi typically have both internal and secreted siderophores that help in both storage and transport of iron [135]. A visual test for the presence of *Neurospora*'s secreted siderophore coprogen [194] employed CAS, or chromeazeurol S dye in agar, used previously in Apergillus [195]. Because the dye is toxic the inoculum needs access to VMM agar containing 5 mM oleate to establish colonies. As the secreted siderophore accumulates, it binds the dye, turning it from a blue-purple to orange. I tested wild type *N. crassa*, and *far* mutant strains for differences in siderophore secretion by inoculation of CAS plates with equal-sized agar plugs. After 7 days of growth and slow color change, I detected a defect in Δ*far-1* (Figure 3.27A). As a control, the experiment was repeated with sucrose as a carbon source, which validated the visual measure of decreased siderophore secretion in Δ*far-1* (Figure 3.27B). Though I found that the siderophore production process is altered in a Δ*far-1* knockout, growth on CAS agar alone does not directly probe the underlying mechanism that alters this output.

After analysis of this finding, I mapped the ChIP-sequencing and RNA-sequencing data back onto the genes for siderophore biosynthesis and transport in the *N. crassa* genome. Under the conditions I assayed, only 5 of 15 of the genes analyzed had binding by ChIP, and fewer than half (3 of 8) genes with significant transcriptional change had FAR-1 or FAR-2 ChIP peaks. One exception was NCU05000, a siderophore transport gene with FAR-2 ChIP enrichment, which was transcribed in butyrate from 6 (Δ*far*-1) to 18 (Δ*far-2*) fold above wild type levels in *far* mutants (data not shown, Table S12). However, the ChIP- and RNA-sequencing data collection were not done with iron deficiency as a challenge, so it is uncertain whether FAR activity would change in the iron-scarce conditions found on in CAS agar. Overall, these data suggest that 1) signals that were not present in the data collected could mediate FAR binding, or 2) a secondary regulator controlled by FAR activity could be affecting siderophore biosynthesis and transport pathways.

Formation of perithecia depends on FAR-2 expression on butyrate medium

Functional categories featuring FAR-enrichment by ChIP included genes involved in asexual and sexual development. In order to test the functional association of the FARs with ascospore development and mating, I set up crosses between *mat a* strains of wild type (NMF262), Δ*far-1* (NMF641), Δ*far-2* (NMF643), and the double mutant, Δ*far-1;* Δ*far-2* (NMF639). The fertilizing ("male") strain was the same for all crosses, *mat A* Δ*far-1;* Δ*far-2* (NMF640). After 14 days, all crosses on oleate and sucrose had developed normal perithecia with ascospores. However, only wild type and Δ*far-1* crosses to the double mutant showed normal perithecial development on butyrate, seen as a cluster of melanized structures at the center of each plate (Figure 3.12C). Based upon expression levels of the transcription factors FAR-1 and FAR-2 in the deletion strains, FAR-2 is expressed at twice the level of wild type in the *Δfar-1* strain grown with butyrate (Figure 3.12A). No perithecia are seen in crosses on butyrate medium with female strains lacking FAR-2 expression, i.e. crosses with Δ*far-2* and Δ*far-1;* Δ*far-2* strains.

FLAG immunoprecipitation of FAR-2 is not clearly enriched in nuclei

Wild type, FAR-1-3XFLAG and FAR-2-3XFLAG strains were all grown and prepared so as to enrich a protein sample for the TF of interest (Table 2.1). The goal of this experiment was to survey post-translational modifications that may be serving as activation signals for regulator activity. After growth and purification as described, the resulting proteins were run out on an SDS-page gel, and then either silver stained or transferred to PVDF for western blot with FLAG antibody (mouse, Sigma F-3165)(Figure 3.28). Whether due to inefficient binding or low protein quantity despite the large tissue size, and supposed concentration by nuclear isolation, the wild type and 3X-FLAG labeled samples for FAR-1 look very similar. This was true for all samples evaluated by silverstained gels; the gel shown is representative (Figure 3.28, top). A western blot

confirmed expression of 3XFLAG-tagged FAR-2, but also showed a loss of far-2 in the eluate. One explanation for this may be that FAR-2 is not found in the nucleus when the strain is grown with sucrose. In contrast, FAR-1 (lane 9) showed a prominent band that supports its nuclear localization in sucrose. These samples are awaiting evaluation by mass spectrometry.

Table 3.1: Mini-heatmap key for Figure 3.17

Relative expression levels for the *pex* genes and genes depicted in Figure 3.17 were quantified as $\log_2$(fold change) from wild type to a *far* mutant. Significance of each WT-mutant comparison was evaluated by Cuffdiff [170], indicated by 'yes' or 'no' in column to the right of each fold change quantity. Genes below the dark line depicted as proteins in the lumen of the peroxisome.

NCU	WTS-dF1S	sig	WTS-dF2S	sig	WTS-ddS	sig	WTB-dF1B	sig	WTB-dF2B	sig	WTB-ddB	sig	WTO-dF1O	sig	WTO-dF2O	sig	WTO-ddO	sig	gene name
NCU00316	0.726	yes	0.090	no	0.906	yes	1.009	yes	-	yes	-	yes	-	yes	-	yes	-	yes	mic-1, ANT1
NCU07578	-	no	0.860	no	-	no	0.472	no	0.762	no	0.143	no	-	yes	0.614	yes	-	yes	mic-26
NCU08118	0.270	no	0.064	no	0.586	no	-	no	0.006	no	-	no	-	yes	0.376	yes	-	yes	pex-1 ATPase
NCU04802	-	no	0.261	no	-	no	0.787	no	0.336	no	0.002	no	-	yes	0.297	yes	-	yes	pex-11
NCU02618	0.023	no	-	no	-	no	-	no	-	no	-	no	0.061	no	-	no	-	no	pex-13
NCU03901	0.151	no	-	no	-	no	0.469	no	0.248	no	0.067	no	-	no	-	no	-	yes	pex-14
NCU02070	-	no	-	no	0.004	no	0.074	no	-	no	-	no	-	yes	-	yes	-	no	pex-2
NCU04062	0.324	no	0.144	no	0.431	no	0.266	no	0.197	no	-	no	-	yes	0.509	yes	0.108	no	pex-20
NCU06637	-	no	0.032	no	-	no	-	no	0.281	no	0.002	no	-	no	0.109	no	-	no	pex-24
NCU00347	0.355	no	-	no	-	no	0.341	no	0.213	no	0.234	no	-	yes	0.246	yes	-	yes	pex-26
NCU06175	0.143	no	0.136	no	0.075	no	0.777	yes	-	no	-	no	-	yes	-	yes	-	yes	pex-3
NCU05564	-	no	0.447	no	-	no	-	no	1.058	yes	0.504	no	-	yes	0.335	yes	-	no	pex-31
NCU01535	0.138	no	-	no	-	no	0.188	no	0.057	no	-	no	-	no	-	no	-	yes	pex-33
NCU02636	-	no	-	no	-	no	-	no	-	no	-	yes	-	no	-	no	-	yes	pex-4
NCU02960	0.339	no	-	no	0.050	no	0.358	no	0.324	no	0.065	no	-	no	0.133	no	-	no	pex-5
NCU08373	0.098	no	0.074	no	0.412	no	0.267	no	0.067	no	-	no	-	no	-	no	-	yes	pex-6
NCU07662	0.328	no	0.307	no	0.249	no	0.758	yes	0.573	no	0.355	no	-	no	0.268	no	-	no	pex-7
NCU00032	-	no	0.358	no	0.062	no	-	no	-	yes	-	no	-	no	-	no	0.144	no	pex-8
NCU03277	0.509	no	-	no	-	no	0.676	no	0.243	no	0.307	no	-	no	-	no	-	no	pex-10
NCU04301	0.584	no	0.103	no	0.357	no	0.698	no	0.440	no	0.363	no	-	no	0.357	no	-	no	pex-19
NCU01850	0.029	no	0.022	no	-	no	-	no	-	no	-	no	-	no	0.103	no	-	no	pex-16
NCU05245	0.342	no	-	no	0.166	no	0.640	no	0.320	no	0.547	no	-	no	0.307	no	-	no	pex-12
NCU02209	0.638	no	-	no	0.734	no	-	no	-	yes	-	yes	0.123	no	0.444	no	-	yes	ods
NCU02408	0.090	no	-	no	0.144	no	-	no	-	yes	-	yes	-	no	0.041	no	-	no	
NCU06694	0.236	no	-	no	0.304	no	0.119	no	0.038	no	0.413	no	0.566	no	0.371	no	1.330	yes	
NCU09497	0.489	no	-	no	0.911	yes	-	yes	-	yes	-	yes	2.192	yes	2.417	yes	-	no	
NCU00580	0.533	no	-	no	0.373	no	1.207	yes	-	no	-	no	-	yes	0.068	yes	-	yes	
NCU07307	0.823	yes	0.066	no	1.628	yes	0.028	no	-	yes	-	yes	1.285	yes	0.370	yes	-	yes	cel-2
NCU07308	0.749	yes	0.265	no	1.676	yes	0.050	no	-	yes	-	yes	1.879	yes	0.459	yes	-	yes	cel-1
NCU08535	0.773	yes	0.376	no	1.998	yes	0.294	no	-	no	-	no	0.569	no	-	no	0.671	no	
NCU09497	0.489	no	-	no	0.911	yes	-	yes	-	yes	-	yes	2.192	yes	2.417	yes	-	no	
NCU08332	-	no	-	no	-	no	-	no	-	no	-	no	-	no	-	no	-	yes	hex-1
NCU09534	-	yes	-	no	-	no	-	no	0.709	no	0.132	no	-	yes	1.695	yes	2.504	yes	HYR1
NCU09770	-	no	0.164	no	0.057	no	1.227	yes	-	yes	-	yes	-	no	-	no	0.302	no	acu-8
NCU04803	-	yes	0.299	no	-	yes	1.084	yes	-	no	-	no	-	yes	0.404	yes	-	yes	npd-1
NCU09931	0.614	no	0.212	no	0.355	no	0.592	no	0.711	no	0.367	no	-	yes	0.321	yes	-	yes	npd-2
NCU00580	0.533	no	-	no	0.373	no	1.207	yes	-	no	-	no	-	yes	0.068	yes	-	yes	
NCU03372	-	no	-	no	-	no	0.487	no	0.241	no	-	yes	-	yes	0.854	yes	-	yes	
NCU06031	0.530	no	-	no	0.240	no	-	no	-	no	-	no	0.240	no	1.011	no	-	yes	rhd
NCU06643	-	no	-	no	-	no	-	no	0.335	no	-	no	-	yes	0.217	yes	-	yes	
NCU05259	0.803	no	-	no	0.648	no	-	no	-	yes	-	yes	0.529	no	0.174	no	-	no	

Table 3.2: Mini-heatmap key for Figure 3.18

Relative expression levels for the TCA cycle and glyoxylate bypass genes depicted in Figure 3.18 were quantified as $\log_2$(fold change) from wild type to a *far* mutant. Significance of each WT-mutant comparison was evaluated by Cuffdiff [170], indicated by 'yes' or 'no' in column to the right of each fold change quantity.

NCU	WTS-dF1S	sig	WTS-dF2S	sig	WTS-ddS	sig	WTB-dF1B	sig	WTB-dF2B	sig	WTB-ddB	sig	WTO-dF1O	sig	WTO-dF2O	sig	WTO-ddO	sig	gene name
NCU07263	0.328	no	0.172	no	0.013	no	2.106	yes	-1.226	no	-1.665	yes	-1.800	yes	0.384	yes	0.288	no	mic-22
NCU01514	-0.415	no	0.061	no	0.401	no	0.963	no	-0.008	no	-0.190	no	-0.335	no	0.457	no	1.106	no	mic-3
NCU08561	0.037	no	0.317	no	0.200	no	1.941	yes	0.229	no	0.295	no	-1.400	yes	0.645	yes	-0.066	no	mic-31
NCU01810	0.292	no	0.055	no	0.315	no	-0.227	no	-0.525	no	-0.848	no	0.267	no	0.019	no	-0.101	no	mic-7
NCU04280	0.582	no	-0.370	no	0.543	no	0.145	no	0.050	no	-0.158	no	0.765	yes	0.925	yes	0.137	no	
NCU01692	0.115	no	0.278	no	0.308	no	1.097	no	-0.701	no	-0.942	no	-0.467	no	0.305	no	0.611	no	tca-1, cit-1
NCU04230	0.225	no	-0.203	no	-0.063	no	1.752	yes	-0.728	no	-0.933	no	-2.047	yes	0.019	yes	-0.200	no	acu-3
NCU10007	0.356	no	0.020	no	0.149	no	1.171	no	-0.568	no	-0.865	no	-1.512	yes	0.205	yes	-1.751	yes	acu-9
NCU00959	0.382	no	-0.249	no	-0.035	no	0.632	no	-0.070	no	-0.382	no	-0.682	no	-0.418	no	-0.394	no	tca-10
NCU07756	0.249	no	0.077	no	-0.271	no	0.486	no	-0.267	no	-0.612	no	-0.705	no	-0.699	no	-0.333	no	tca-11
NCU08336	0.113	no	0.094	no	0.141	no	0.689	no	-0.450	no	-0.554	no	-0.725	no	-0.857	no	0.115	no	tca-12
NCU03031	0.320	no	0.053	no	-0.019	no	0.393	no	-0.182	no	-0.598	no	-0.770	yes	-0.700	yes	-0.121	no	tca-13
NCU10008	0.145	no	0.037	no	-0.281	no	0.436	no	-0.258	no	-0.542	no	-0.558	no	0.038	no	-0.567	no	tca-14
NCU04899	-0.029	no	-0.033	no	0.124	no	0.936	no	-0.200	no	-0.257	no	-0.573	no	0.219	no	0.549	no	tca-15
NCU06211	0.433	no	0.080	no	0.295	no	1.318	yes	-0.880	no	-0.842	no	-0.437	no	0.428	no	-0.502	no	tca-16
NCU00720	0.409	no	-0.450	no	-0.349	no	-0.255	no	-0.714	no	-0.677	no	0.048	no	-0.154	no	-0.478	no	tca-17
NCU02482	0.371	no	0.266	no	0.676	no	1.445	yes	-1.704	yes	-1.989	yes	0.055	no	-0.099	no	0.740	no	tca-2
NCU02366	0.142	no	0.142	no	0.570	no	0.784	no	0.037	no	0.043	no	-0.377	no	-0.080	no	0.494	no	tca-3
NCU07697	-0.099	no	0.331	no	0.125	no	0.009	no	0.642	no	0.393	no	0.006	no	0.049	no	-0.264	no	tca-4
NCU03857	0.347	no	-0.072	no	0.787	no	1.351	yes	-0.137	no	0.092	no	0.141	no	0.498	no	0.709	no	tca-5
NCU00775	0.096	no	0.163	no	0.087	no	-0.112	no	0.440	no	0.260	no	-0.008	no	0.118	no	-0.162	no	tca-6
NCU05425	0.209	no	0.189	no	0.487	no	0.570	no	0.699	no	0.595	no	-0.454	no	0.185	no	0.708	no	tca-7
NCU01227	0.237	no	-0.171	no	0.169	no	0.232	no	0.185	no	-0.006	no	0.179	no	0.350	no	-0.112	no	tca-8
NCU08471	0.282	no	-0.154	no	0.069	no	-0.063	no	-0.107	no	-0.281	no	0.267	no	0.294	no	0.532	no	tca-9
NCU01611	0.105	no	0.095	no	0.190	no	1.507	yes	0.442	no	0.707	no	-0.783	no	0.984	no	1.346	yes	
NCU08002	0.347	no	0.189	no	0.487	no	1.526	yes	-0.121	no	-0.384	no	-1.166	yes	1.139	yes	2.275	yes	
NCU02269	0.680	no	-0.745	no	0.151	no	-0.712	no	-1.133	no	-1.254	no	0.966	no	1.076	no	0.451	no	
NCU07784	0.176	no	0.168	no	0.131	no	-0.193	no	-0.194	no	-0.509	no	-0.184	no	0.359	no	-0.125	no	
NCU05075	0.127	no	-0.471	no	-0.155	no	0.800	no	0.665	no	0.561	no	0.164	no	0.676	no	-0.147	no	
NCU10732	-0.298	no	-0.747	no	-0.348	no	1.077	no	-1.261	yes	-1.084	no	-1.016	yes	0.213	yes	-0.930	yes	
NCU02481	0.310	no	0.334	no	0.597	no	1.142	no	-0.795	no	-1.042	no	-0.346	no	-0.048	no	0.569	no	
NCU06032	0.110	no	0.228	no	0.392	no	-0.892	yes	-0.714	no	-0.806	no	-0.952	yes	0.385	yes	-0.828	yes	
NCU00187	-0.284	no	0.461	no	-0.038	no	1.770	yes	2.036	yes	2.250	yes	1.043	yes	1.063	yes	0.006	no	mig-11
NCU00680	0.316	no	0.045	no	0.340	no	1.432	yes	-1.141	no	-1.375	no	-0.004	no	-0.108	no	0.541	no	
NCU01417	0.222	no	0.211	no	0.164	no	-0.378	no	-0.428	no	-0.098	no	0.522	no	0.341	no	0.928	yes	

Table 3.3: Mini-heatmap key for Figure 3.19

Relative expression levels for the beta-oxidation genes depicted in Figure 3.19 were quantified as $\log_2$(fold change) from wild type to a *far* mutant. Significance of each WT-mutant comparison was evaluated by Cuffdiff [170], indicated by 'yes' or 'no' in column to the right of each fold change quantity.

NCU	WTS-dF1S	sig	WTS-dF2S	sig	WTS-ddS	sig	WTB-dF1B	sig	WTB-dF2B	sig	WTB-ddB	sig	WTO-dF1O	sig	WTO-dF2O	sig	WTO-ddO	sig	gene name
NCU03556	0.812	no	-0.386	no	0.001	no	0.834	no	0.224	no	-0.090	no	-1.720	yes	0.177	yes	-1.228	yes	mic-14, pmp47
NCU01751	0.123	no	-0.146	no	0.002	no	0.334	no	0.404	no	0.266	no	-0.759	no	0.632	no	0.430	no	
NCU10009	0.266	no	0.013	no	0.624	no	0.596	no	0.535	no	0.821	no	0.703	no	-0.090	no	0.087	no	
NCU08382	-0.192	no	0.586	no	0.210	no	0.612	no	0.634	no	0.739	no	-0.906	yes	0.489	yes	0.701	no	
NCU08977	0.712	no	-0.195	no	0.131	no	0.220	no	0.024	no	-0.073	no	-1.062	yes	0.005	yes	-0.323	no	
NCU03415	-0.133	no	0.115	no	-0.168	no	1.088	no	0.401	no	0.682	no	-0.025	no	0.461	no	1.373	yes	cbs-3
NCU00378	0.276	no	-0.141	no	0.019	no	0.844	no	0.591	no	1.067	yes	0.425	no	0.392	no	0.556	no	
NCU07053	0.113	no	-0.489	no	-1.102	yes	-0.640	no	-0.543	no	-1.049	no	-0.081	no	-0.755	no	-0.809	no	
NCU01654	0.537	no	0.210	no	0.471	no	0.658	no	0.528	no	0.241	no	-1.566	yes	0.445	yes	-1.049	yes	acs-1
NCU06063	-0.333	no	-0.524	no	-0.012	no	0.433	no	-0.259	no	0.098	no	-0.007	no	-0.141	no	-1.608	no	acs-5
NCU08935	0.243	no	0.026	no	0.021	no	0.462	no	0.219	no	0.089	no	0.039	no	0.084	no	-0.297	no	acs-7
NCU01181	-0.299	no	0.268	no	-0.544	no	-0.036	no	-0.192	no	-0.969	no	-0.788	no	0.082	no	-1.123	yes	acd-3
NCU08924	0.554	no	-0.131	no	0.263	no	0.842	no	0.852	no	0.589	no	-1.219	yes	-0.215	yes	-0.741	no	acd-2
NCU02287	0.608	no	0.843	yes	0.449	no	0.708	no	1.410	yes	0.897	no	-2.422	yes	0.718	yes	-0.619	no	acd-1
NCU09885	-0.223	no	0.126	no	-0.453	no	0.089	no	0.364	no	0.376	no	0.268	no	0.183	no	0.206	no	
NCU06543	0.634	no	0.082	no	0.303	no	1.031	yes	0.554	no	0.316	no	-0.627	no	0.249	no	0.519	no	
NCU00299	0.539	no	-0.042	no	-0.143	no	0.754	no	0.633	no	-0.369	no	-1.243	yes	-0.087	yes	-1.279	yes	
NCU03542	-0.115	no	0.248	no	-0.472	no	-0.024	no	0.632	no	-1.039	yes	-3.151	yes	0.436	yes	-3.026	yes	
NCU06647	0.124	no	0.153	no	0.209	no	0.689	no	-0.136	no	-0.643	no	-1.075	yes	0.184	yes	-0.759	no	
NCU08828	-0.132	no	0.596	no	-0.013	no	0.941	yes	0.853	no	0.301	no	-2.446	yes	0.523	yes	-0.980	no	fox-2
NCU09238	0.086	no	-0.096	no	0.200	no	-0.414	no	-0.406	no	-0.543	no	-0.345	no	0.090	no	-0.057	no	fox2-like
NCU04796	0.128	no	0.745	no	0.213	no	0.667	no	0.871	yes	0.495	no	-2.519	yes	0.856	yes	-1.436	yes	
NCU09646	0.543	no	0.124	no	0.245	no	1.220	yes	0.154	no	-1.008	yes	-1.003	yes	-0.372	yes	-1.694	yes	
NCU05558	0.017	no	0.132	no	-0.452	no	0.291	no	0.188	no	0.118	no	-0.023	no	0.199	no	0.317	no	
NCU06032	0.110	no	0.228	no	0.392	no	-0.892	yes	-0.714	no	-0.806	no	-0.952	yes	0.385	yes	-0.828	yes	acs-6
NCU06448	0.345	no	0.122	no	-0.083	no	0.579	no	0.461	no	0.149	no	0.254	no	-0.031	no	0.860	yes	
NCU06382	-0.138	no	0.036	no	-0.185	no	0.302	no	0.503	no	0.330	no	-1.447	yes	0.642	yes	-2.321	yes	
NCU08358	0.132	no	-0.285	no	0.393	no	0.089	no	0.058	no	0.652	no	0.681	yes	0.171	yes	2.898	yes	

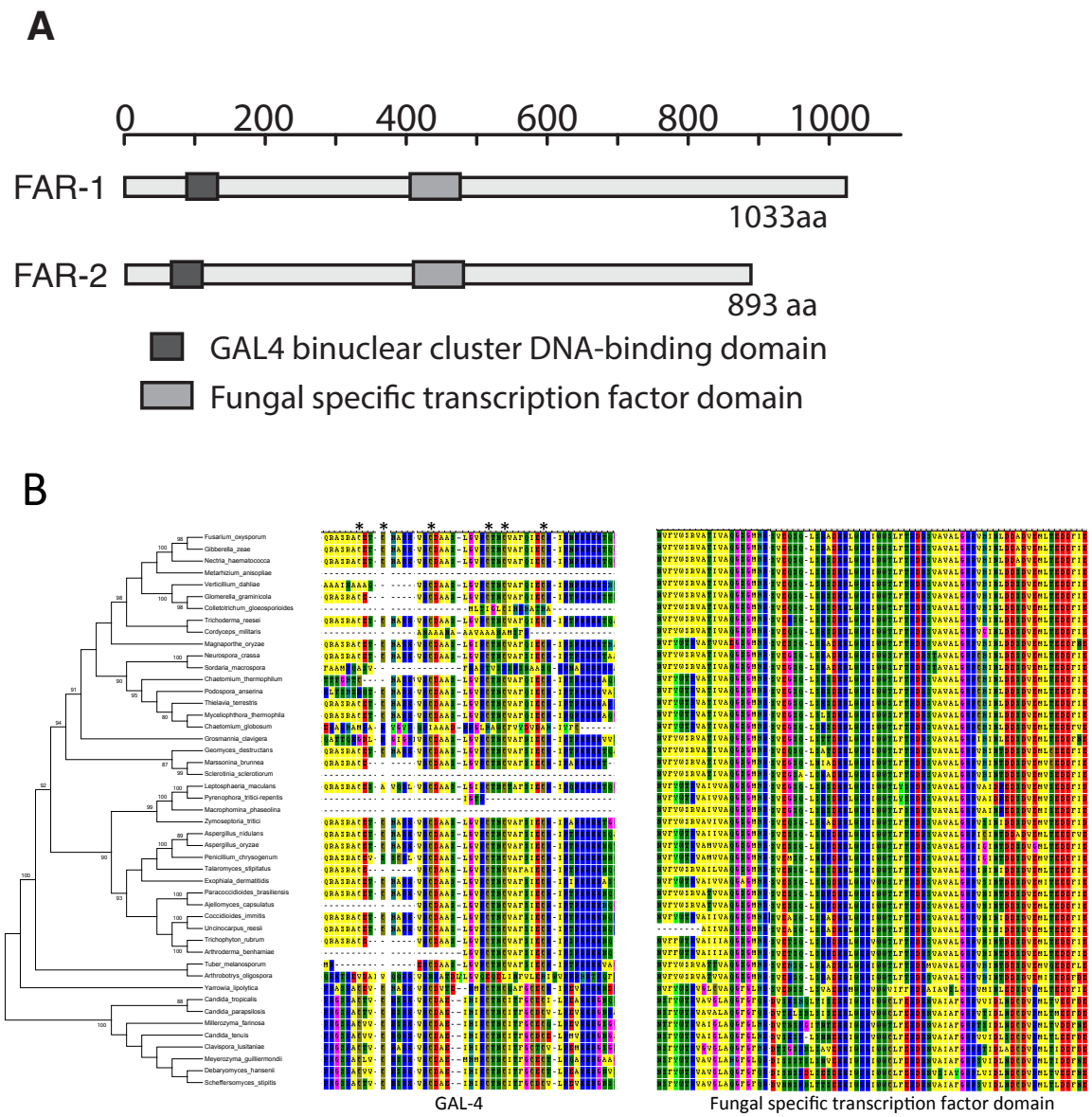

Figure 3.1: FAR-1 and FAR-2 Protein domains and evolution
(A) Protein domain placement along FAR-1 and FAR-2 as determined by RNA- and Sanger sequencing of cDNAs. These motifs were localized along the protein by ELM, Eukaryotic Linear Motif resource [110]. (B) A ClustalW alignment of the FAR-1 GAL-4 domain and Fungal specific transcription factor domain in line with the alignment tree for FAR-1 (Figure 1.4) using MEGA[149]. The 6 cysteines of the *N. crassa* GAL4 domain are marked with asterisks along the top. Interestingly, some homologues of FAR-1 seem to lack this DNA binding sequence. The hemiasomycetes with a FAR-1 homolog have a conserved but distinct amino acid identities compared to other true ascomycetes.

A

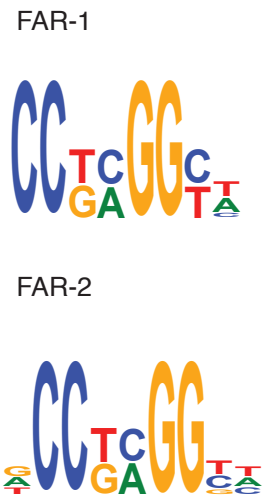

B

Figure 3.2: FAR-1 and FAR-2 binding motifs determined by ChIP-seq
(A) Binding motifs represented from WebLogo3, found bioinformatically by analysis in Scope[176], and confirmed as a significant motif by Bioprospector [178], and Weeder [177]. The called and annotated peaks from Chromosome 1 for both FAR-1 (sucrose was chosen) and FAR-2 (butyrate) were collected from conditions in which binding is found using IGV [196]. Motif discovery was limited to peaks from a single chromosome due to limited submission size. It should be noted that though the sequence occurs many times, not all are bound, and even neighboring sequences may be bound unequally. (B) Sequence logo shows consensus sequence found in other organisms and its reverse compliment. Explanatory arrows clarify the 5' CC and 3' GG bases in sequence logos for FAR-1 and FAR-2.

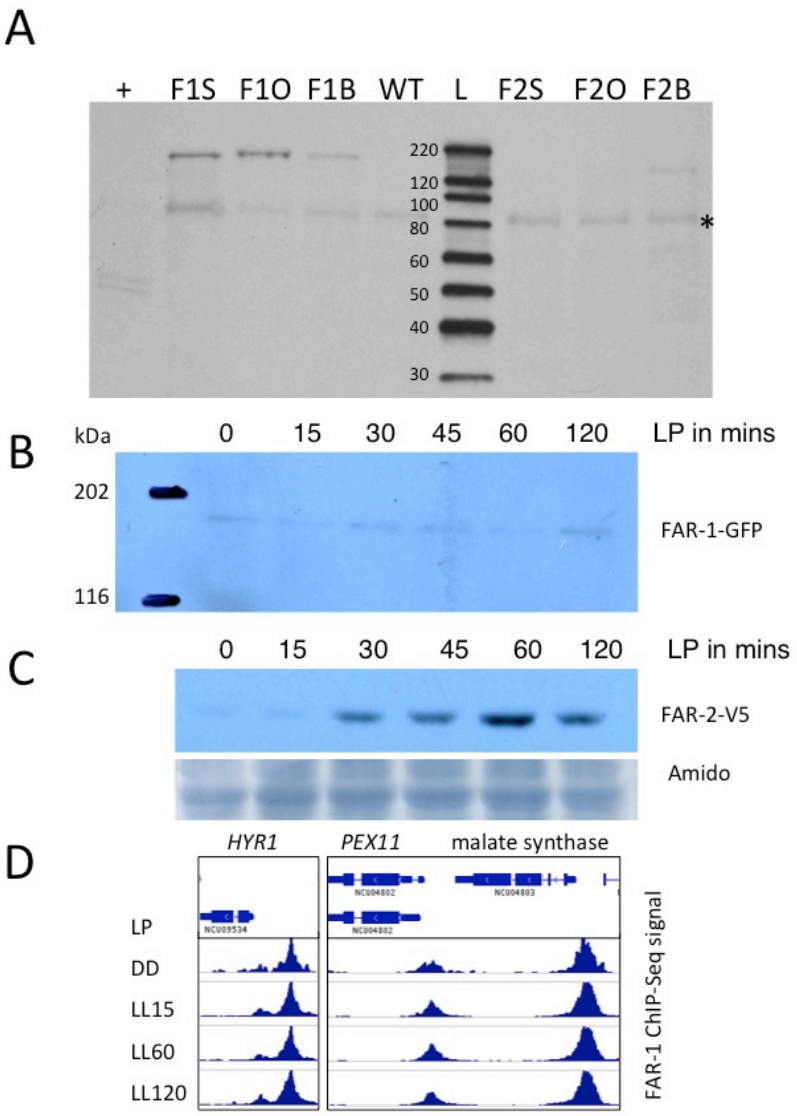

Figure 3.3: Western blot analysis of FAR-1 and FAR-2

(A) Detection of GFP-tagged FAR-1 and FAR-2. Samples were grown overnight in minimal media containing sucrose, and then transferred to a new carbon source as indicated for four hrs before lyophilization. Samples were loaded as indicated +:CenH3:gfp (positive control), F1S:FAR-1 in 1.5% sucrose, F1O:FAR-1 in 5mM oleate, F1B:FAR-1 in 5mM butyrate, WT:Wildtype (NMF261) grown in sucrose, F2S:FAR-2 in 1.5% sucrose, F2O:FAR-2 in 5mM oleate, F2B:FAR-2 in 5mM butyrate. Asterisk marks a background band always detected with the GFP antibody (sc9996) and serves as a loading control. Expected sizes for FAR-1-GFP is 142 kDa, and for FAR-2-GFP is 126 kDa including the size of the epitope tag. Exposure was for 10 minutes. (B) Expression of FAR-1-GFP is not induced by light (LP, light pulse for number of minutes indicated). (C) Expression of FAR-2-V5 is inducible by light (B + C were done by Rigzin Dekhang, Texas A&M University). (D) representative view of bona fide FAR-1 binding sites over a light induction from 0 to 120 minutes (IGV, [196]).

A

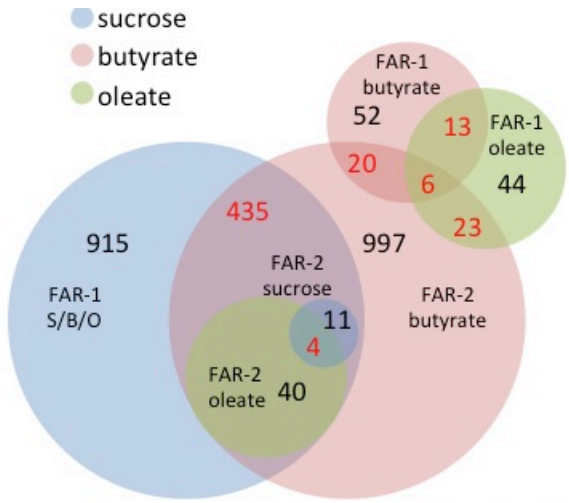

ChIP Sample	ChIP peaks	Changing transcripts near ChIP peaks
FAR-1_suc/but/ol	915	1404
FAR-1_butyrate	52	76
FAR-1_oleate	44	65
FAR-1 TOTAL	998	
FAR-2 sucrose	11	18
FAR-2_butyrate (TOTAL)	997	1566
FAR-2 oleate	40	69
FAR-1_suc/ol/but + FAR-2_suc + FAR-2_ol	4	7
FAR-1_suc/ol/but + FAR-2_but	435	701
FAR-1_but + FAR-2_but	20	28
FAR-1_ol + FAR-2_but	23	30
FAR-1_but + FAR-1_ol	13	18
FAR-1_but + FAR-1_ol + FAR-2_but	6	7

B

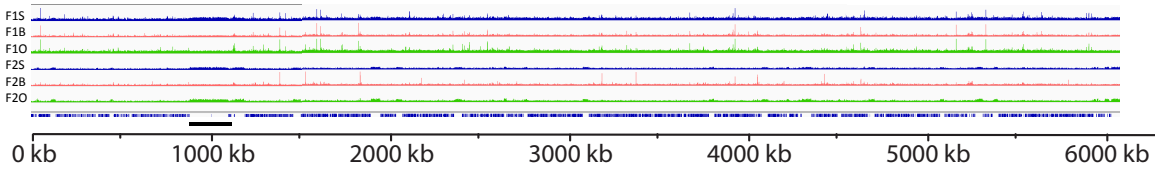

Figure 3.4: FAR-1 and FAR-2 ChIP analysis summary
(A) Venn diagram showing distribution and overlap of ChIP peaks and affected transcripts near these peaks for FAR-1 and FAR-2. Blue numbers indicate transcripts changing between one or more RNA-sequencing conditions within a strain or a condition. Numbers in the overlapping regions (red) are a subset of the black numbers shown. (B) Images from IGV showing ChIP reads for FAR-1 and FAR-2 in sucrose (blue, F1S, F2S), butyrate (red, F1B, F2B), and oleate (green, F1O, F2O). ChIP sequencing for FAR-2 in sucrose and oleate show general genome sequencing background negatively correlating to gene density. Gene distribution is shown along the bottom of the ChIP tracks in blue, and placement of centromere is marked with a black bar.

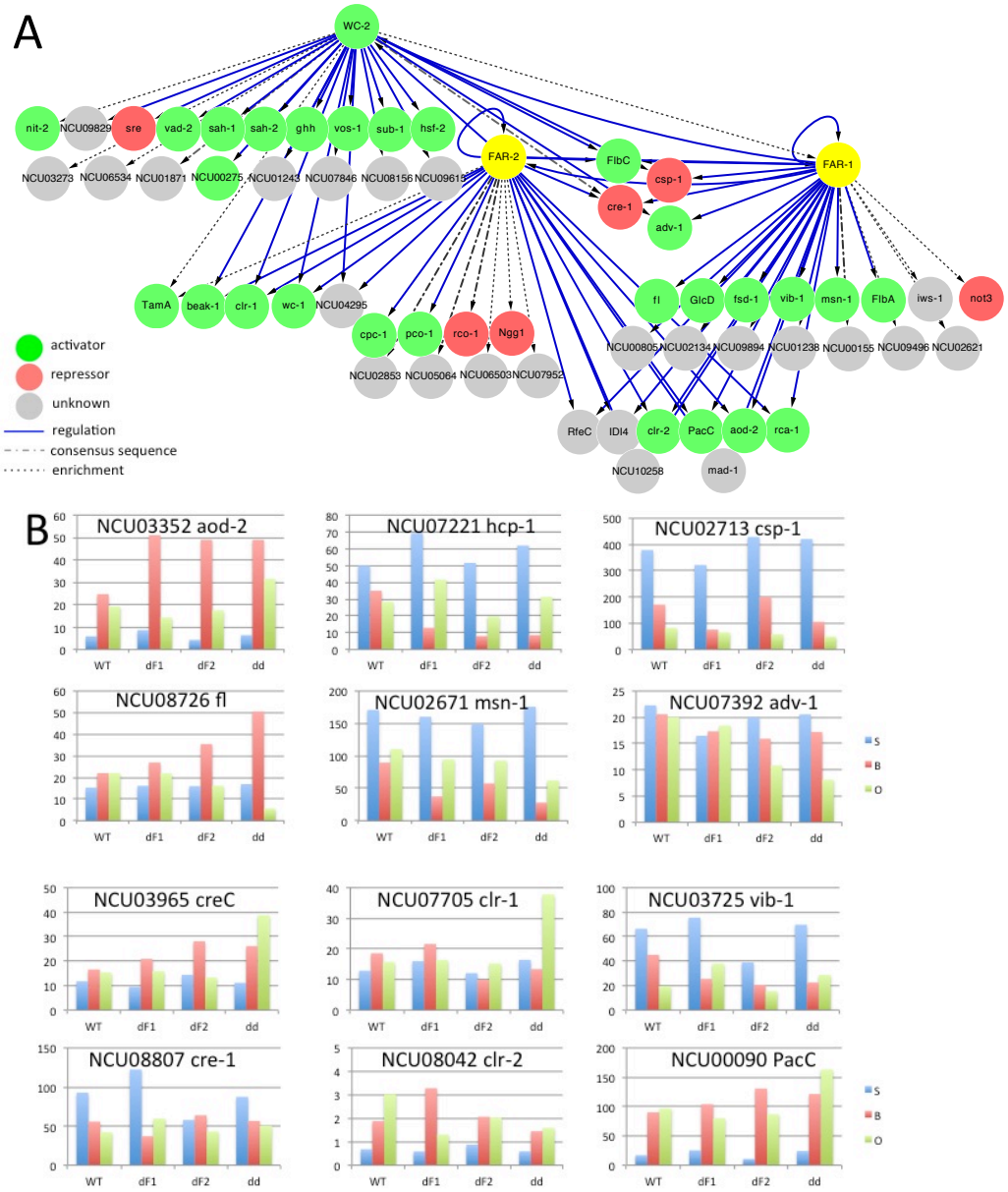

Figure 3.5: WC-2 and FAR-1 and FAR-2 transcription factor network
(A) FAR-1 and FAR-2 transcription factor network, including data from WC-2 [7]. Represented are transcription factor proteins that have ChIP binding sites as directed by arrow heads. Solid blue lines indicate a significant difference in transcript level in a comparison between a wild type and a FAR mutant as measured by Cuffdiff. Dot-dash lines indicate ChIP binding, with transcript level change due to treatment rather than genotype. Grey dotted lines are genes with a ChIP peak but no transcriptional change detected. (B) Transcript levels of selected transcription factor genes measured by FPKM from RNA-sequencing. Note the high expression levels of *clr-1* and *creC* in oleate of the double knockout.

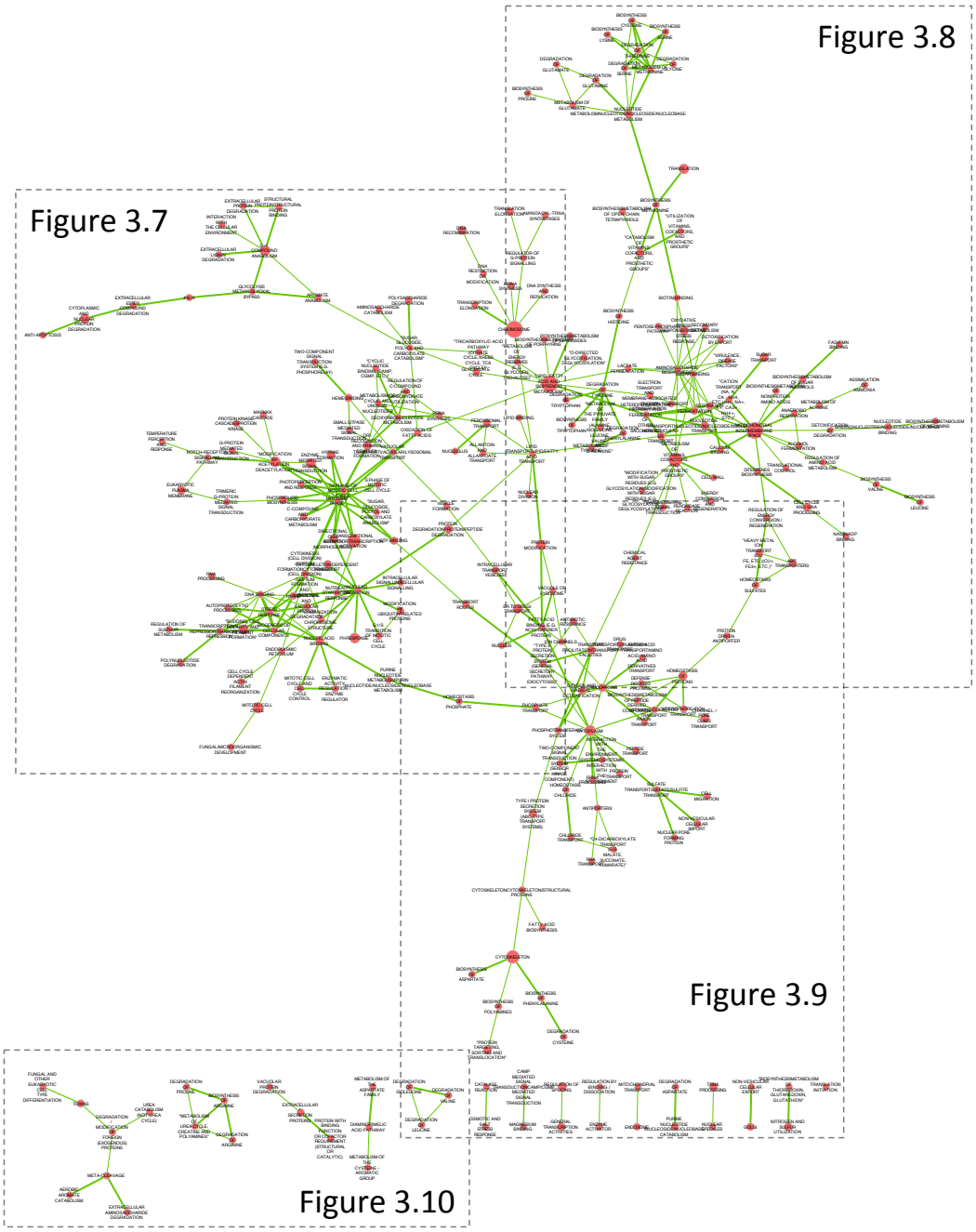

Figure 3.6: Overview of FunCat analysis visualized in Cytoscape for FAR-1 and FAR-2 functional categories

FAR-1 and FAR-2 ChIP targets evaluated by their functional category and overlap. Meanings in the visualization include: relative node size (small is less significant, large is more significant) and number of genes in the overlap between connected functional categories, indicated by green line width. Image was generated using Map Enrichment [168] through Cytoscape[167].

A

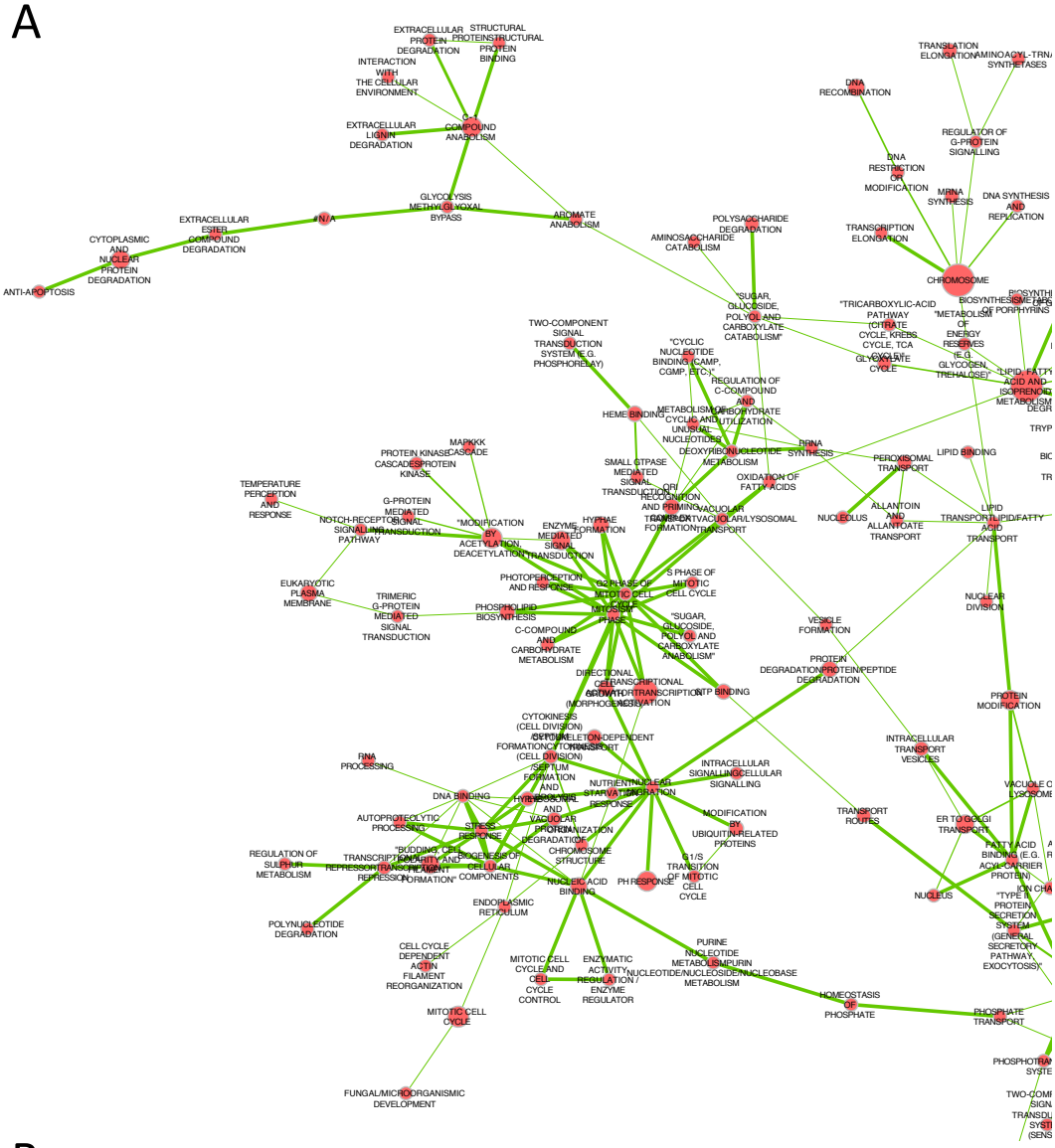

B

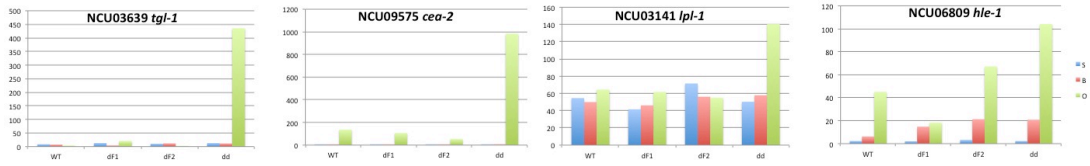

Figure 3.7: FunCat visualization: upper left network and lipase expression
(A) Note the prominent categories of transcriptional activation, and linkage to meiotic and mitotic cell cycle. Functions of "Lipid, Fatty Acid and Isoprenoid metabolism", and chromosome associated functions have a significant presence. (B) Four lipases with FAR binding sites. Both tgl-1 and cea-2 are dramatically overexpressed in a Δ*far-1*;Δ*far-2* strain grown with oleate.

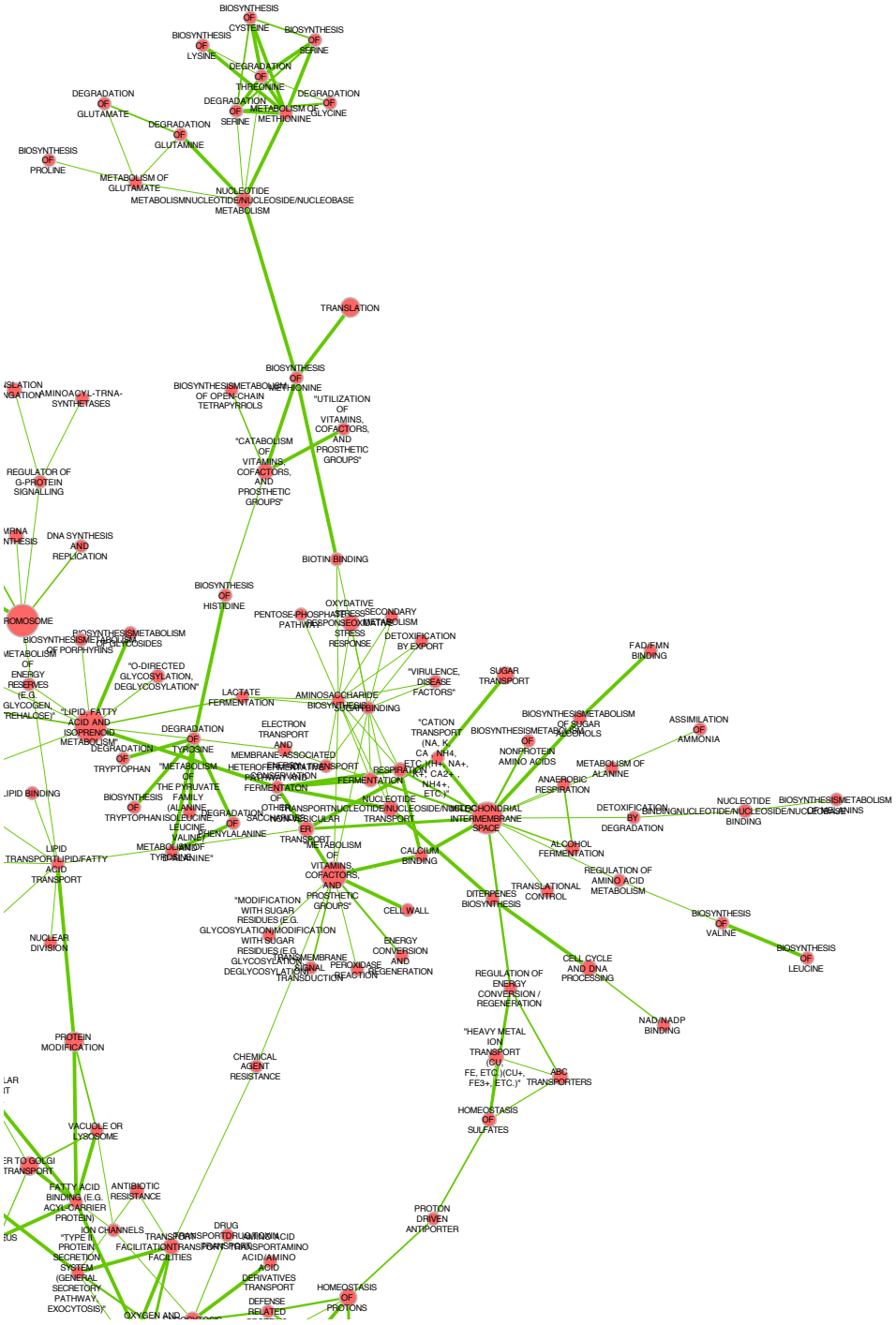

Figure 3.8: FunCat visualization: upper right network

As expected of TFs involved in regulation of transcripts encoding TCA cycle enzymes, localization to the mitochondrial innermembrane space is significant. The FARs also have links to other parts of metabolism such as amino acid biosynthesis and degradation. The category of 'prosthetic groups and co-factors' includes heme binding. proteins

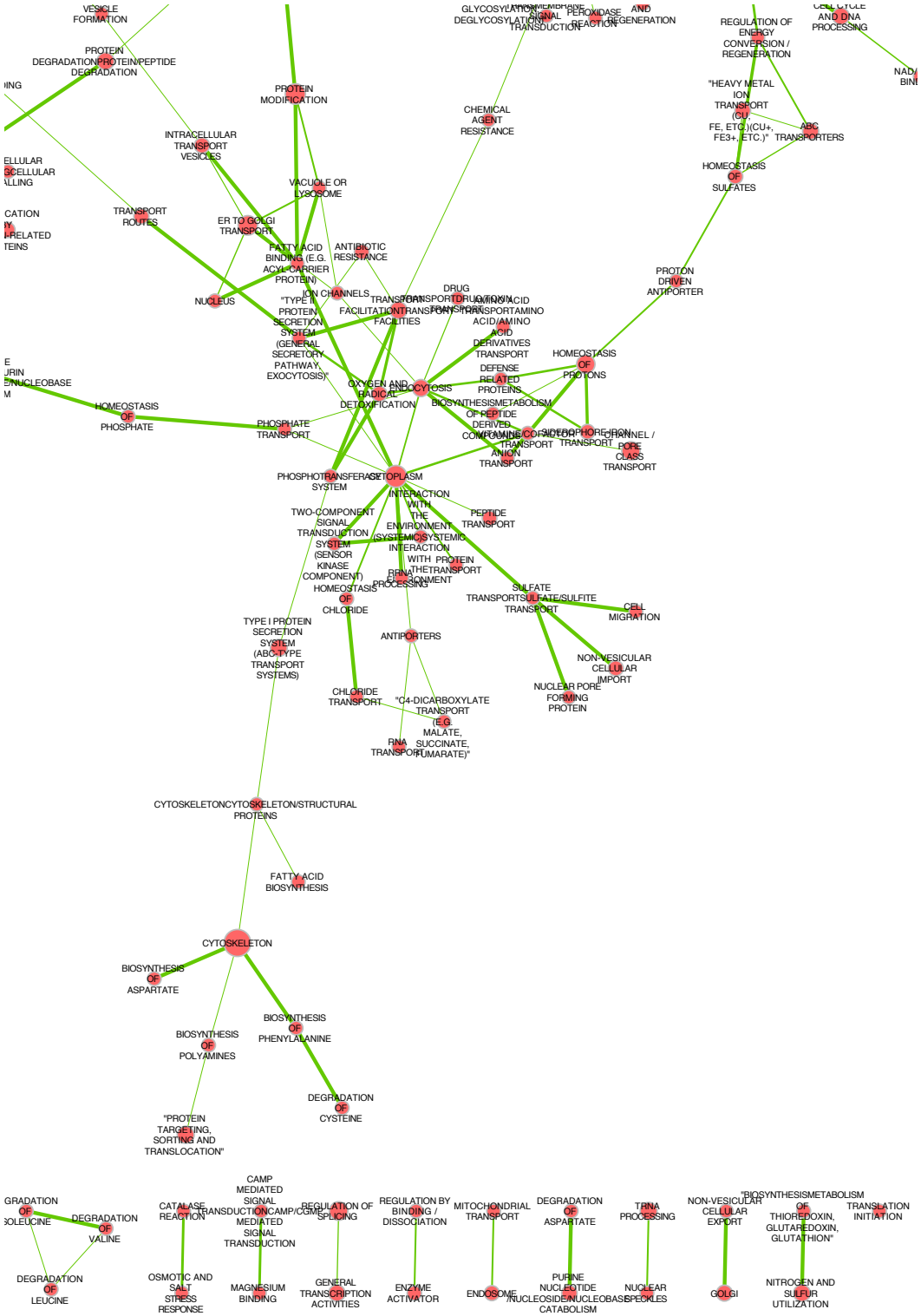

Figure 2.9: FunCat visualization: lower center and right of paired networks
Many general transport mechanisms are evident here, as well as transport of heavy metal ions, and ABC transporters, some of which are utilized for fatty acid trafficking.

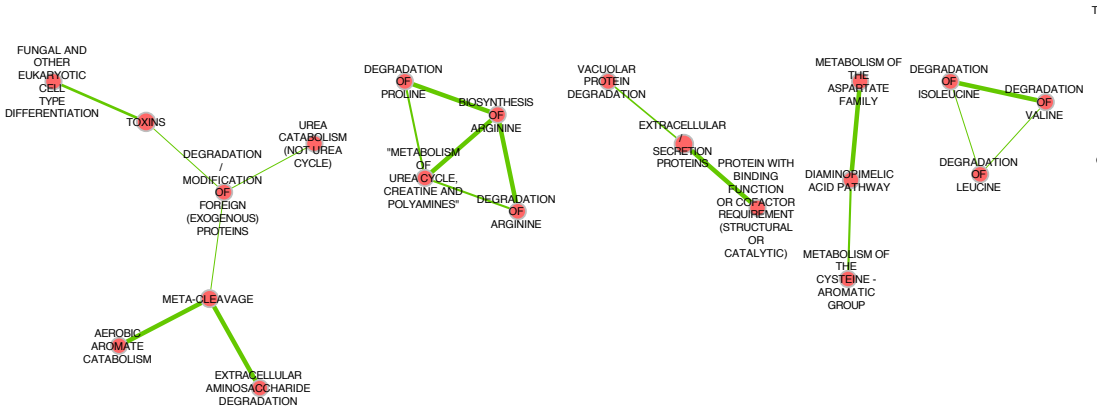

Figure 3.10: FunCat visualization: left of paired networks
Protein and amino acid degradation functions are found among FAR ChIP peaks, seen at the top.

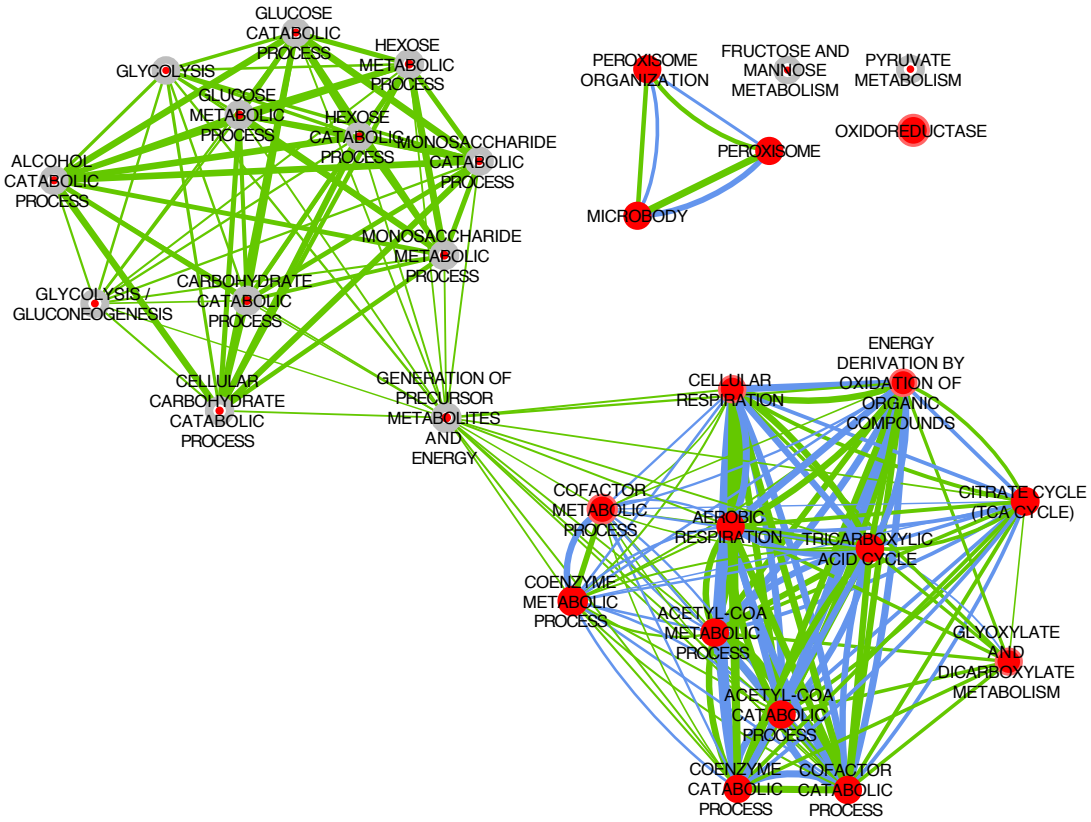

Figure 3.11: David GO analysis network of FAR-1 and FAR-2 ChIP targets
Green connectors represent genes with common placement among connected nodes for FAR-2, Blue connectors are common for FAR-1. The width of these connectors is based on the number of genes in each category that overlap. The size of the core is proportional to the total number of genes in the category for FAR-1; the width of the rim is proportional to the total number of genes in the category for FAR-2. Color--grey (less important) to red (significant) reflects the relative significance of the number of genes relative to those found in the genome, based upon p-value found in David. Therefore a large red center ringed by red is significant for both FAR-1 and FAR-2. A small red core ringed by a large grey rim has few or no representatives from the FAR-1 ChIP set, but a number of genes from the FAR-2 dataset, and is considered less significant due to insufficient overlap with FAR-1.

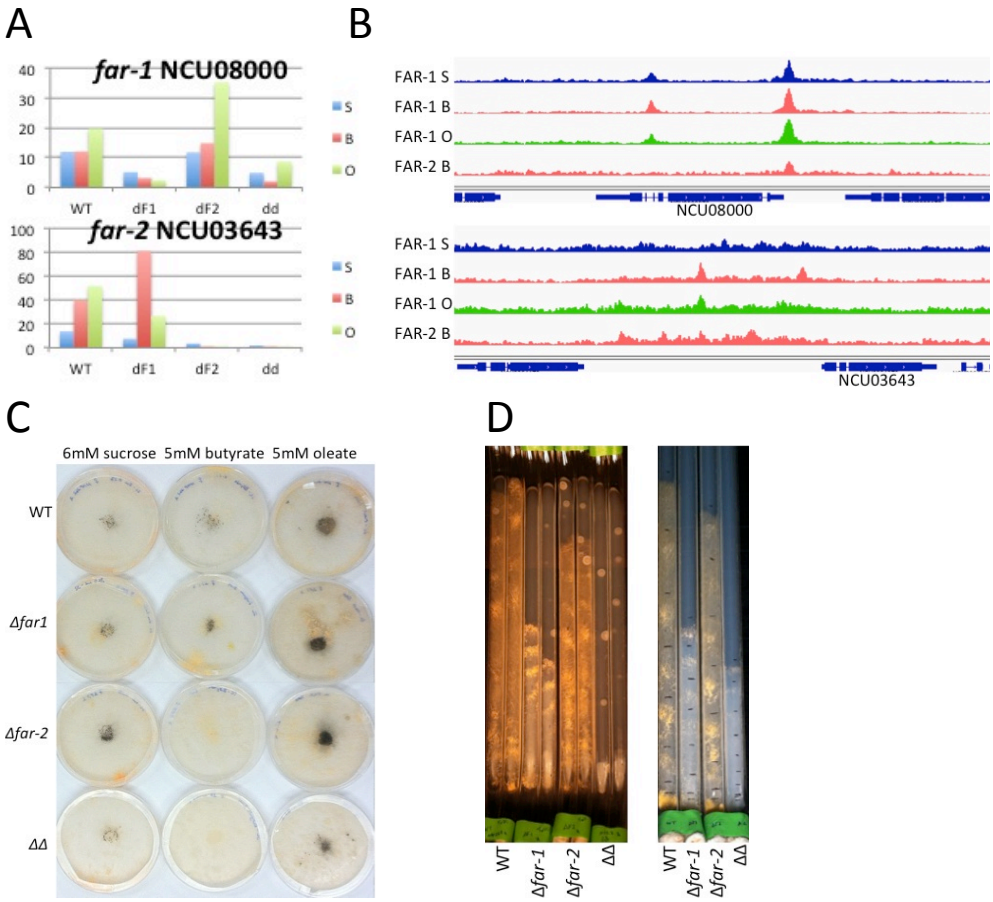

Figure 3.12: Perithecial production is *Δfar-2* dependent on butyrate
(A) Expression levels of *far-1* and *far-2* in all strains used for RNA-Seq. Transcript counts of *far-1* in the Δ*far-1*; Δ*far-2* strain are not above genomic sequencing background noise and may be DNA contamination, supported by reads in introns and an abrupt loss of transcript signal at the bounds of the untranslated regions. (B) ChIP peaks for both FAR-1 and FAR-2 near the *far-1* and *far-2* genes. The peaks near *far-2* fell below the stringent requirements for a FAR-1 peak, despite presence of the consensus sequence. (C) Crosses between *mat a* WT, Δ*far-1*, Δ*far-2*, and Δ*far-1*; Δ*far-2* (ΔΔ) with the Δ*far-1*; Δ*far-2 mat A* strain (NMF640, Table 2.1). This experiment tests the necessity of FAR-1 and FAR-2 for perithecia formation. Expression data for *far-1* and *far-2* during growth on different carbon sources shows that each is overexpressed when the other is lost, FAR-1 in oleate, and FAR-2 in butyrate. Perithecial formation is dependent upon high levels of FAR-2 on butyrate by these data. (D) Race tubes showing pigmentation and conidiation in WT, and single and double *far* mutants when grown with 5 mM oleate (left). Growth is representative of previous trials despite contaminant fungi. The orange pigment is less evident in Δ*far-1* mutant strains. An increase in growth of the ΔΔ strain is marked here. I have previously observed a ΔΔ growth rate increase following extremely slow linear growth after other race tubes finished.

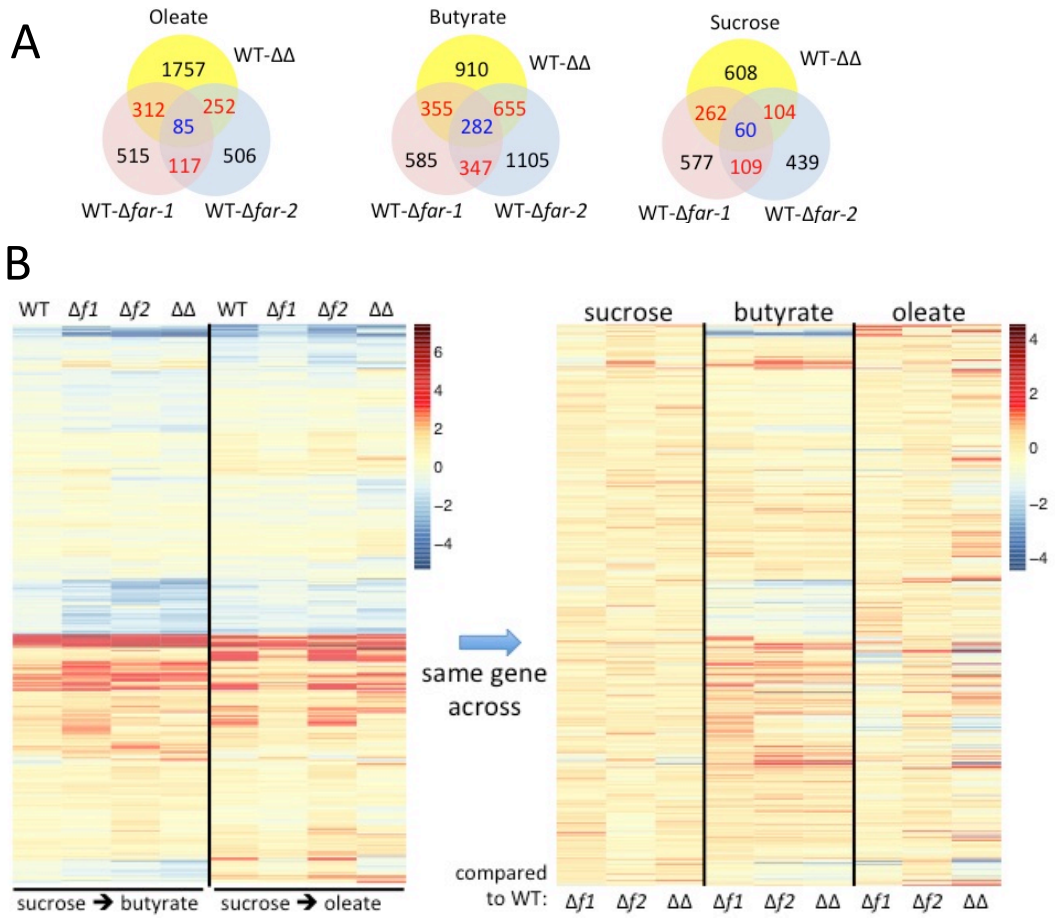

Figure 3.13: RNA-sequencing data summary: FAR-1 and FAR-2 can both decrease and increase transcript levels of specific genes

(A) Cuffdiff analysis of *far* mutants compared to wild type showing the transcripts that differ significantly in their expression level in different carbon sources. Wild type cDNA counts (FPKM) were compared to those in Δ*far-1,* Δ*far-2*, and the double Δ*far-1;* Δ*far-2* mutant (ΔΔ). (B) Heat maps of transcript levels of genes near intervals with both FAR-1 and FAR-2 ChIP peaks. Expression is represented as $\log_2$ (fold change FPKM), with blue showing a decrease in level from first condition to second condition listed in the lower labels (eg, WT in sucrose compared to WT in butyrate). Comparisons of expression in the strain indicated in sucrose and the same strain in butyrate and oleate are shown in the left panel. This is a reflection of how the transcript is changing as a result of carbon source only. The right panel shows the same genes as in the left panel but visualized by comparing expression of wild type to the single or double *far* mutant in the same condition. Genes both increase and decrease relative to WT upon loss of FAR-1 and/or FAR-2 functionality. Genes are the same horizontally from the left heat map to the right. Scales in the right panel were set to ± 4.5 for comparison.

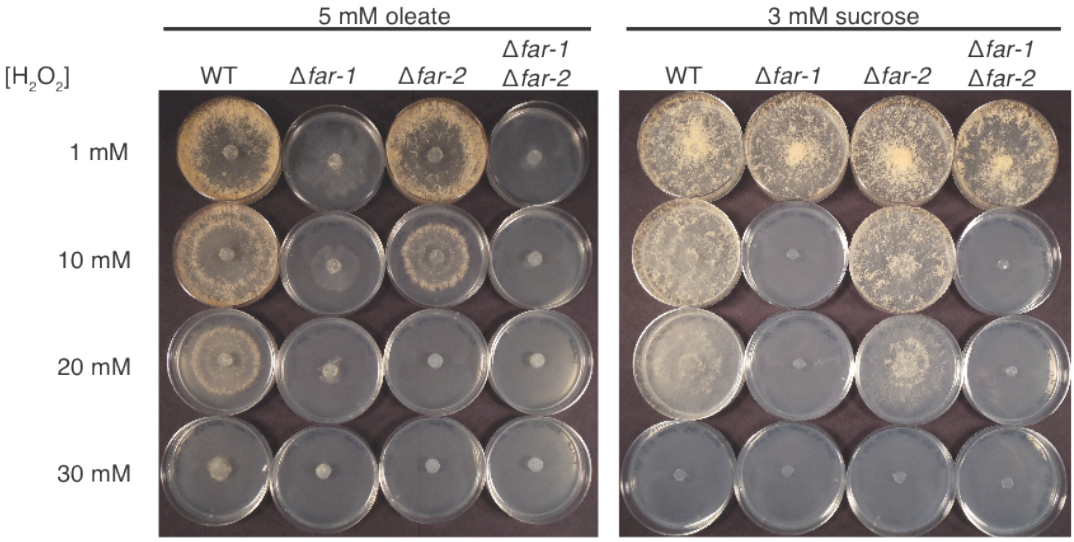

Figure 3.14: *Δfar-1* is susceptible to hydrogen peroxide stress
Linear growth and conidiation are affected in the presence of increasing concentrations of hydrogen peroxide in media with oleate as carbon source (left panel). This response is less robust on sucrose medium (right panel).

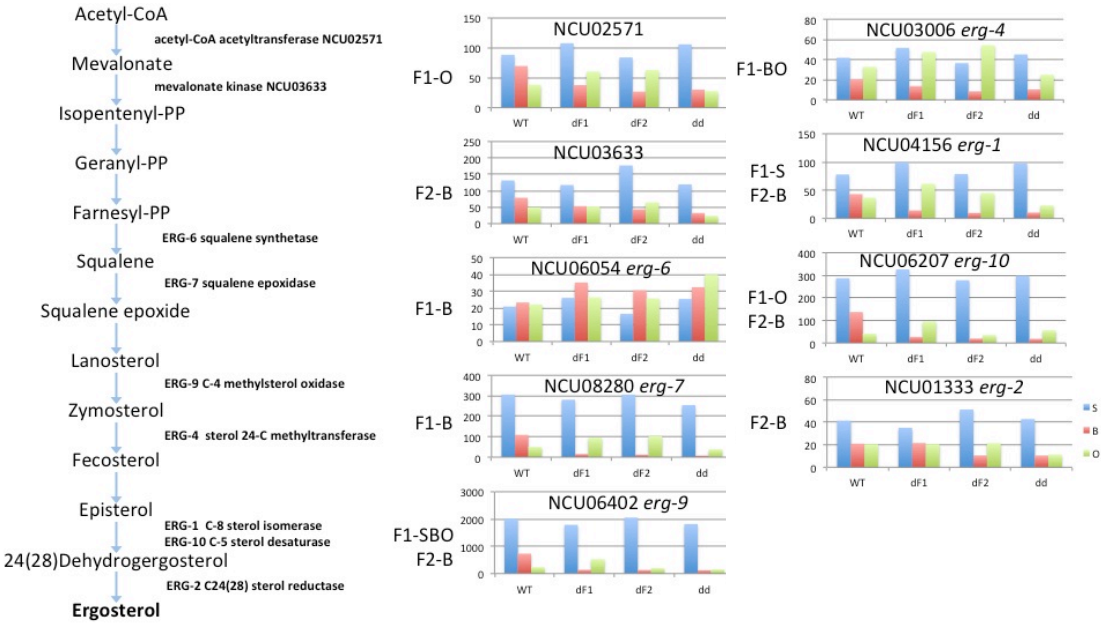

Figure 3.15: Expression levels of transcripts encoding enzymes in the ergosterol pathway in *far* mutants

Genes represented are near ChIP peaks either for FAR-1, FAR-2 or both noted to the left of each bargraph. Transcript levels change significantly between RNA-seq conditions in at least one comparison: carbon sources for a single strain or between strains in one condition.

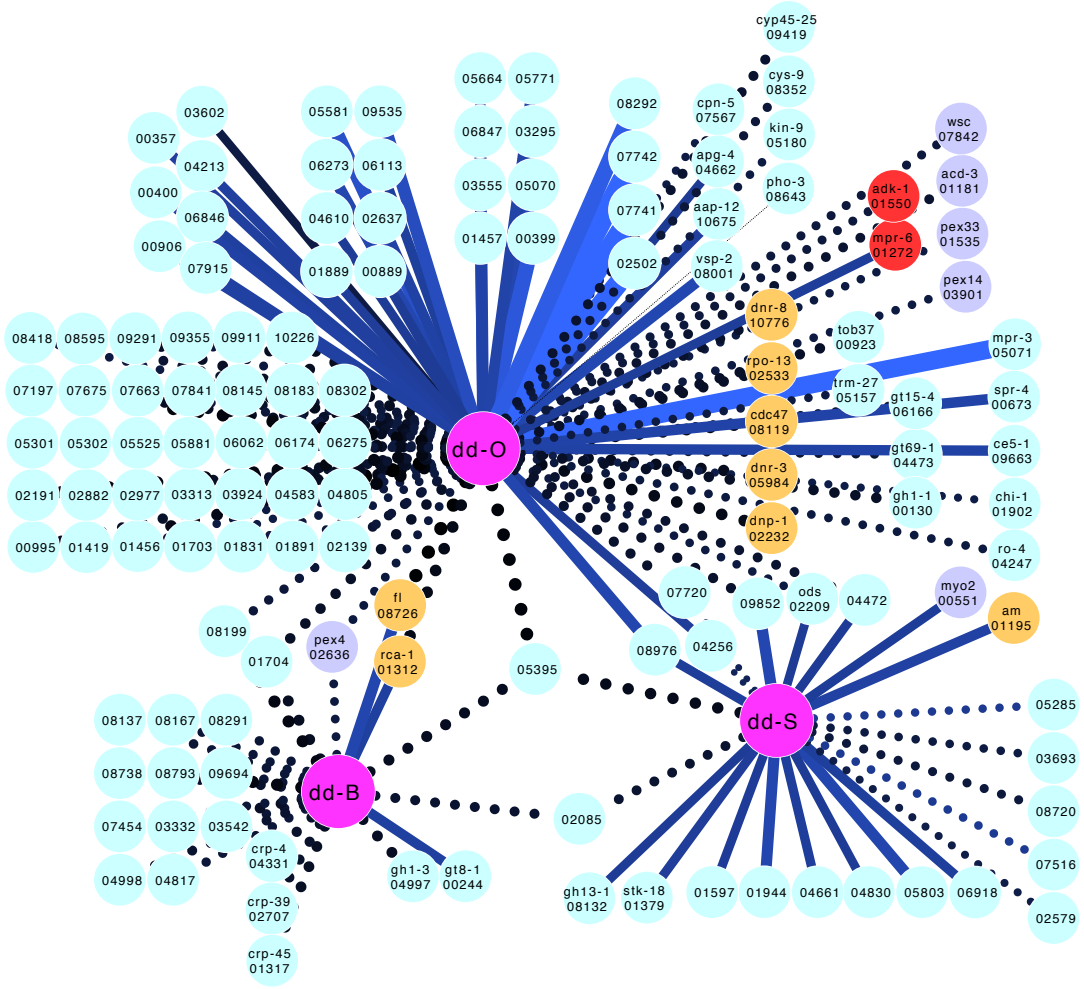

Figure 3.16: FARs redundantly regulate genes
Transcript levels of FAR ChIP targets (bound by both FAR-1 and FAR-2) in the Δ*far-1; Δfar-2* (ΔΔ) mutant were significantly different from those in wild type, but not from either of the single Δ*far-1* or Δ*far-2* mutants. The majority of transcripts displaying redundant regulation are found in oleate, leading to the suggestion that FAR transcriptional activity is most essential for normal growth on this carbon source. Fuchsia: treatment of the Δ*far-1; Δfar-2* mutant in which connected nodes changed significantly, Red: mitochondrial protein, Purple: glyoxysome protein, Orange: nuclear protein, Teal: no designated location. Connector lines (edges) denote the relationship between expression levels in wild type and ΔΔ: wider dotted and blacker is a decrease in expression in ΔΔ compared to wild type; Solid and more blue is an increase in ΔΔ relative to wild type. NCU numbers are represented by digits. Gene names are noted where applicable. Particularly of note is the myo2 protein that was found associated with the peroxisome pore import protein pex14. [197]. Of a total 134 genes, 15 pairs of genes (30 or 22%) are found located directly adjacent to one another, suggesting co-regulation.

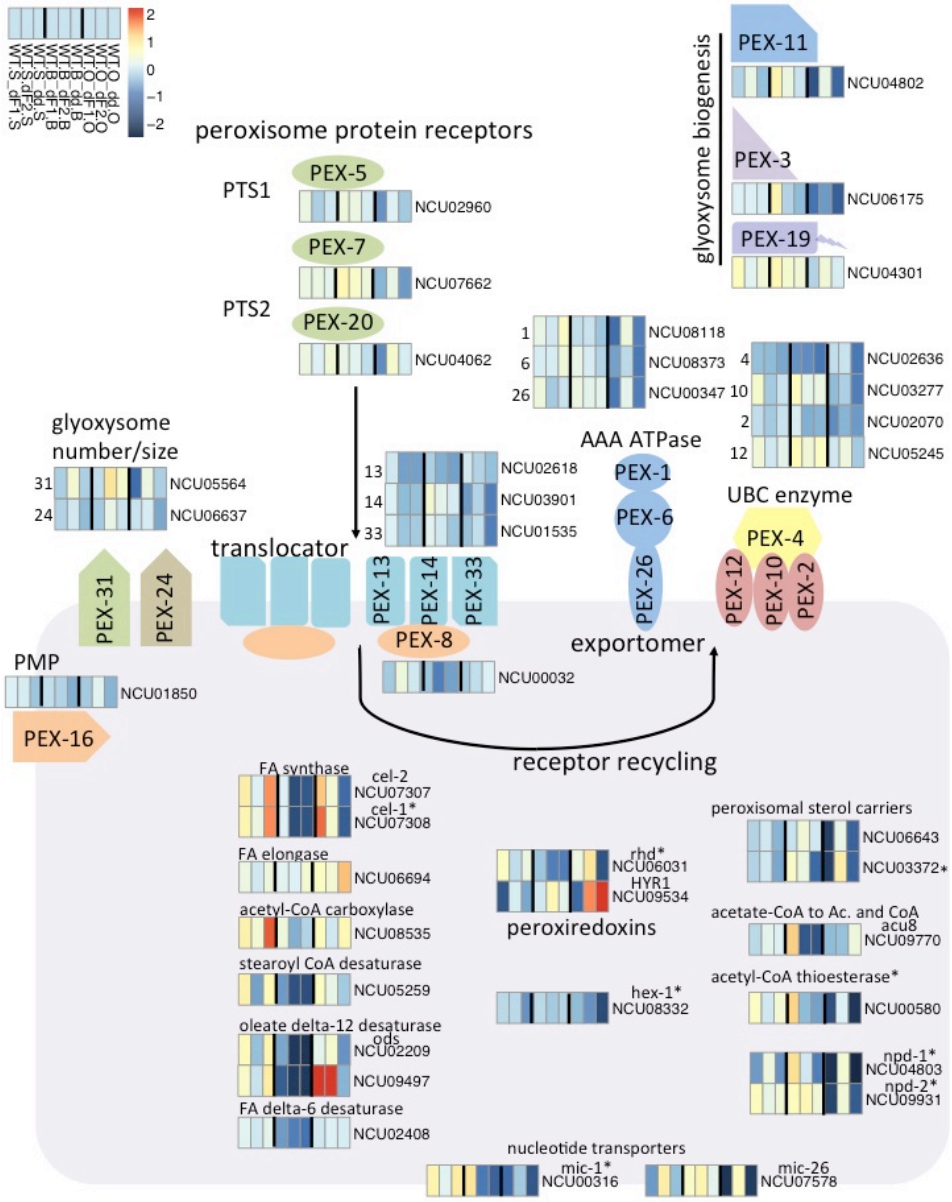

Figure 3.17: Peroxisome import machinery, and pex proteins identified for peroxisome/glyoxysome biogenesis and content maintenance

Gene names marked with an asterisk (*) have been experimentally localized to the glyoxysome [141]. Arrows indicate the presumed delivery path of peroxisomal proteins, and recycling of the import receptors (PTS1 and PTS2 types) via ubiquitination and ATPase activity of the exportomer [198]. The glyoxysomal lumen is depicted with localized detoxification, fatty acid synthesis and desaturation enzymes. Vertical black bars on each expression level heatmap divide carbon sources: sucrose, butyrate, and oleate left to right represented for each mutant relative to wild type. Legend at top left corner shows a value of zero on the $\log_2$(change) scale used to color the mini-heatmaps. Values and significance of comparisons are detailed in table 3.1.

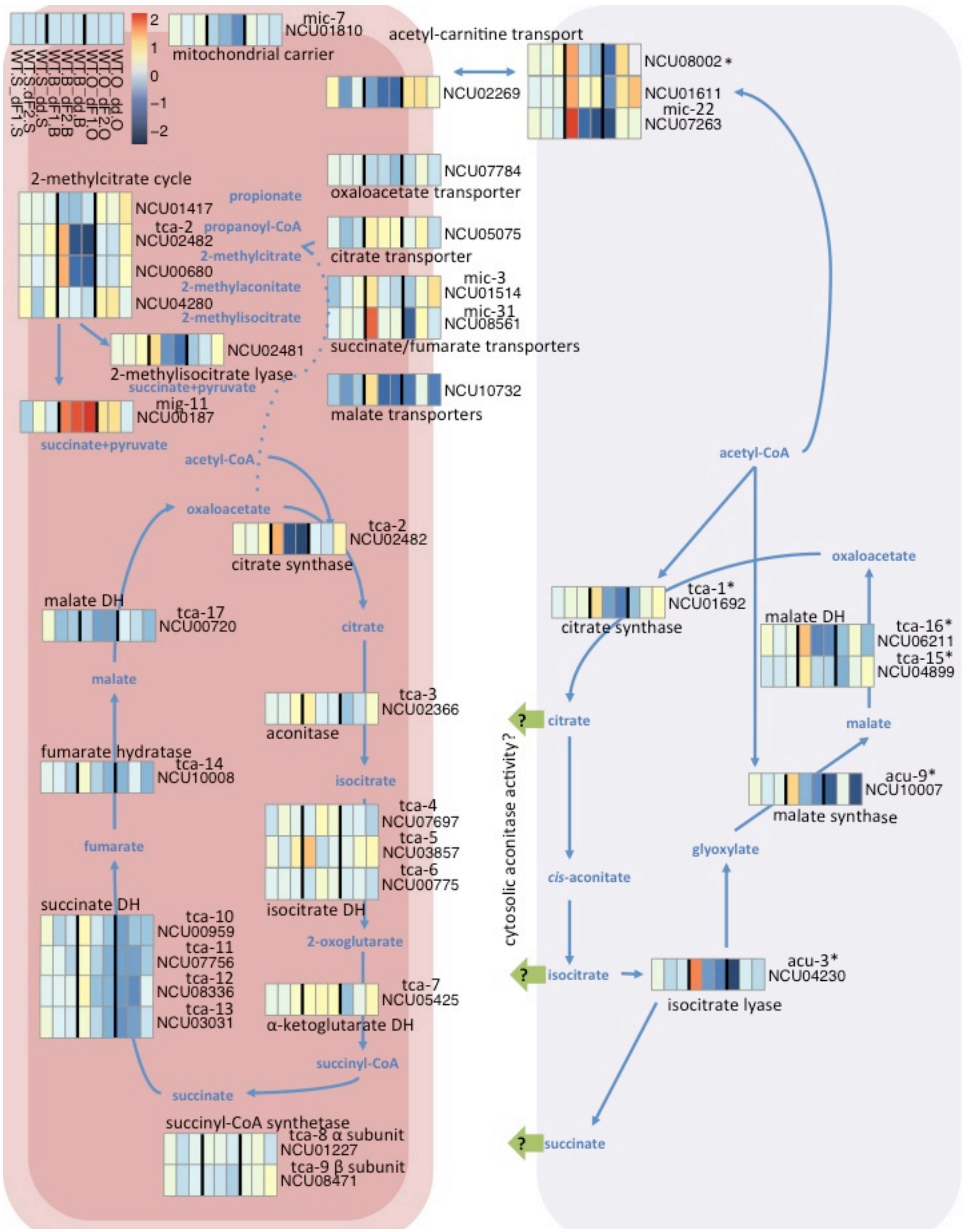

Figure 3.18: Expression levels of the mitochondrial TCA cycle and glyoxylate bypass in *far* mutants

The TCA cycle and 2-methylcitrate cycle enzymes are depicted in a mitochondrion (pink, left), as well as known transporters for TCA cycle intermediates associated with the inner mitochondrial membrane (top). Glyoxylate bypass enzymes (purple, right) and acetyl-CoA transporters annotated as being associated with the glyoxysome. Gene names marked with an asterisk (*) have been experimentally localized to the glyoxysome [141]. Vertical black bars on each expression level heatmap divide carbon sources: sucrose, butyrate, and oleate left to right. DH: dehydrogenase. Values and significance of comparisons are detailed in table 3.2.

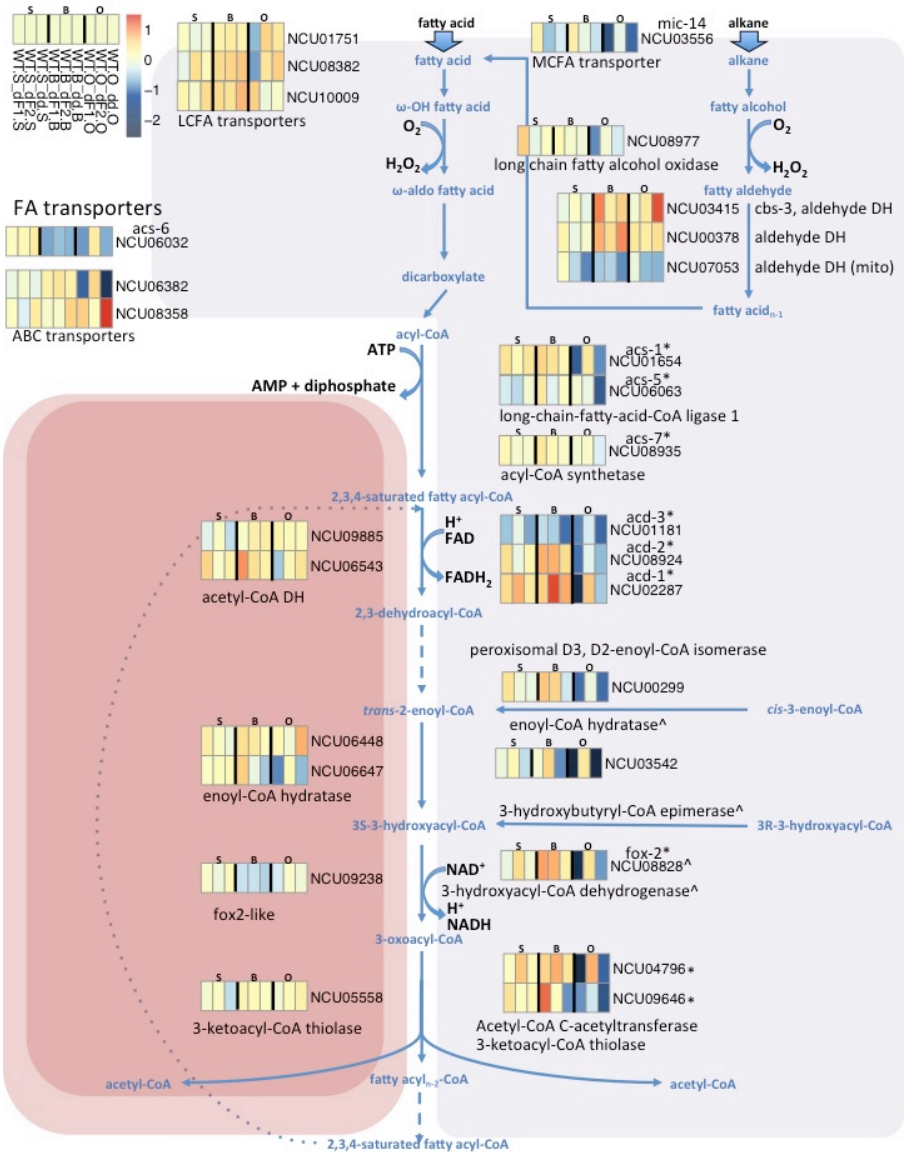

Figure 3.19: Expression levels for enzymes involved in omega-oxidation, and beta-oxidation in *far* mutants

In Neurospora, β-oxidation processes are found in both the mitochondrion (pink, left) and the glyoxysome (right). Conditions in each box of individual heat maps are as found in the legend, colored according to the $\log_2$ (fold change FPKM) in expression between WT and each mutant strain for sucrose, butyrate and oleate carbon sources. These reactions serve to reduce electron carriers to fuel the TCA cycle, and produce acetyl-CoA for biosynthetic reactions. Dashed blue lines are spontaneous reactions, the dotted line re-starts the cycle. The multifunctional enzyme FOX-2 carries out three reactions marked with (^). Gene names marked with an asterisk (*) have been experimentally localized to the glyoxysome, DH: dehydrogenase. Values and significance of comparisons are detailed in table 3.3.

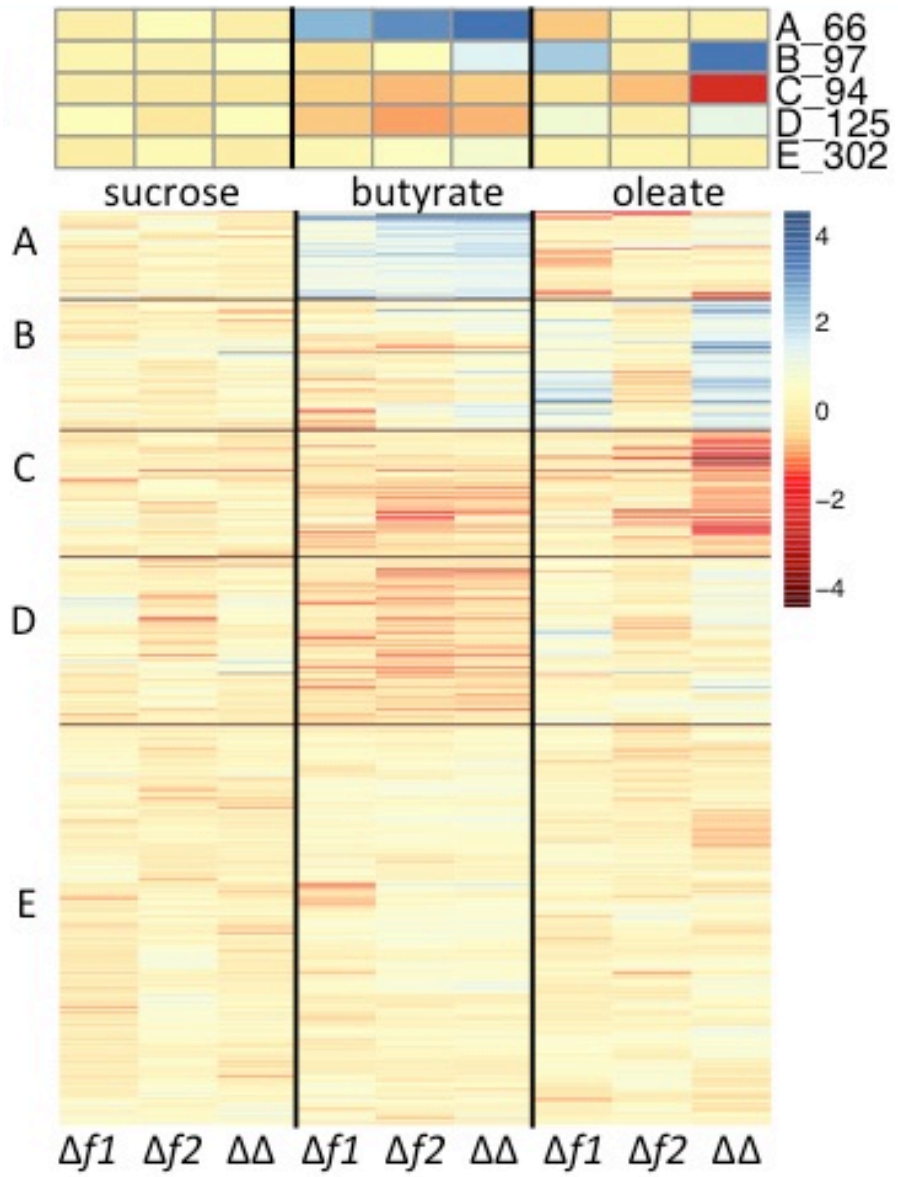

Figure 3.20: RNA-Sequencing clustering of ChIP target genes produces five gene expression centers

Expression data from the right panel of 3.13 was clustered around 5 centers, yielding these averages after 5000 repetitions using a minimal squared distance from the center, pictured top. The number of genes in each cluster is reflected to the right of the letter denoting each center, top. General trends for gene expression in each cluster include: A: FAR dependent regulation in butyrate (Figure 3.21), B: FAR-1 dependent regulation in oleate (Figure 3.22), C: FAR repression in oleate or a secondary activator (Figure 3.23), D: FAR repression in butyrate or a secondary activator and FAR-1 dependence in oleate (Figure 3.24). E: minimal change under experimental conditions tested.

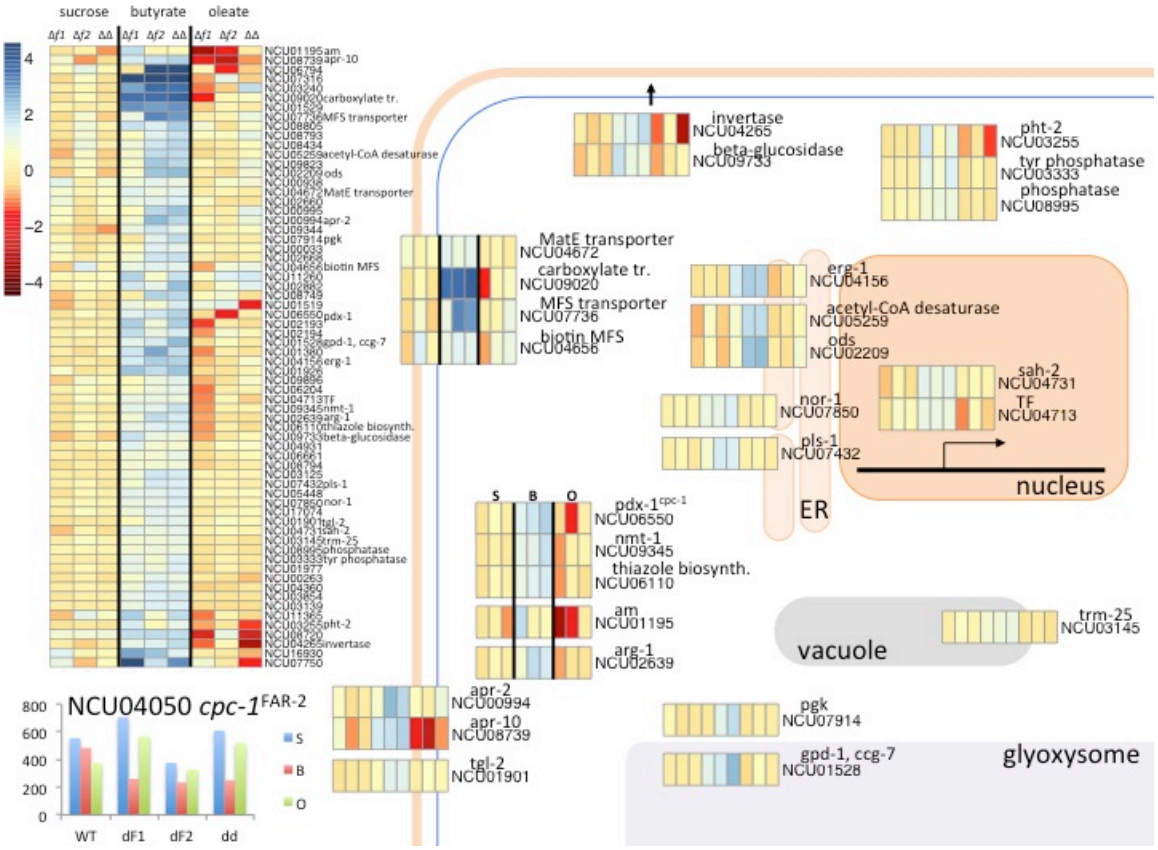

Figure 3.21: Cluster A heatmap with subcellular depiction of transcript levels
Heatmap (left) produced based upon $\log_2$(expression change) between wild type and FAR mutants and conditions listed at the top of each column from centers determined in Figure 3.20. Gene products depicted within the cell are labeled next to a corresponding NCU number. Genes in this grouping show transcript levels lower than wild type in butyrate without FAR functionality. Cluster A contains genes encoding protein functions of transport, polysaccharide cleavage, transcription factor activity, fatty acid modification, amino acid biosynthesis, phosphatase activity, protease and lipase activity and glycolysis/gluconeogenesis enzymes. Altered expression of transcription factor *cpc-1* in butyrate in the FAR mutants may be an instance of a secondary regulatory effect on amino acid biosynthetic enzymes. The solid orange line represents the cell wall, while the blue line inside it represents the plasma membrane.

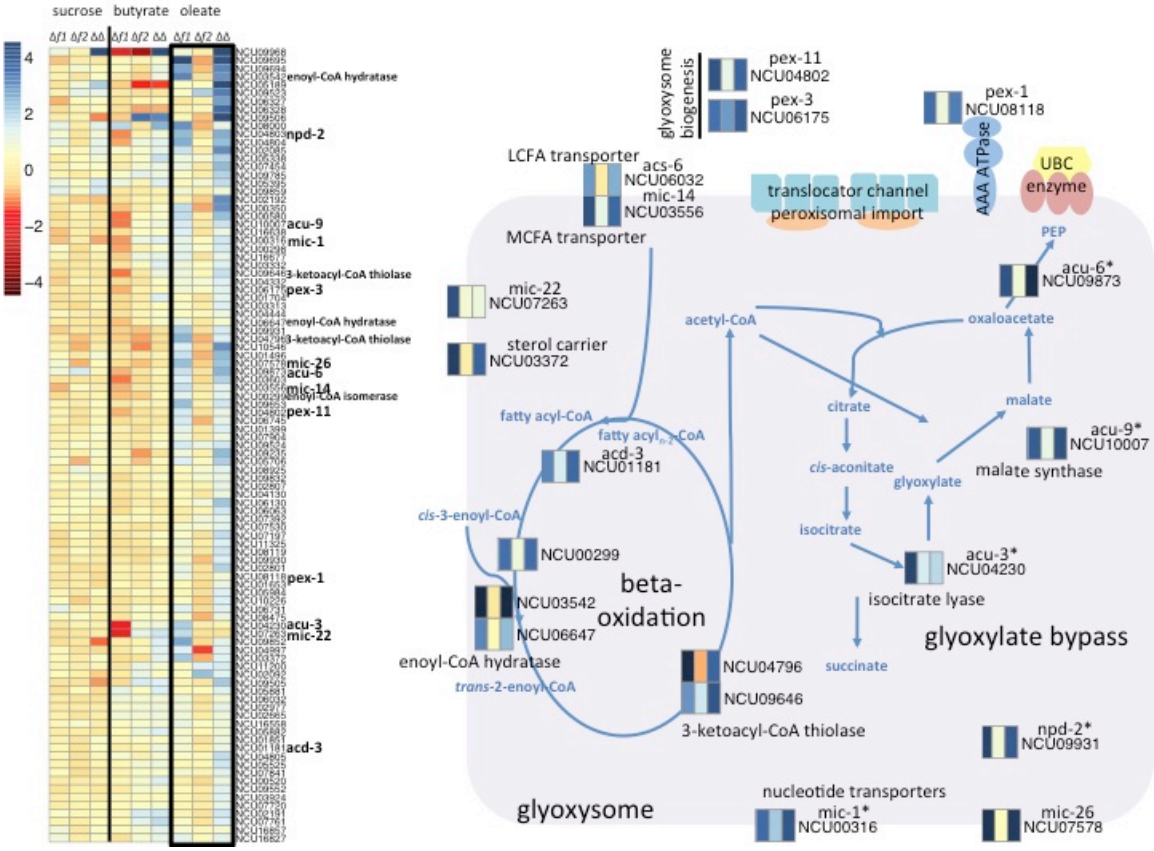

Figure 3.22: Cluster B heatmap with subcellular depiction of transcript levels
Heatmap (left) produced based upon $\log_2$(expression change) between wild type and FAR mutants and conditions listed at the top of each column from centers determined in Figure 3.20. Gene products depicted within the cell are labeled next to a corresponding NCU number. Genes in this grouping show transcript levels lower than wild type in FAR-1 mutant strains in oleate. Cluster B contains genes encoding protein functions of beta-oxidation and the glyoxylate bypass, nucleotide and carbon source transport, pex proteins for glyoxysome biogenesis and population, and detoxification activity. The light purple compartment represents the glyoxysome of *Neurospora crassa*, or the non-catalase containing microbody similar to the peroxisome in other organisms.

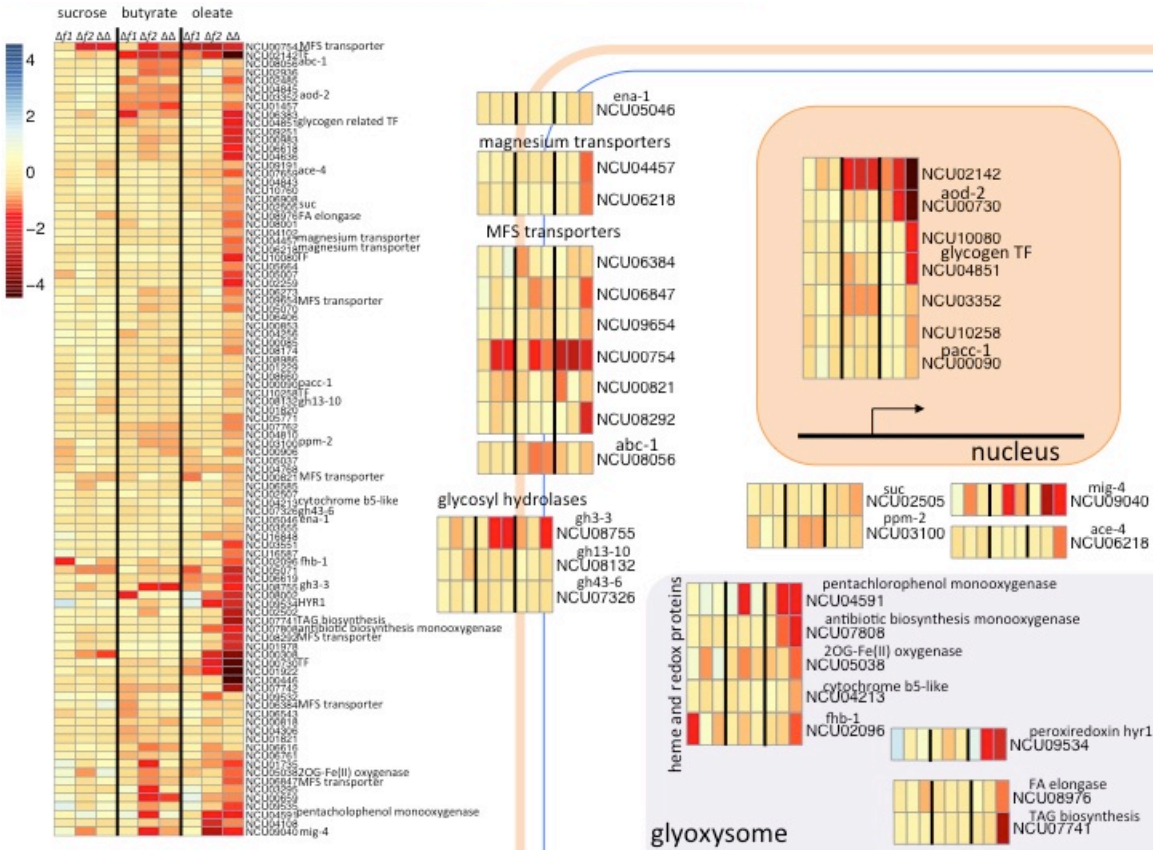

Figure 3.23: Cluster C heatmap with subcellular depiction of transcript levels
Heatmap (left) produced based upon $\log_2$(expression change) between wild type and FAR mutants and conditions listed at the top of each column from centers determined in Figure 3.20. Gene products depicted within the cell are labeled next to a corresponding NCU number. Genes in this grouping show transcript levels higher than wild type levels particularly in the Δ*far-1*; Δ*far-2* mutant in oleate (far left column). Cluster C contains genes encoding protein functions of transcriptional regulation, metal and small molecule transport, polysaccharide hydrolysis, fatty acid biosynthesis, reduction-oxidation activity, response to reactive oxygen species, and glycolysis. The solid orange line represents the cell wall, while the blue line inside it represents the plasma membrane.

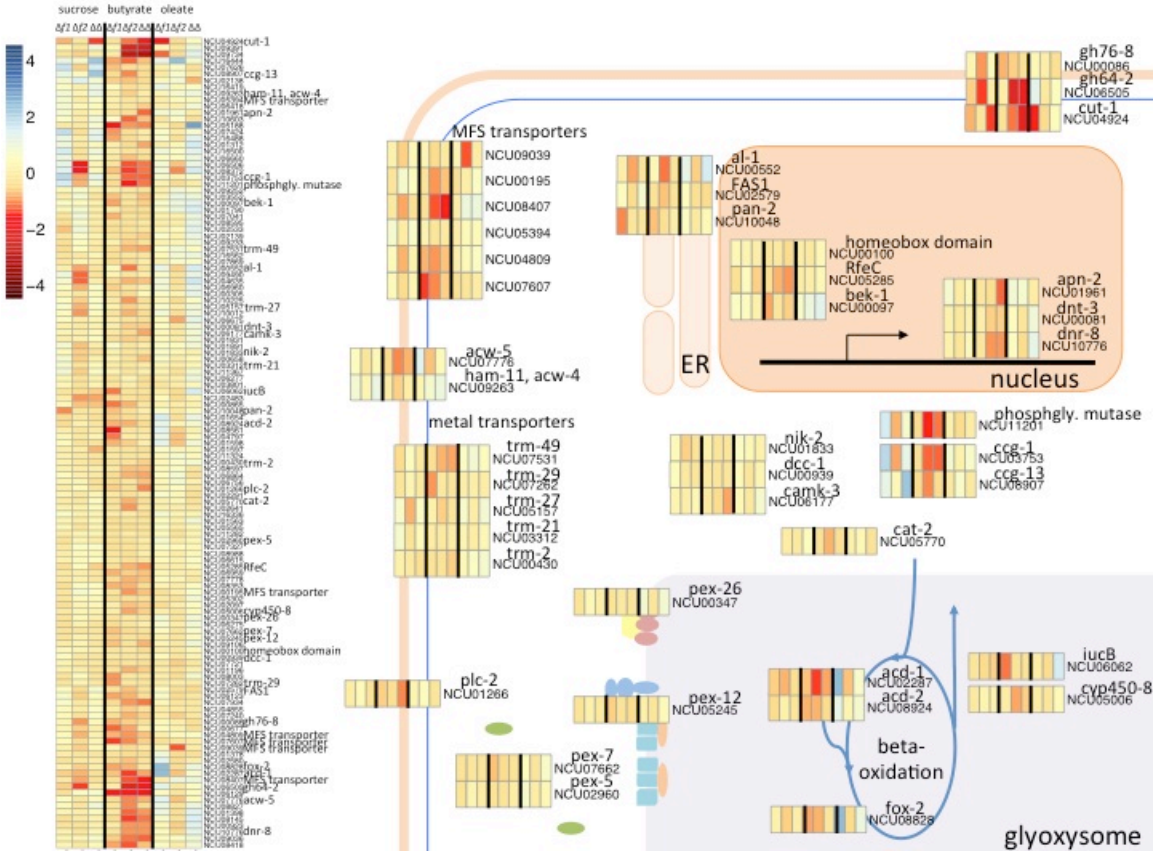

Figure 3.24: Cluster D heatmap with subcellular depiction of transcript levels
Heatmap (left) produced based upon $\log_2$(expression change) between wild type and FAR mutants and conditions listed at the top of each column from centers determined in Figure 3.20. Gene products depicted within the cell are labeled next to a corresponding NCU number. Genes in this grouping show transcript levels higher than those in wild type in butyrate, and lower than wild type in FAR-1 mutants in oleate or sucrose. Cluster D contains genes encoding protein functions of transcriptional regulation, DNA repair, polysaccharide cleavage, metal and small molecule transport, kinase activity, clock output proteins, glyoxysome protein trafficking and transport, beta-oxidation, and biosynthesis of carbon-rich products. The solid orange line represents the cell wall, while the blue line inside it represents the plasma membrane.

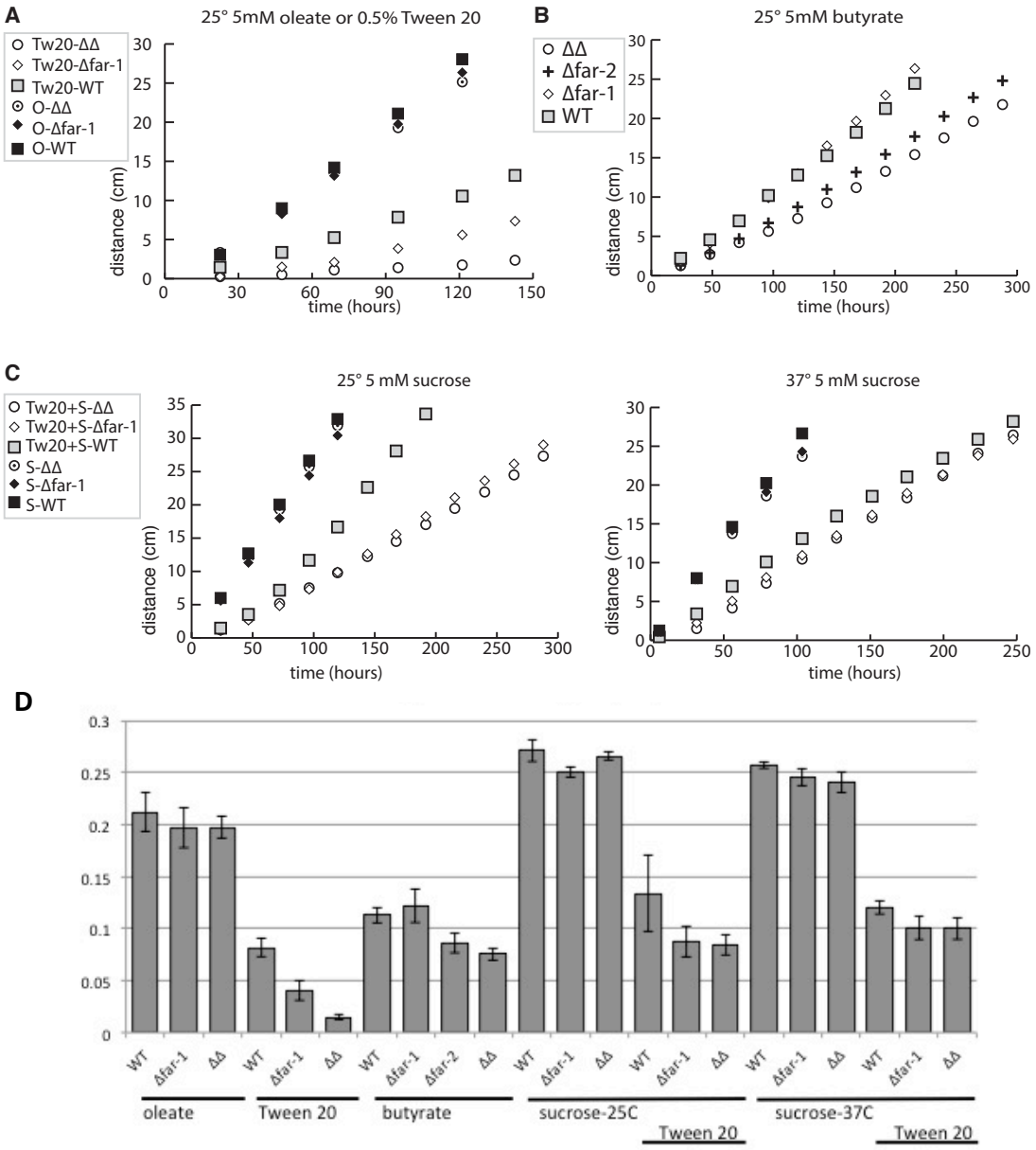

Figure 3.25: Linear growth of *far* mutants

(A) Linear growth of wild type (WT), Δ*far-1*, and Δ*far-1;* Δ*far-2*(ΔΔ) strains on oleate (O) or Tween-20 alone. The Δ*far-1* strain shows a Tween20-dependent slower growth rate. Δ*far-2* growth followed that of WT (not shown, see Figure 3.26). (B) Linear growth of WT, Δ*far-1*, Δ*far-2*, and ΔΔ on butyrate. (C) A test of temperature dependent growth rates on sucrose (S) and sucrose with Tween 20. Within this temperature range, sensitivity to Tween 20 with strains grown at room temperature decreases to equivalent growth rates at 37°C. (D) Growth rates in cm/hr from race tube assays shown in A to C. Standard deviations are indicated. Experiments were replicated 3 times.

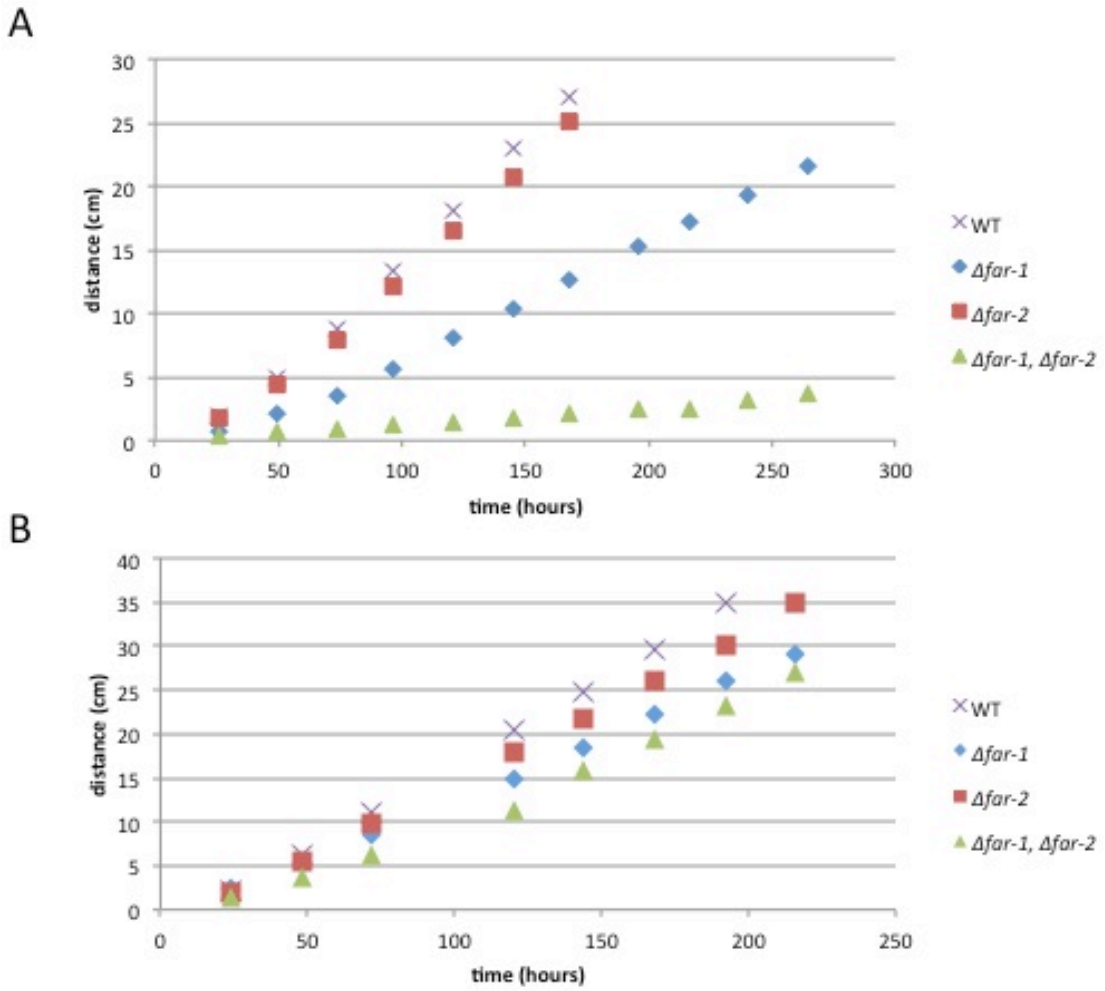

Figure 3.26: Additional race tube experiments show wild type and Δfar-2 grow at the same rate on oleate + 0.5% Tween 20, and growth rates are similar for all strains on Tween 80.

(A) Linear growth rates of strains with genotypes of Δ*far-1*, Δ*far-2*, and Δ*far-1;* Δ*far-2* on 5 mM oleate + 0.5% Tween 20. Wild type and Δfar-2 strains grow at a similar rate while in the presence of Tween 20, while strains with a *Δfar-1* mutation show a growth rate defect. The double mutant Δ*far-1;* Δ*far-2* growth rate defect is greatly decreased compared to that of Δ*far-1* suggesting an additive effect without FAR-2. (B) Strains in race tubes with 5 mM oleate and 0.5% Tween 80 grow at a similar rate.

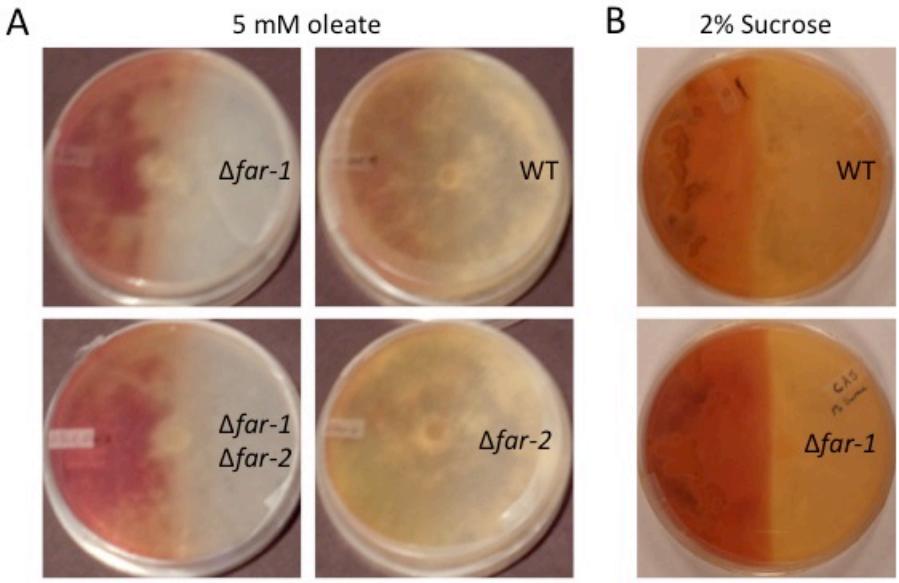

Figure 3.27: Δ*far-1* siderophore secretion is reduced
Plates of CAS (left half of plates) and VMM (right half) agar were inoculated with agar plugs of strains of interest to show secretion of siderophores either on 5 mM oleate (A) or 2% (w/v) sucrose (B). The decrease in siderophore secretion of Δfar-1 is not carbon specific, but is more pronounced on oleate.

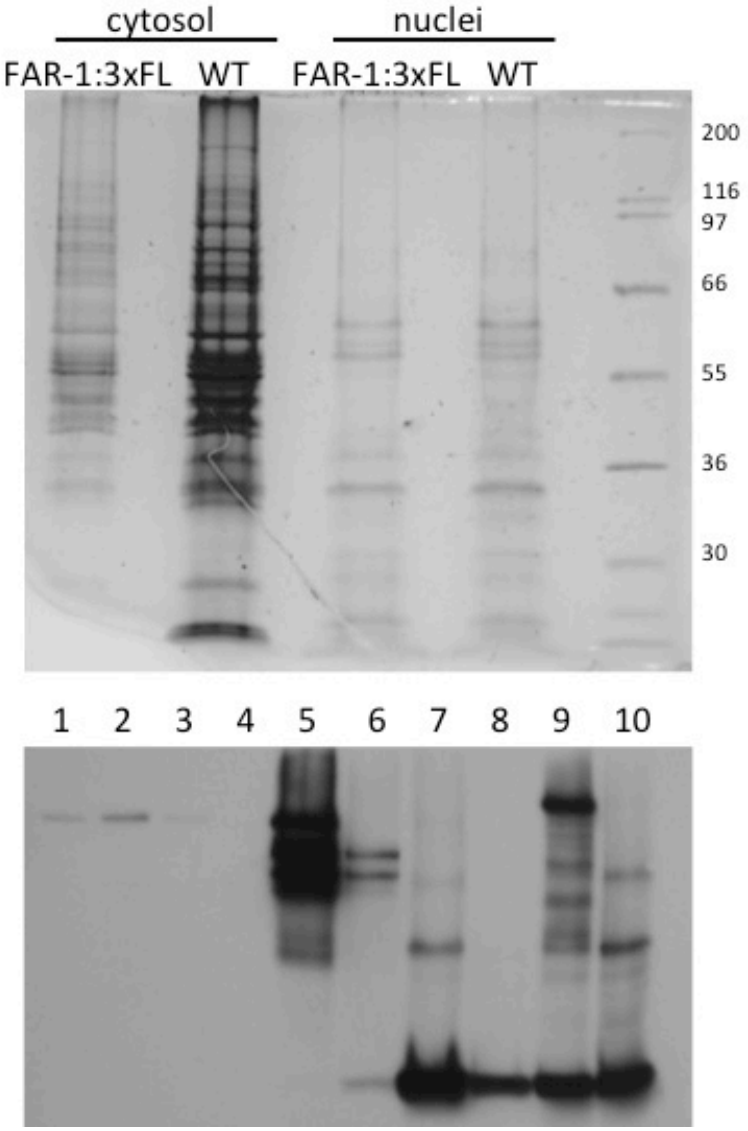

Figure 3.28: Silverstain and western of FAR-1-3xFL immunoprecipitation
Top: Silverstain of protein from a FLAG isolation of FAR-1/3xFL with nuclear isolation. No enrichment for the transcription factor is visible on the gel, but it can be detected by western blot. Image is representative of gels for other FLAG isolations. Bottom: Western blot of TEB97.5 (NMF658), FAR-2-3xFL in a nuclear isolation and FLAG immunoprecipitation in preparation for mass spectrometry. Lane contents are as follows: 1:second pellet 2:first pellet 3:far-2 Whole Cell Extract 4:Ladder 5:far-2 'cytosol' supernatant from nuclear extract 6:wild type 'cytosol' 7:FAR-2 nuclei grown in butyrate 8:wild type nuclei grown in butyrate 9:FAR-1 nuclei grown in sucrose (positive control) 10: wild type nuclei grown in sucrose.

Chapter 4: Discussion: Transcriptional Networks Controlled by the Fatty Acid Regulators, FAR-1 and FAR-2

ChIP finds sequence specific genome-wide binding of the FARs

ChIP- and RNA-sequencing informs us about FAR binding to chromatin and the effects on transcription that these TFs exert. However, the characterization of a specific phenotype caused by a fatty acid regulator is a challenge. Many of the genes that are regulated by FAR-1 and FAR-2 encode core metabolic enzymes, such as TCA cycle proteins, and are not solely regulated by FAR activity. RNA sequencing suggests that the FARs most often are activators, but can also either act as repressors or activate expression of a repressor that in turn acts to suppress transcription of genes under the conditions I tested (Figure 3.13B).

Fatty acid metabolism has attracted attention before this study, as outlined in the introductory chapter. Previously, *A. nidulans* FarA and FarB had been shown to regulate two genes of the glyoxylate cycle, five genes required for beta-oxidation, the peroxin *PEX11*, and several acetyl-CoA/carnitine transporters. Findings with *C. albicans* and *Y.lipolytica* echoed these findings, as homologs of the above genes as well as additional genes (e.g. *PEX5*) were identified as FAR targets [104], [105]. Two plant pathogens, *A. oryzae* and *F. oxysporum*, have been functionally studied for lipase regulation relevant to pathogenicity and breakdown of plastics [114], [199]. I set out to accomplish a genome-wide analysis of FARs, with the goal to dramatically increase the knowledge of genes directly or indirectly regulated by *N. crassa* FAR-1 and FAR-2. One prediction was that my study would result in detailed and better understanding of fungal transcriptional networks that govern fatty acid anabolism and catabolism. One way this was accomplished was through increasing what we know about the number and types of genes associated with FAR binding sites by ChIP and GO analysis.

It is acknowledged that the program (FunCat, http://mips.gsf.de/cgi-bin/proj/funcatDB/search_advanced.pl) used for assessing *N. crassa* gene ontologies is

outdated. The tools available for Neurospora-specific functional categorization also limit the size of web-submissions. I took this into account by obtaining the functional categories database for Neurospora, and adding the most recent annotation from the Neurospora crassa genome (Broad Institute). However, in light of the large portion of the genome—nearly 10%—which is potentially affected if all FAR binding sites are active, a limitation to more significant peaks was warranted. That being said, as I discussed for PEX proteins, the strongest binding by ChIP does not mean strongest induction or repression of transcription. Refined analyses using re-construction of the unmaintained functional category database has confirmed what I found in early analyses.

RNA-sequencing models transcript expression as affected by *far* mutants in metabolic and biosynthetic pathways

Promoters of *pex* genes are strongly bound by FAR-1 but are not the most affected in a *far-1* mutant

The peroxisomal import machinery is particularly important for transporting the enzymes of the glyoxylate cycle into the lumen of the glyoxysome. In *C. albicans*, a lack of *pex5* will cause retention of isocitrate lyase (Icl) and malate synthase (Mls) in the cytosol [200]. Interestingly, this does not hinder their function, in that these strains are able to grow on ethanol and acetate. However, on medium with long fatty acid chains, a lack of these enzymes does present a problem. Under these circumstances, Tween 20 and oleate slow or stop growth of *C. albicans Δicl* strains, as their compartmentalization is required for efficient use of beta-oxidation products [105]. Woronin body formation and function—to plug septal pores after hyphal damage—is dependent upon formation of a large hexagonal crystal of the protein HEX-1 (NCU09228). PEX-1 localization within microbodies is dependent upon the function of the pore and receptor transport protein PEX-13, as Δ*pex-13* resulted in HEX-1 localization in the cytosol [201].

Enzymes involved in omega-oxidation, such as aldehyde dehydrogenase may be active in ethanol degradation in the peroxisome in other organisms [202]. cbs-3 (NCU03415) or carnitine biosynthesis-3, NCU07053, and NCU00378, however, are downstream of detoxification by catalases, which have been shown to occur in aerial hyphae and conidia, and bound to cell walls, specifically not in the microbodies [184]. Evidence suggesting this may be only part of the story is in the co-purification of cat-4 with the woronin body protein hex-1 [184]. More localization studies are needed.

Lipid metabolism requires access to enzymes or substrates by transporters

While two-carbon (2C) carbon sources such as acetate and ethanol are metabolized by enzymes in the cytosol and the mitochondrion, longer fatty acids are first taken into the cell by non-vesicular transport mechanisms (e.g. NCU06032, *acs-6*). Fatty acids may be acted upon in the cytosol or transported into the lumen of the glyoxysome by fatty acid-CoA transporters such as the half ABC transporters NCU01751 and NCU08382 [203], [204]. In *Candida boidinii* Δ*pmp47*, levels of beta-oxidation were affected on laurate, a medium chain fatty acid; this effect disappeared when the peroxisomes were permeabilized with Triton-X100, leading to the conclusion that Pmp47 is involved in the conversion of laurate to lauroyl-CoA [203] N. *Neurospora* MIC-14 (NCU03556) is the homologue of yeast peroxisomal membrane protein Pmp47, and also a target of both FAR-1 and FAR-2 binding by ChIP.

In order to draw any correlation between degree of differential expression and destination compartment, a parallel dataset of enzymes localized to microbodies specific to my experimental conditions would be necessary. This is an instance where bioinformatics and gene ontology data may be misleading, and experimental data is the most informative. Proteins with PTS1 and PTS2 signals were localized to Neurospora glyoxysomes, but constituted just half of the identified lumen contents while the remaining proteins were PTS-less [141]. A number of the PTS-less proteins are part of

the TCA cycle and glyoxylate bypass such as citrate synthase TCA-1 (NCU01692), and malate dehydrogenase subunits TCA-15 (NCU04899) and TCA-16 (NCU06211).

Though we have uncovered a lot of interesting biology, a lot of it remains to be verified, including direct links to gene regulation. As an example, the extreme over-expression (*tgl-1* and *cea-2*, Figure 13.7B) seen for some of the FAR targets as determined by ChIP is similar to that for other transcripts that do not have FAR binding sites and thus no direct connection with FAR-1 or FAR-2 (NCU02333 or *arg-1*, NCU00194 or *ota*, NCU00762, and several genes involved in ergosterol biosynthesis). Assuming a core six-nucleotide recognition site, the likelihood of finding the consensus binding sequence for FARs is $(1/4)^6$, or once in every 4096 bases; because the binding sequence can be recognized on either strand the likelihood is closer to twice this. Given the size of the genome, which is close to 44 Mb, the binding site should occur at least 10,742 times. As a result, it is no surprise that many binding 'peaks' are called, in fact on the order of thousands of peaks, when using a programmed peak caller such as MACS2 [164]. Deciphering which of these peaks are real requires the use of a reporter assay. Previous work by Hynes et al focused on direct response of transcriptional activity to different fatty acids by means of a reporter.

Replicates of cultures for RNA extraction for a total of twelve different conditions—four strains in three carbon sources--were grown separately over the course of several days. Though the environmental variation can be high, even in incubators, a true biological response should be resolvable from day-to-day variation that does not occur as a result of the treatment. The RNA- sequencing overview is reflective of the conjunction of both ChIP and RNA sequencing data by the filter of genes near FAR ChIP peaks. Future experiments could test the self/sister regulation by ablation of the DNA consensus motifs near each gene, and assaying transcript levels of FAR-1 and FAR-2 in oleate and butyrate.

Further testing the mechanism underlying FAR activation

To address the question of how the two FAR transcription factors are regulated, one of the first possibilities for regulation of activity could be by phosphorylation. I performed a western blot of FAR-1 (size 115 kDa) with and without phosphatase treatment using CIAP (calf intestinal alkaline phosphatase) for 1 hour to remove phosphate modifications from the protein. The resulting band sizes showed no difference. Another approach I took was a native western blot to determine whether a potential complex containing an allosteric molecule would run at a different size if tissues were isolated from different carbon sources. ChIP was done in a number of experiments to test potential conditions that might affect FAR-1 binding, including deletion of *wc-2* (i.e. the gene encoding WC-2, one of the two TFs involved in the core oscillator regulating circadian rhythms), hydrogen peroxide treatment, and growth in different carbon sources. Formaldehyde reactivity with hydrogen peroxide removed any meaningful data (i.e. the ChIP-sequencing was genomic background) captured by formaldehyde crosslinking during ChIP. No obvious changes were detected as a result of the *wc-2* deletion, leading to the conclusion that FAR-1 specifically is acting independently of WC-2 activity, rather than in concert with it as a binding partner as suggested from results with *Nectria haematococa* [108] (Figure 2.6).

Phenotypes associate gene ontology to growth, stress response and development

Tween 20 susceptbility of Δ*far-1* may be membrane-based

The basis of the slow growth phenotype of *N. crassa* induced by Tween 20 seems to be a physical phenomenon, also seen as growth retardation in combination with rich carbon sources (Figure 3.25C). Work on other fungi can help to build a hypothesis as to the underlying cause of this phenotype. The FAR-1 homolog CTF1 in *C. albicans* has been shown to regulate beta-oxidation, and glyoxylate bypass enzymes [105]. The growth defect on Tween 20 has been found in *C. albicans* mutants for isocitrate lyase *icl1*, *fox2*, and *ctf1*. Serial dilutions on Tween 40 showed a slight decrease in survival for

the Δ*ctf1* strain compared to wild type, while the *icl1* and *fox2* mutants did not grow at all. Because the dominant side chain found in Tween 20 is the 12-carbon mono-laurate, defects in medium chain length fatty acid transport [203] or activation enzyme, i.e. Faa2 homolog ACS-1 (NCU01654, Figure 3.19) in the peroxisomal lumen may be a possible explanation for the growth defect [105], [121]. This defect would be relieved as chain length increases and regulation by FAR-1/CTF1 takes over, such as seen in growth on Tween 80 (Figure 3.26). The *C. albicans* mutants tested for growth on different types of Tween also are significantly regulated by the FARs in *N. crassa*, and decrease significantly in Δ*far-1* compared to wild type on oleate (Figure 3.18, *acu-3*; Figure 3.19, *fox-2*).

Mechanisms for toxicity of fatty acid in fungi include inhibition of beta-oxidation, inhibition of fatty acid synthesis, and insertion into fungal membranes [205]. It is thought that membranes containing lower amounts of sterols are more susceptible to insertion toxicity and underlying disorder [206]. The idea that the fatty acids themselves or an aberrant mix of membrane components are toxic is attractive given the phenotype of slow growth seen when multiple carbon sources are present, including agar, and either sucrose or oleate in addition to the carbon in the Tween 20 detergent (Figure 3.25 and Figure 3.26). This idea is supported by studies of ergosterol/cholesterol membrane content, which increases when organisms are exposed to higher temperature as a buffer for membrane viscosity [207], [208]. A temperature-dependent rather than FAR-dependent increase in ergosterol production might be an explanation for why higher temperatures relieved the growth defect relative to wild type (Figure 3.25C).

The energetically expensive production of ergosterol is dependent upon the presence of oxygen, functional heme cofactors, as well as a ready source of carbon precursors for assembly [208]. The Δ*far-1* strain exhibits phenotypes including decreased siderophore secretion, peroxide detoxification defects, and decreases in transcription of many relevant genes to ergosterol production and lipid modification

(Figure 3.15, Figure 3.17). These interrelated characteristics further support the hypothesis that the Tween 20 defect is membrane-based. This may be clarified by future quantification of the ergosterol and saturated/unsaturated lipid content of the membranes of the *far* mutants.

H_2O_2 stress susceptibility could have a variety of underlying causes

The multi-compartment localization of beta-oxidation, and TCA-glyoxylate cycle of *Neurospora* have evolved to interact with different substrates—shorter carbon sources and ethanol degradation for mitochondria, and longer fatty acids in the peroxisome [209]. Sequestration of these enzymes also helps to contain toxins and harmful byproducts that may damage other parts of the cell. Compartmentalization of enzymatic activities may be regulated by redox homeostasis, as suggested by the conditional splicing or translational of glycolysis enzyme transcripts containing a peroxisomal targeting signal in *Ustilago* [210]. The same proteins for *Neurospora* were found to conditionally contain PTS sequences through the same mechanisms when evaluated by GFP-expression fusions in yeast [210]. FAR-1 regulation is important to transcript levels of glyoxysomal enzymes of the glyoxylate cycle and beta-oxidation (Figure 3.17, Figure 3.18, Figure 3.19), namely malate synthase (*acu-9*), isocitrate lyase (*acu-3*), and malate dehydrogenases (*tca-15, tca-16*). Experiments cataloging the proteins associated with *Neurospora*'s microbodies, as well as parts of the peroxisomal import complex have dispelled many assumptions of protein localization [141], [197]. Conditions that might change localization of proteins from the cytosol to the glyoxysome have not yet been addressed. Bioinformatic placement of many of TCA cycle and metabolic enzymes to the mitochondrion raises the question of whether there are not other proteins that function in the glyoxysome which have not yet been found.

The reasoning behind testing hydrogen peroxide toxicity was linked to the beta-oxidation, antioxidant, and PEX protein ChIP targets found for FAR-1. Transcription of *pex* genes for proteins integral to the glyoxysome was shown to be negatively regulated

in a *far-1* mutant (Figure 3.17). Genes encoding enzymes that participate in detoxification of ROS also have binding sites, ROS which may be generated by beta-oxidation, light signaling, or exogenous sources. Subsequent RNA-sequencing work demonstrated that these genes are transcriptionally regulated. However, the phenotyping experiment does not address the mechanism or cause of what we observe, and in this way the genome-wide data set is both strong and weak. I can hypothesize about underlying mechanisms, however. At the level of a regulatory network, these causes are additive, and sometimes synergistic, and may have many contributing genes that each result in similar phenotypes. The strength of genome-wide data is that I may be able to uncover relationships between gene expression dynamics that are not obvious by other means.

The siderophore secretion defect of Δ*far-1* is caused by indirect regulation

Iron is a part of a heme cofactor, often found in enzymes catalyzing oxidation-reduction reactions [211]. Obtaining iron for biological use necessitates binding and endocytosis of iron atoms with an appropriate oxidation state, as well as maintaining an intracellular store for growing tissues. Neurospora has two primary siderophores, coprogen for secretion and ferricrocin for storage[212]. These molecules may be found in altered amounts within differentiated cells such as conidia[212]. Siderophores can be many different shapes, but have been found to be synthesized in the peroxisome [213]. Measure of the output of the secreted coprogen siderophore was qualitatively evaluated in this work (Figure 3.27). However, the step at which a FAR-1 mediated change occurred is uncertain, be it the transcriptional regulation of genes for biosynthesis, a defect in biosynthesis protein localization, a defect in the organelle for production, or secretion. For stricter measure of iron uptake, assays like Mossbauer spectroscopy may be employed [194]. An alteration in carbon source raises the possibility that the carbon requirements for siderophore biosynthesis are altered along with affecting the transcription of enzymes in ergosterol production (Figure 3.15) and

gluconeogenesis such as *pg*k (NCU09714) *gpd-1* (NCU01528) in a FAR-1 dependent manner. Work in *A. nidulans* on shows that PacC controls transcription of siderophore biosynthesis genes a pH dependent manner, with transcription occurring from an alkaline-detecting PacC mimic, but not an acidic-detecting mimic [214]. In *N. crassa*, the gene encoding PacC shows significant peaks for both FAR-2 and all conditions of FAR-1 (Figure 3.5), suggesting this may be an additional regulator affecting siderophore synthesis. Transcription of *pacC* is higher in the *far* double mutant than in the wild type strain, suggesting the FARs could be acting as transcriptional repressors. Indeed, there is also the possibility that PacC may incite yet another regulator. This is part of the work of TF network building, to clarify the complexity of response pathways *in vitro*.

Future studies may measure siderophore secretion more accurately from liquid medium, with a number of colorimetric assays that have recently become available such as the SideroTec kit from emergenbio, or for identification purposes, HPLC [213].

Perithecial development may be linked to peroxisomal function

FAR-2 seems to be necessary for perithecial development on butyrate. By testing perithecium formation, I did not simply test for genes that are functionally related to development of melanized sexual structures. I also challenged *N. crassa* to produce the necessary nutritional feedstocks and regulatory conditions for their development. FAR perturbation widely influences other regulators and metabolic enzymes alike. Interestingly, enzymes of the glyoxylate cycle and those implicated in channeling the necessary nutrients from lipid reserves to developing fruiting bodies are found in the peroxisome, and are also implicated in meiotic development [215]. Studies in *Gibberella zea* (anamorph *Fusarium graminearum*) have found the glyoxylate cycle essential to the breakdown of fatty acids, and the expression of isocitrate lyase of the glyoxylate shunt to be necessary for perthecial formation [215]. A *Podospora anserina pex2* mutant is sterile, because of the lacking of this RING-finger protein, which acts in recycling peroxin receptors back to the cytosol. Instead of fusing, nuclei dividing for

crozier formation make a “crozier tree”, and the fungus never undergoes meiosis [216]. Peroxisomes provide unique functions in different fungal lineages, maintaining appropriate levels of ROS for differentiation, and rounds of generation and clearance for use as a chemical signal [215]. Analysis of *pex* mutants, and mutants in proteins involved in carbon source trafficking, as well as the initial genes implicated in ascospore development under the conditions I used for crosses may shed more light on the failure to develop normal perithecia.

Chapter 5: General Conclusions: Transcriptional Networks Controlled by the Fatty Acid Regulators, FAR-1 and FAR-2

The detection, perpetuation, and response to environmental signals requires both fast response, like the opening of an ion channel, but also the slower activity of transcriptional change, altering the transcriptome, and subsequently the proteome of a cell on the order of minutes to hours. Through assays like ChIP, I have been able to take a snapshot of the probability that a sequence specific transcription factor (TF) will bind to DNA. However, this binding does not take place along a naked piece of DNA, but rather surrounded by other TFs, histone proteins, chromatin modifiers and remodelers, as well as DNA and RNA polymerases. We do not yet fully understand how TFs that occur in *cis* interact to compete or cooperate in their DNA binding activity. The work I presented here describes the activities of two TFs that bind the same consensus sequence, but cause outcomes unique to each protein. It is part of a growing body of work to characterize TFs in the filamentous fungus *N. crassa*.

Every cell is reliant upon transport proteins for access to carbon sources and micronutrients like iron. Transduction of nutritional substrate availability drives the combined activity of TFs that have evolved to recognize specific DNA sequence elements. Each TF may influence diverse genes in order to make the appropriate enzymes, cellular compartments, damage control proteins, and additional transporters for nutrient utilization. Using bioinformatic characterization of the genes potentially bound (as determined by ChIP-sequencing), followed by transcriptome characterization (by RNA-sequencing), I have greatly expanded the known network of genes influenced by the fatty acid regulators. Mutant analysis highlighted genes bound by FAR-1 and FAR-2, both individually and redundantly. Given the breadth of new functions associated with the FARs, I tested the influence of *far* mutants on linear growth rate, siderophore production, hydrogen peroxide stress, and sexual structure development. In future and ongoing work, I am characterizing the post-translational modifications of FAR-2 and

FAR-1 by mass spectrometry, which I hypothesize control transcriptional activator behavior, rather than "simple" binding to promoter sites.

The strengths of TF characterization

The combination of ChIP- and RNA-sequencing data is able to reveal much more about the outcome of TF interaction on genome-wide transcription than previous techniques available. This approach can be used to best effect in a genetically tractable organism like *N. crassa*, but can inform the logic networks of activators and repressor in transcriptional regulation throughout much of eukaryotic cell biology. I have been able to use the same computational and analytical techniques developed for the FAR proteins for a variety of other TFs. Each set of experiments has undertaken a test of conditions specific to the activation of one TF (ADV-1, light; AOD-2, chloramphenicol), which will assemble a cell-wide transcription factor network. With my annotation programs, I have generated a tool for quickly providing meaning to sequencing data.

Additionally, I catalogued a dataset that will better define the gap between TF binding and transcript production. I have genome-wide data that establishes that the most strongly bound DNA sequences do not necessarily mean that nearby gene transcripts are the most affected by the loss of the TF. Following our work on WC-2, this work addresses a fraction of the next tier of TFs, the two FARs, which in turn induce or repress transcription of a third tier of TF genes. Among these TFs are some that are also second tier TFs, characterized by their response to light (*csp-1*), suggesting feedback or cross regulation. There are some that are truly third tier, e.g. those that effect cellulose breakdown (*vib-1, clr-2*). Additional TFs in this and following tiers remain to be explored for their effects across the genome.

Both the process of beta-oxidation and the enzymes involved have been extensively characterized in bacteria, and eukaryotes [88], [127], [209]. Similarly, peroxisome biogenesis has been dissected in yeast and *Neurospora* [99], [140]. Mutant generation and phenotypic analysis is a powerful tool to define which proteins are necessary for an observable trait. The complete loss of a beta-oxidation or TCA cycle

enzyme may tell us what that one protein does. However once we know one function a protein has, the question remains—what dictates when and how much of the protein is made? By my extensive characterization of two TFs which control fatty acid utilization-related gene transcription, I have begun to unravel control of pathways fungi use for enzymes driving the central metabolism of the TCA cycle, and how these paths cross into adjacent, but previously unrelated regulation such as metal homeostasis.

Learning from RNA-sequencing

RNA-sequencing data confirmed that many of the transcripts are expressed at very low levels under the conditions tested. With the insights gained from RNA-sequencing data, I would choose to monitor activity from promoters that have a FAR binding site, and respond dramatically when strains are grown on different carbon sources. Another consideration might be using a gene that can be monitored in parallel with its product, such as an enzyme that has an accessible colorimetric assay like a lipase (Figure 3.7B). In this way, we may monitor transcription from the promoter with a reporter, but also capture potential differences in post-transcriptional or post-translational regulation. These particular lipases are also an interesting candidate for a reporter based upon the body of scientific literature citing the of FAR-1 and -2 homologs for lipase/cutinase regulation [109], [114].

Whether global or local regulation of a reporter, I have learned that TF network analysis becomes more worthwhile the larger the scale of analysis. My efforts to do all the steps from wet lab to dry lab, growth and analysis of ChIP and RNA replicates, the processing, bioinformatics, and visualization myself was meaningful in part because of its size. In order to address the size and complexity of a phenomenon like transcriptional regulation, it requires large coordinate efforts such as those of the ENCODE projects for *D. melanogaster*, *C. elegans*, and human cell lines. My contact with all of the steps, as well as the collaborators of the Neurospora PO1 project, essentially the ENCODE project for this fungus, emphasized the need to share and coordinate data

production and analyses. With our collective data, we have an opportunity to unravel the regulation, cross-regulation, and signaling connections between the FARs, WC-2, ADV-1, and all the TFs in our growing network.

Significance

The goal of this work was initially to define how or if WC-2 or light induction affected the activity and abundance of FAR-1. However, what we found was that a nearby DNA sequence, even if bound by a TF, does not always lead to activity in any given condition, for both FAR-1 and FAR-2. Additionally, we found widespread affects from TF mutants that were independent of FAR binding sites and linkage to the control of other TF genes. Though the signal for activation is under investigation, we found that TF activities of the FARs have global effects. Through my work on building transcription factor networks and FAR-binding independent transcriptome alterations, we have also established that while the FARs are important they are only two DNA-binding TFs among many. The systematic characterization of the *N. crassa* TF network will provide insights where reporter assays and limited target analyses fail.

Through this work I have found many ways to digest and make data accessible. The rich dataset I have annotated is a resource for hypothesis formation concerning TF networks, and the differential regulation of genes on the carbon sources sucrose, oleate, and butyrate. The regulators I characterize here may inform the bioengineering of regulatory pathways for biofuel production, such as triacyl-glycerol production in the lipogenous yeast *Yarrowia lipolytica* [138].

Ongoing and future studies

Detection of post-translational modifications of FAR-1 and FAR-2 by mass spectrometry

Our experiments to localize FAR-1 along the genome of *N. crassa* showed that in changing carbon sources, this TF does not dramatically alter its DNA association.

Supporting RNA-sequencing data shows that transcription of genes near FAR-1 peaks is affected by a change in carbon source. Regulation of FAR-1 by post-translational modification would explain its ability to alter the transcriptome, but this hypothesis remains to be tested. I have immunoprecipitated FAR-1 tagged with a 3xFLAG moiety in sucrose, and oleate. These samples await analysis to determine if any modifications can be detected.

In contrast, FAR-2 changes its DNA association depending upon carbon source, by our ChIP assay. Mammalian PPARs beta and gamma show ligand dependent nuclear localization [217]. A fungal example of a TF which shuttles between the cytoplasm and the nucleus is the WCC, the circadian transcriptional activator mentioned in the introduction [218]. I hypothesize that the poor FAR-2 ChIP signal is due to similar TF shuttling between the cytoplasm and the nucleus. Other evidence which supports this was a loss of FAR-2 signal seen by western from isolated nuclei compared to input and cytosol of the same strain (Figure 2.23). I hope to test this further with a smaller scale cell fractionation assay. Based upon FAR-2's cellular localization, immunoprecipitation procedure may need further optimization before sample analysis. I hope by these means to collect evidence about the control of FAR transcriptional activity.

References

[1] K. A. Borkovich, L. A. Alex, O. Yarden, M. Freitag, G. E. Turner, N. D. Read, S. Seiler, D. Bell-Pedersen, J. Paietta, N. Plesofsky, M. Plamann, M. Goodrich-Tanrikulu, U. Schulte, G. Mannhaupt, F. E. Nargang, A. Radford, C. Selitrennikoff, J. E. Galagan, J. C. Dunlap, J. J. Loros, D. Catcheside, H. Inoue, R. Aramayo, M. Polymenis, E. U. Selker, M. S. Sachs, G. A. Marzluf, I. Paulsen, R. Davis, D. J. Ebbole, A. Zelter, E. R. Kalkman, R. O'Rourke, F. Bowring, J. Yeadon, C. Ishii, K. Suzuki, W. Sakai, and R. Pratt, "Lessons from the Genome Sequence of Neurospora crassa: Tracing the Path from Genomic Blueprint to Multicellular Organism," *Microbiol. Mol. Biol. Rev.*, vol. 68, no. 1, pp. 1–108, Mar. 2004.

[2] X. He, R. Chatterjee, S. John, H. Bravo, B. K. Sathyanarayana, S. C. Biddie, P. C. FitzGerald, J. A. Stamatoyannopoulos, G. L. Hager, and C. Vinson, "Contribution of nucleosome binding preferences and co-occurring DNA sequences to transcription factor binding," *BMC Genomics*, vol. 14, p. 428, 2013.

[3] N. R. Zabet, R. Foy, and B. Adryan, "The Influence of Transcription Factor Competition on the Relationship between Occupancy and Affinity," *PLoS ONE*, vol. 8, no. 9, p. e73714, Sep. 2013.

[4] Y. H. Fu and G. A. Marzluf, "nit-2, the major nitrogen regulatory gene of Neurospora crassa, encodes a protein with a putative zinc finger DNA-binding domain," *Mol. Cell. Biol.*, vol. 10, no. 3, pp. 1056–1065, Mar. 1990.

[5] M. S. Chae, C. E. Nargang, I. A. Cleary, C. C. Lin, A. T. Todd, and F. E. Nargang, "Two zinc-cluster transcription factors control induction of alternative oxidase in Neurospora crassa," *Genetics*, vol. 177, no. 4, pp. 1997–2006, Dec. 2007.

[6] G. Sancar, C. Sancar, B. Brügger, N. Ha, T. Sachsenheimer, E. Gin, S. Wdowik, I. Lohmann, F. Wieland, T. Höfer, A. Diernfellner, and M. Brunner, "A global circadian repressor controls antiphasic expression of metabolic genes in Neurospora," *Mol. Cell*, vol. 44, no. 5, pp. 687–697, Dec. 2011.

[7] K. M. Smith, G. Sancar, R. Dekhang, C. M. Sullivan, S. Li, A. G. Tag, C. Sancar, E. L. Bredeweg, H. D. Priest, R. F. McCormick, T. L. Thomas, J. C. Carrington, J. E. Stajich, D. Bell-Pedersen, M. Brunner, and M. Freitag, "Transcription Factors in Light and Circadian Clock Signaling Networks Revealed by Genomewide Mapping of Direct Targets for Neurospora White Collar Complex," *Eukaryot. Cell*, vol. 9, no. 10, pp. 1549–1556, Jul. 2010.

[8] Z. Wang, M. Gerstein, and M. Snyder, “RNA-Seq: a revolutionary tool for transcriptomics,” *Nat. Rev. Genet.*, vol. 10, no. 1, pp. 57–63, Jan. 2009.

[9] B. Alberts, *Molecular biology of the cell*. New York: Garland Science, 2008.

[10] J. Kadonaga, “Regulation of RNA Polymerase II Transcription by Sequence-Specific DNA Binding Factors,” *Cell*, vol. 116, no. 2, pp. 247–257, Jan. 2004.

[11] A. V. Morozov, “Protein-DNA binding specificity predictions with structural models,” *Nucleic Acids Res.*, vol. 33, no. 18, pp. 5781–5798, Oct. 2005.

[12] B. B. Tuch, D. J. Galgoczy, A. D. Hernday, H. Li, and A. D. Johnson, “The Evolution of Combinatorial Gene Regulation in Fungi,” *PLoS Biol.*, vol. 6, no. 2, p. e38, 2008.

[13] V. Orlando, H. Strutt, and R. Paro, “Analysis of chromatin structure by in vivo formaldehyde cross-linking,” *Methods San Diego Calif*, vol. 11, no. 2, pp. 205–214, Feb. 1997.

[14] B. Ren, “Genome-Wide Location and Function of DNA Binding Proteins,” *Science*, vol. 290, no. 5500, pp. 2306–2309, Dec. 2000.

[15] H. Li and R. Durbin, “Fast and accurate short read alignment with Burrows-Wheeler transform,” *Bioinforma. Oxf. Engl.*, vol. 25, no. 14, pp. 1754–1760, Jul. 2009.

[16] B. Langmead, C. Trapnell, M. Pop, and S. L. Salzberg, “Ultrafast and memory-efficient alignment of short DNA sequences to the human genome,” *Genome Biol.*, vol. 10, no. 3, p. R25, 2009.

[17] C. R. Lickwar, F. Mueller, S. E. Hanlon, J. G. McNally, and J. D. Lieb, “Genome-wide protein-DNA binding dynamics suggest a molecular clutch for transcription factor function,” *Nature*, vol. 484, no. 7393, pp. 251–255, Apr. 2012.

[18] T. C. Voss, R. L. Schiltz, M.-H. Sung, P. M. Yen, J. A. Stamatoyannopoulos, S. C. Biddie, T. A. Johnson, T. B. Miranda, S. John, and G. L. Hager, “Dynamic exchange at regulatory elements during chromatin remodeling underlies assisted loading mechanism,” *Cell*, vol. 146, no. 4, pp. 544–554, Aug. 2011.

[19] Q. Cheng, M. Kazemian, H. Pham, C. Blatti, S. E. Celniker, S. A. Wolfe, M. H. Brodsky, and S. Sinha, “Computational Identification of Diverse Mechanisms Underlying Transcription Factor-DNA Occupancy,” *PLoS Genet.*, vol. 9, no. 8, p. e1003571, Aug. 2013.

[20] E. Gin, A. C. R. Diernfellner, M. Brunner, and T. Höfer, “The Neurospora photoreceptor VIVID exerts negative and positive control on light sensing to achieve adaptation,” *Mol. Syst. Biol.*, vol. 9, May 2013.

[21] Y.-S. Bahn, C. Xue, A. Idnurm, J. C. Rutherford, J. Heitman, and M. E. Cardenas, “Sensing the environment: lessons from fungi,” *Nat. Rev. Microbiol.*, vol. 5, no. 1, pp. 57–69, Jan. 2007.

[22] A. C. Froehlich, “White Collar-1, a Circadian Blue Light Photoreceptor, Binding to the frequency Promoter,” *Science*, vol. 297, no. 5582, pp. 815–819, Jul. 2002.

[23] R. H. Davis and D. D. Perkins, “TIMELINENeurospora: a model of model microbes,” *Nat. Rev. Genet.*, vol. 3, no. 5, pp. 397–403, May 2002.

[24] E. Selker, “Premeiotic Instability Of Repeated Sequences In Neurospora Crassa,” *Annu. Rev. Genet.*, vol. 24, no. 1, pp. 579–613, Jan. 1990.

[25] E. U. Selker, N. A. Tountas, S. H. Cross, B. S. Margolin, J. G. Murphy, A. P. Bird, and M. Freitag, “The methylated component of the Neurospora crassa genome,” *Nature*, vol. 422, no. 6934, pp. 893–897, Apr. 2003.

[26] A. Radford, “Metabolic Highways of Neurospora crassa Revisited,” in *Advances in Genetics*, vol. 52, Elsevier, 2004, pp. 165–207.

[27] W. J. Belden, L. F. Larrondo, A. C. Froehlich, M. Shi, C.-H. Chen, J. J. Loros, and J. C. Dunlap, “The band mutation in Neurospora crassa is a dominant allele of ras-1 implicating RAS signaling in circadian output,” *Genes Dev.*, vol. 21, no. 12, pp. 1494–1505, Jun. 2007.

[28] M. L. Sargent and W. R. Briggs, “The effects of light on a circadian rhythm of conidiation in neurospora,” *Plant Physiol.*, vol. 42, no. 11, pp. 1504–1510, Nov. 1967.

[29] Y. Yoshida, T. Maeda, B. Lee, and K. Hasunuma, “Conidiation rhythm and light entrainment in superoxide dismutase mutant in Neurospora crassa,” *Mol. Genet. Genomics MGG*, vol. 279, no. 2, pp. 193–202, Feb. 2008.

[30] E. Bunning, *The Physiological Clock: Endogenous Diurnal and Biological Chronometry : by Erwin Bunning*. Springer-Verlag, 1964.

[31] J. F. Feldman and M. N. Hoyle, “Isolation of circadian clock mutants of Neurospora crassa,” *Genetics*, vol. 75, no. 4, pp. 605–613, Dec. 1973.

[32] H. Wijnen and M. W. Young, “Interplay of Circadian Clocks and Metabolic Rhythms,” *Annu. Rev. Genet.*, vol. 40, no. 1, pp. 409–448, Dec. 2006.

[33] C. L. Baker, J. J. Loros, and J. C. Dunlap, “The circadian clock of Neurospora crassa: Neurospora crassa circadian clock,” *FEMS Microbiol. Rev.*, vol. 36, no. 1, pp. 95–110, Jan. 2012.

[34] A. M. Pregueiro, “The Neurospora Checkpoint Kinase 2: A Regulatory Link Between the Circadian and Cell Cycles,” *Science*, vol. 313, no. 5787, pp. 644–649, Aug. 2006.

[35] Y. Yang, Q. He, P. Cheng, P. Wrage, O. Yarden, and Y. Liu, “Distinct roles for PP1 and PP2A in the Neurospora circadian clock,” *Genes Dev.*, vol. 18, no. 3, pp. 255–260, Feb. 2004.

[36] Z. A. Lewis, A. Correa, C. Schwerdtfeger, K. L. Link, X. Xie, R. H. Gomer, T. Thomas, D. J. Ebbole, and D. Bell-Pedersen, “Overexpression of White Collar-1 (WC-1) activates circadian clock-associated genes, but is not sufficient to induce most light-regulated gene expression in Neurospora crassa,” *Mol. Microbiol.*, vol. 45, no. 4, pp. 917–931, 2002.

[37] V. D. Gooch, A. Mehra, L. F. Larrondo, J. Fox, M. Touroutoutoudis, J. J. Loros, and J. C. Dunlap, “Fully Codon-Optimized luciferase Uncovers Novel Temperature Characteristics of the Neurospora Clock,” *Eukaryot. Cell*, vol. 7, no. 1, pp. 28–37, Aug. 2007.

[38] P. Ballario, P. Vittorioso, A. Magrelli, C. Talora, A. Cabibbo, and G. Macino, “White collar-1, a central regulator of blue light responses in Neurospora, is a zinc finger protein.,” *EMBO J.*, vol. 15, no. 7, p. 1650, 1996.

[39] H. Linden and G. Macino, “White collar 2, a partner in blue-light signal transduction, controlling expression of light–regulated genes in Neurospora crassa,” *EMBO J.*, vol. 16, no. 1, pp. 98–109, 1997.

[40] M. Olmedo, C. Ruger-Herreros, E. M. Luque, and L. M. Corrochano, “A complex photoreceptor system mediates the regulation by light of the conidiation genes con-10 and con-6 in Neurospora crassa,” *Fungal Genet. Biol. FG B*, vol. 47, no. 4, pp. 352–363, Apr. 2010.

[41] C.-H. Chen, C. S. Ringelberg, R. H. Gross, J. C. Dunlap, and J. J. Loros, “Genome-wide analysis of light-inducible responses reveals hierarchical light signalling in Neurospora,” *EMBO J.*, vol. 28, no. 8, pp. 1029–1042, Mar. 2009.

[42] Q. He and Y. Liu, “Molecular mechanism of light responses in Neurospora: from light-induced transcription to photoadaptation,” *Genes Dev.*, vol. 19, no. 23, pp. 2888–2899, Dec. 2005.

[43] J. J. Loros, S. A. Denome, and J. C. Dunlap, “Molecular cloning of genes under control of the circadian clock in Neurospora,” *Science*, vol. 243, no. 4889, pp. 385–388, Jan. 1989.

[44] D. Bell-Pedersen, J. C. Dunlap, and J. J. Loros, “The Neurospora circadian clock-controlled gene, ccg-2, is allelic to eas and encodes a fungal hydrophobin required for formation of the conidial rodlet layer,” *Genes Dev.*, vol. 6, no. 12A, pp. 2382–2394, Dec. 1992.

[45] D. Bell-Pedersen, M. L. Shinohara, J. J. Loros, and J. C. Dunlap, “Circadian clock-controlled genes isolated from Neurospora crassa are late night- to early morning-

specific," *Proc. Natl. Acad. Sci. U. S. A.*, vol. 93, no. 23, pp. 13096–13101, Nov. 1996.

[46] M. L. Shinohara, A. Correa, D. Bell-Pedersen, J. C. Dunlap, and J. J. Loros, "Neurospora Clock-Controlled Gene 9 (ccg-9) Encodes Trehalose Synthase: Circadian Regulation of Stress Responses and Development," *Eukaryot. Cell*, vol. 1, no. 1, pp. 33–43, Feb. 2002.

[47] H. Zhu, M. Nowrousian, D. Kupfer, H. V. Colot, G. Berrocal-Tito, H. Lai, D. Bell-Pedersen, B. A. Roe, J. J. Loros, and J. C. Dunlap, "Analysis of expressed sequence tags from two starvation, time-of-day-specific libraries of Neurospora crassa reveals novel clock-controlled genes," *Genetics*, vol. 157, no. 3, pp. 1057–1065, Mar. 2001.

[48] B. Grimaldi, P. Coiro, P. Filetici, E. Berge, J. R. Dobosy, M. Freitag, E. U. Selker, and P. Ballario, "The Neurospora crassa White Collar-1 dependent blue light response requires acetylation of histone H3 lysine 14 by NGF-1," *Mol. Biol. Cell*, vol. 17, no. 10, pp. 4576–4583, Oct. 2006.

[49] N. Gyöngyösi, D. Nagy, K. Makara, K. Ella, and K. Káldi, "Reactive oxygen species can modulate circadian phase and period in Neurospora crassa," *Free Radic. Biol. Med.*, vol. 58, pp. 134–143, May 2013.

[50] Y. Yoshida, H. Iigusa, N. Wang, and K. Hasunuma, "Cross-Talk between the Cellular Redox State and the Circadian System in Neurospora," *PLoS ONE*, vol. 6, no. 12, p. e28227, Dec. 2011.

[51] J. M. Dreyfuss, J. D. Zucker, H. M. Hood, L. R. Ocasio, M. S. Sachs, and J. E. Galagan, "Reconstruction and Validation of a Genome-Scale Metabolic Model for the Filamentous Fungus Neurospora crassa Using FARM," *PLoS Comput. Biol.*, vol. 9, no. 7, p. e1003126, Jul. 2013.

[52] F. J. Corpas, J. B. Barroso, and L. A. del Río, "Peroxisomes as a source of reactive oxygen species and nitric oxide signal molecules in plant cells," *Trends Plant Sci.*, vol. 6, no. 4, pp. 145–150, Apr. 2001.

[53] K. Yamashita, A. Shiozawa, S. Banno, F. Fukumori, A. Ichiishi, M. Kimura, and M. Fujimura, "Involvement of OS-2 MAP kinase in regulation of the large-subunit catalases CAT-1 and CAT-3 in Neurospora crassa," *Genes Genet. Syst.*, vol. 82, no. 4, pp. 301–310, Aug. 2007.

[54] T. M. Lamb, C. S. Goldsmith, L. Bennett, K. E. Finch, and D. Bell-Pedersen, "Direct transcriptional control of a p38 MAPK pathway by the circadian clock in Neurospora crassa," *PloS One*, vol. 6, no. 11, p. e27149, 2011.

[55] S. Banno, R. Noguchi, K. Yamashita, F. Fukumori, M. Kimura, I. Yamaguchi, and M. Fujimura, "Roles of putative His-to-Asp signaling modules HPT-1 and RRG-2, on

viability and sensitivity to osmotic and oxidative stresses in Neurospora crassa," *Curr. Genet.*, vol. 51, no. 3, pp. 197–208, Jan. 2007.

[56] Y. Zhang, R. Lamm, C. Pillonel, S. Lam, and J.-R. Xu, "Osmoregulation and fungicide resistance: the Neurospora crassa os-2 gene encodes a HOG1 mitogen-activated protein kinase homologue," *Appl. Environ. Microbiol.*, vol. 68, no. 2, pp. 532–538, Feb. 2002.

[57] J. Zhu, X. Yu, B. Xie, X. Gu, Z. Zhang, and S. Li, "Transcriptomic profiling-based mutant screen reveals three new transcription factors mediating menadione resistance in Neurospora crassa," *Fungal Biol.*, vol. 117, no. 6, pp. 422–430, Jun. 2013.

[58] T. R. Hughes and C. G. de Boer, "Mapping Yeast Transcriptional Networks," *Genetics*, vol. 195, no. 1, pp. 9–36, Sep. 2013.

[59] H. Lavoie, H. Hogues, and M. Whiteway, "Rearrangements of the transcriptional regulatory networks of metabolic pathways in fungi," *Curr. Opin. Microbiol.*, vol. 12, no. 6, pp. 655–663, Dec. 2009.

[60] C. H. Yuh, H. Bolouri, and E. H. Davidson, "Genomic cis-regulatory logic: experimental and computational analysis of a sea urchin gene," *Science*, vol. 279, no. 5358, pp. 1896–1902, Mar. 1998.

[61] I. V. Grigoriev, R. Nikitin, S. Haridas, A. Kuo, R. Ohm, R. Otillar, R. Riley, A. Salamov, X. Zhao, F. Korzeniewski, T. Smirnova, H. Nordberg, I. Dubchak, and I. Shabalov, "MycoCosm portal: gearing up for 1000 fungal genomes," *Nucleic Acids Res.*, Dec. 2013.

[62] A. B. Stergachis, E. Haugen, A. Shafer, W. Fu, B. Vernot, A. Reynolds, A. Raubitschek, S. Ziegler, E. M. LeProust, J. M. Akey, and J. A. Stamatoyannopoulos, "Exonic Transcription Factor Binding Directs Codon Choice and Affects Protein Evolution," *Science*, vol. 342, no. 6164, pp. 1367–1372, Dec. 2013.

[63] T. Schlitt and A. Brazma, "Modelling in molecular biology: describing transcription regulatory networks at different scales," *Philos. Trans. R. Soc. B Biol. Sci.*, vol. 361, no. 1467, pp. 483–494, Mar. 2006.

[64] M. B. Gerstein, Z. J. Lu, E. L. Van Nostrand, C. Cheng, B. I. Arshinoff, T. Liu, K. Y. Yip, R. Robilotto, A. Rechtsteiner, K. Ikegami, P. Alves, A. Chateigner, M. Perry, M. Morris, R. K. Auerbach, X. Feng, J. Leng, A. Vielle, W. Niu, K. Rhrissorrakrai, A. Agarwal, R. P. Alexander, G. Barber, C. M. Brdlik, J. Brennan, J. J. Brouillet, A. Carr, M.-S. Cheung, H. Clawson, S. Contrino, L. O. Dannenberg, A. F. Dernburg, A. Desai, L. Dick, A. C. Dose, J. Du, T. Egelhofer, S. Ercan, G. Euskirchen, B. Ewing, E. A. Feingold, R. Gassmann, P. J. Good, P. Green, F. Gullier, M. Gutwein, M. S. Guyer, L. Habegger, T. Han, J. G. Henikoff, S. R. Henz, A. Hinrichs, H. Holster, T. Hyman, A. L.

Iniguez, J. Janette, M. Jensen, M. Kato, W. J. Kent, E. Kephart, V. Khivansara, E. Khurana, J. K. Kim, P. Kolasinska-Zwierz, E. C. Lai, I. Latorre, A. Leahey, S. Lewis, P. Lloyd, L. Lochovsky, R. F. Lowdon, Y. Lubling, R. Lyne, M. MacCoss, S. D. Mackowiak, M. Mangone, S. McKay, D. Mecenas, G. Merrihew, D. M. Miller, A. Muroyama, J. I. Murray, S.-L. Ooi, H. Pham, T. Phippen, E. A. Preston, N. Rajewsky, G. Ratsch, H. Rosenbaum, J. Rozowsky, K. Rutherford, P. Ruzanov, M. Sarov, R. Sasidharan, A. Sboner, P. Scheid, E. Segal, H. Shin, C. Shou, F. J. Slack, C. Slightam, R. Smith, W. C. Spencer, E. O. Stinson, S. Taing, T. Takasaki, D. Vafeados, K. Voronina, G. Wang, N. L. Washington, C. M. Whittle, B. Wu, K.-K. Yan, G. Zeller, Z. Zha, M. Zhong, X. Zhou, modENCODE Consortium, J. Ahringer, S. Strome, K. C. Gunsalus, G. Micklem, X. S. Liu, V. Reinke, S. K. Kim, L. W. Hillier, S. Henikoff, F. Piano, M. Snyder, L. Stein, J. D. Lieb, and R. H. Waterston, "Integrative Analysis of the Caenorhabditis elegans Genome by the modENCODE Project," *Science*, vol. 330, no. 6012, pp. 1775–1787, Dec. 2010.

[65] The modENCODE Consortium, S. Roy, J. Ernst, P. V. Kharchenko, P. Kheradpour, N. Negre, M. L. Eaton, J. M. Landolin, C. A. Bristow, L. Ma, M. F. Lin, S. Washietl, B. I. Arshinoff, F. Ay, P. E. Meyer, N. Robine, N. L. Washington, L. Di Stefano, E. Berezikov, C. D. Brown, R. Candeias, J. W. Carlson, A. Carr, I. Jungreis, D. Marbach, R. Sealfon, M. Y. Tolstorukov, S. Will, A. A. Alekseyenko, C. Artieri, B. W. Booth, A. N. Brooks, Q. Dai, C. A. Davis, M. O. Duff, X. Feng, A. A. Gorchakov, T. Gu, J. G. Henikoff, P. Kapranov, R. Li, H. K. MacAlpine, J. Malone, A. Minoda, J. Nordman, K. Okamura, M. Perry, S. K. Powell, N. C. Riddle, A. Sakai, A. Samsonova, J. E. Sandler, Y. B. Schwartz, N. Sher, R. Spokony, D. Sturgill, M. van Baren, K. H. Wan, L. Yang, C. Yu, E. Feingold, P. Good, M. Guyer, R. Lowdon, K. Ahmad, J. Andrews, B. Berger, S. E. Brenner, M. R. Brent, L. Cherbas, S. C. R. Elgin, T. R. Gingeras, R. Grossman, R. A. Hoskins, T. C. Kaufman, W. Kent, M. I. Kuroda, T. Orr-Weaver, N. Perrimon, V. Pirrotta, J. W. Posakony, B. Ren, S. Russell, P. Cherbas, B. R. Graveley, S. Lewis, G. Micklem, B. Oliver, P. J. Park, S. E. Celniker, S. Henikoff, G. H. Karpen, E. C. Lai, D. M. MacAlpine, L. D. Stein, K. P. White, M. Kellis, D. Acevedo, R. Auburn, G. Barber, H. J. Bellen, E. P. Bishop, T. D. Bryson, A. Chateigner, J. Chen, H. Clawson, C. L. G. Comstock, S. Contrino, L. C. DeNapoli, Q. Ding, A. Dobin, M. H. Domanus, J. Drenkow, S. Dudoit, J. Dumais, T. Eng, D. Fagegaltier, S. E. Gadel, S. Ghosh, F. Guillier, D. Hanley, G. J. Hannon, K. D. Hansen, E. Heinz, A. S. Hinrichs, M. Hirst, S. Jha, L. Jiang, Y. L. Jung, H. Kashevsky, C. D. Kennedy, E. T. Kephart, L. Langton, O.-K. Lee, S. Li, Z. Li, W. Lin, D. Linder-Basso, P. Lloyd, R. Lyne, S. E. Marchetti, M. Marra, N. R. Mattiuzzo, S. McKay, F. Meyer, D. Miller, S. W. Miller, R. A. Moore, C. A. Morrison, J. A. Prinz, M. Rooks, R. Moore, K. M. Rutherford, P. Ruzanov, D. A. Scheftner, L. Senderowicz, P. K. Shah, G. Shanower, R. Smith, E. O. Stinson, S. Suchy, A. E. Tenney, F. Tian, K. J. T. Venken, H. Wang, R. White, J. Wilkening, A. T. Willingham, C. Zaleski, Z. Zha, D. Zhang, Y. Zhao, and J. Zieba, "Identification of Functional Elements and Regulatory Circuits by Drosophila modENCODE," *Science*, vol. 330, no. 6012, pp. 1787–1797, Dec. 2010.

[66] C. Tian, J. Li, and N. L. Glass, “Exploring the bZIP transcription factor regulatory network in Neurospora crassa,” *Microbiology*, vol. 157, no. 3, pp. 747–759, Nov. 2010.

[67] S. MacPherson, M. Larochelle, and B. Turcotte, “A Fungal Family of Transcriptional Regulators: the Zinc Cluster Proteins,” *Microbiol. Mol. Biol. Rev.*, vol. 70, no. 3, pp. 583–604, Sep. 2006.

[68] M. Salazar, W. Vongsangnak, G. Panagiotou, M. R. Andersen, and J. Nielsen, “Uncovering transcriptional regulation of glycerol metabolism in Aspergilli through genome-wide gene expression data analysis,” *Mol. Genet. Genomics*, vol. 282, no. 6, pp. 571–586, Sep. 2009.

[69] W. H. Meijer, L. Gidijala, S. Fekken, J. A. K. W. Kiel, M. A. van den Berg, R. Lascaris, R. A. L. Bovenberg, and I. J. van der Klei, “Peroxisomes are required for efficient penicillin biosynthesis in Penicillium chrysogenum,” *Appl. Environ. Microbiol.*, vol. 76, no. 17, pp. 5702–5709, Sep. 2010.

[70] S. T. Coradetti, J. P. Craig, Y. Xiong, T. Shock, C. Tian, and N. L. Glass, “Conserved and essential transcription factors for cellulase gene expression in ascomycete fungi,” *Proc. Natl. Acad. Sci.*, vol. 109, no. 19, pp. 7397–7402, Apr. 2012.

[71] J. Sun and N. L. Glass, “Identification of the CRE-1 Cellulolytic Regulon in Neurospora crassa,” *PLoS ONE*, vol. 6, no. 9, p. e25654, Sep. 2011.

[72] E. A. Znameroski and N. L. Glass, “Using a model filamentous fungus to unravel mechanisms of lignocellulose deconstruction,” *Biotechnol. Biofuels*, vol. 6, no. 1, p. 6, 2013.

[73] P. Silar, “Hyphal Interference: Self Versus Non-self Fungal Recognition and Hyphal Death,” in *Biocommunication of Fungi*, G. Witzany, Ed. Dordrecht: Springer Netherlands, 2012, pp. 155–170.

[74] A. Sørensen, M. Lübeck, P. Lübeck, and B. Ahring, “Fungal Beta-Glucosidases: A Bottleneck in Industrial Use of Lignocellulosic Materials,” *Biomolecules*, vol. 3, no. 3, pp. 612–631, Sep. 2013.

[75] T. Potapova, “Cell-to-Cell Communication in the Tip Growth of Mycelial Fungi,” in *Biocommunication of Fungi*, G. Witzany, Ed. Dordrecht: Springer Netherlands, 2012, pp. 103–114.

[76] C. Ziv, R. Gorovits, and O. Yarden, “Carbon source affects PKA-dependent polarity of Neurospora crassa in a CRE-1-dependent and independent manner,” *Fungal Genet. Biol.*, vol. 45, no. 2, pp. 103–116, Feb. 2008.

[77] M. J. De Vit, J. A. Waddle, and M. Johnston, “Regulated nuclear translocation of the Mig1 glucose repressor,” *Mol. Biol. Cell*, vol. 8, no. 8, pp. 1603–1618, Aug. 1997.

[78] B. Turcotte, X. B. Liang, F. Robert, and N. Soontorngun, “Transcriptional regulation of nonfermentable carbon utilization in budding yeast,” *FEMS Yeast Res.*, vol. 10, no. 1, pp. 2–13, Feb. 2010.

[79] J. M. Gancedo, “Yeast carbon catabolite repression,” *Microbiol. Mol. Biol. Rev. MMBR*, vol. 62, no. 2, pp. 334–361, Jun. 1998.

[80] H.-J. Schüller, “Transcriptional control of nonfermentative metabolism in the yeast Saccharomyces cerevisiae,” *Curr. Genet.*, vol. 43, no. 3, pp. 139–160, Jun. 2003.

[81] R. R. McCartney and M. C. Schmidt, “Regulation of Snf1 kinase. Activation requires phosphorylation of threonine 210 by an upstream kinase as well as a distinct step mediated by the Snf4 subunit,” *J. Biol. Chem.*, vol. 276, no. 39, pp. 36460–36466, Sep. 2001.

[82] J. Horák, “Regulations of sugar transporters: insights from yeast,” *Curr. Genet.*, vol. 59, no. 1–2, pp. 1–31, Mar. 2013.

[83] R. Jiang and M. Carlson, “Glucose regulates protein interactions within the yeast SNF1 protein kinase complex,” *Genes Dev.*, vol. 10, no. 24, pp. 3105–3115, Dec. 1996.

[84] M. Simon, M. Binder, G. Adam, A. Hartig, and H. Ruis, “Control of peroxisome proliferation in Saccharomyces cerevisiae by ADR1, SNF1 (CAT1, CCR1) and SNF4 (CAT3),” *Yeast Chichester Engl.*, vol. 8, no. 4, pp. 303–309, Apr. 1992.

[85] F. V. Mayer, R. Heath, E. Underwood, M. J. Sanders, D. Carmena, R. R. McCartney, F. C. Leiper, B. Xiao, C. Jing, P. A. Walker, L. F. Haire, R. Ogrodowicz, S. R. Martin, M. C. Schmidt, S. J. Gamblin, and D. Carling, “ADP Regulates SNF1, the Saccharomyces cerevisiae Homolog of AMP-Activated Protein Kinase,” *Cell Metab.*, vol. 14, no. 5, pp. 707–714, Nov. 2011.

[86] R. Ghillebert, E. Swinnen, J. Wen, L. Vandesteene, M. Ramon, K. Norga, F. Rolland, and J. Winderickx, “The AMPK/SNF1/SnRK1 fuel gauge and energy regulator: structure, function and regulation,” *FEBS J.*, vol. 278, no. 21, pp. 3978–3990, Nov. 2011.

[87] J. Sun, C. Tian, S. Diamond, and N. L. Glass, “Deciphering Transcriptional Regulatory Mechanisms Associated with Hemicellulose Degradation in Neurospora crassa,” *Eukaryot. Cell*, vol. 11, no. 4, pp. 482–493, Feb. 2012.

[88] Y. Kang, D. T. Nguyen, M. S. Son, and T. T. Hoang, “The Pseudomonas aeruginosa PsrA responds to long-chain fatty acid signals to regulate the fadBA5 -oxidation operon,” *Microbiology*, vol. 154, no. 6, pp. 1584–1598, Jun. 2008.

[89] D. S. Rubink and W. W. Winder, “Effect of phosphorylation by AMP-activated protein kinase on palmitoyl-CoA inhibition of skeletal muscle acetyl-CoA carboxylase,” *J. Appl. Physiol.*, vol. 98, no. 4, pp. 1221–1227, Apr. 2005.

[90] S. Kersten, B. Desvergne, and W. Wahli, “Roles of PPARs in health and disease,” *Nature*, vol. 405, no. 6785, pp. 421–424, May 2000.

[91] R. Nielsen, T. A. Pedersen, D. Hagenbeek, P. Moulos, R. Siersbaek, E. Megens, S. Denissov, M. Borgesen, K.-J. Francoijs, S. Mandrup, and H. G. Stunnenberg, “Genome-wide profiling of PPAR :RXR and RNA polymerase II occupancy reveals temporal activation of distinct metabolic pathways and changes in RXR dimer composition during adipogenesis,” *Genes Dev.*, vol. 22, no. 21, pp. 2953–2967, Nov. 2008.

[92] L. Michalik, J. Auwerx, J. P. Berger, V. K. Chatterjee, C. K. Glass, F. J. Gonzalez, P. A. Grimaldi, T. Kadowaki, M. A. Lazar, S. O’Rahilly, C. N. A. Palmer, J. Plutzky, J. K. Reddy, B. M. Spiegelman, B. Staels, and W. Wahli, “International Union of Pharmacology. LXI. Peroxisome proliferator-activated receptors,” *Pharmacol. Rev.*, vol. 58, no. 4, pp. 726–741, Dec. 2006.

[93] B. P. Kota, T. H.-W. Huang, and B. D. Roufogalis, “An overview on biological mechanisms of PPARs,” *Pharmacol. Res. Off. J. Ital. Pharmacol. Soc.*, vol. 51, no. 2, pp. 85–94, Feb. 2005.

[94] M. Ammerschlaeger, “Characterization of the Species-Specificity of Peroxisome Proliferators in Rat and Human Hepatocytes,” *Toxicol. Sci.*, vol. 78, no. 2, pp. 229–240, Jan. 2004.

[95] J. Vamecq and N. Latruffe, “Medical significance of peroxisome proliferator-activated receptors,” *The Lancet*, vol. 354, no. 9173, pp. 141–148, Jul. 1999.

[96] C. Phelps, V. Gburcik, E. Suslova, P. Dudek, F. Forafonov, N. Bot, M. MacLean, R. J. Fagan, and D. Picard, “Fungi and animals may share a common ancestor to nuclear receptors,” *Proc. Natl. Acad. Sci. U. S. A.*, vol. 103, no. 18, pp. 7077–7081, May 2006.

[97] A. Gurvitz and H. Rottensteiner, “The biochemistry of oleate induction: Transcriptional upregulation and peroxisome proliferation,” *Biochim. Biophys. Acta BBA - Mol. Cell Res.*, vol. 1763, no. 12, pp. 1392–1402, Dec. 2006.

[98] C. Wolfrum, “Fatty acids and hypolipidemic drugs regulate peroxisome proliferator-activated receptors alpha - and gamma -mediated gene expression via liver fatty acid binding protein: A signaling path to the nucleus,” *Proc. Natl. Acad. Sci.*, vol. 98, no. 5, pp. 2323–2328, Feb. 2001.

[99] W. H. Kunau and A. Hartig, “Peroxisome biogenesis in Saccharomyces cerevisiae,” *Antonie Van Leeuwenhoek*, vol. 62, no. 1–2, pp. 63–78, Aug. 1992.

[100] M. Albertini, W. Girzalsky, M. Veenhuis, and W. H. Kunau, “Pex12p of Saccharomyces cerevisiae is a component of a multi-protein complex essential for peroxisomal matrix protein import,” *Eur. J. Cell Biol.*, vol. 80, no. 4, pp. 257–270, Apr. 2001.

[101] R. Erdmann, F. F. Wiebel, A. Flessau, J. Rytka, A. Beyer, K.-U. Fröhlich, and W.-H. Kunau, “PAS1, a yeast gene required for peroxisome biogenesis, encodes a member of a novel family of putative ATPases,” *Cell*, vol. 64, no. 3, pp. 499–510, Feb. 1991.

[102] R. Erdmann, M. Veenhuis, D. Mertens, and W. H. Kunau, “Isolation of peroxisome-deficient mutants of Saccharomyces cerevisiae,” *Proc. Natl. Acad. Sci. U. S. A.*, vol. 86, no. 14, pp. 5419–5423, Jul. 1989.

[103] F. Lutzoni, F. Kauff, C. J. Cox, D. McLaughlin, G. Celio, B. Dentinger, M. Padamsee, D. Hibbett, T. Y. James, E. Baloch, M. Grube, V. Reeb, V. Hofstetter, C. Schoch, A. E. Arnold, J. Miadlikowska, J. Spatafora, D. Johnson, S. Hambleton, M. Crockett, R. Shoemaker, G.-H. Sung, R. Lücking, T. Lumbsch, K. O’Donnell, M. Binder, P. Diederich, D. Ertz, C. Gueidan, K. Hansen, R. C. Harris, K. Hosaka, Y.-W. Lim, B. Matheny, H. Nishida, D. Pfister, J. Rogers, A. Rossman, I. Schmitt, H. Sipman, J. Stone, J. Sugiyama, R. Yahr, and R. Vilgalys, “Assembling the fungal tree of life: progress, classification, and evolution of subcellular traits,” *Am. J. Bot.*, vol. 91, no. 10, pp. 1446–1480, Oct. 2004.

[104] N. Poopanitpan, S. Kobayashi, R. Fukuda, H. Horiuchi, and A. Ohta, “An ortholog of farA of Aspergillus nidulans is implicated in the transcriptional activation of genes involved in fatty acid utilization in the yeast Yarrowia lipolytica,” *Biochem. Biophys. Res. Commun.*, vol. 402, no. 4, pp. 731–735, Nov. 2010.

[105] M. A. Ramirez and M. C. Lorenz, “The Transcription Factor Homolog CTF1 Regulates -Oxidation in Candida albicans,” *Eukaryot. Cell*, vol. 8, no. 10, pp. 1604–1614, Aug. 2009.

[106] M. J. Hynes, S. L. Murray, A. Duncan, G. S. Khew, and M. A. Davis, “Regulatory Genes Controlling Fatty Acid Catabolism and Peroxisomal Functions in the Filamentous Fungus Aspergillus nidulans,” *Eukaryot. Cell*, vol. 5, no. 5, pp. 794–805, May 2006.

[107] D. Li and P. E. Kolattukudy, “Cloning of Cutinase Transcription Factor 1, a Transactivating Protein Containing Cys6Zn2 Binuclear Cluster DNA-binding Motif,” *J. Biol. Chem.*, vol. 272, no. 19, pp. 12462–12467, May 1997.

[108] D. Li, T. Sirakova, L. Rogers, W. F. Ettinger, and P. E. Kolattukudy, “Regulation of constitutively expressed and induced cutinase genes by different zinc finger transcription factors in Fusarium solani f. sp. pisi (Nectria haematococca),” *J. Biol. Chem.*, vol. 277, no. 10, pp. 7905–7912, Mar. 2002.

[109] G. Bravo-Ruiz, C. Ruiz-Roldán, and M. I. G. Roncero, “Lipolytic System of the Tomato Pathogen *Fusarium oxysporum* f. sp. *lycopersici*,” *Mol. Plant. Microbe Interact.*, vol. 26, no. 9, pp. 1054–1067, Sep. 2013.

[110] H. Dinkel, S. Michael, R. J. Weatheritt, N. E. Davey, K. Van Roey, B. Altenberg, G. Toedt, B. Uyar, M. Seiler, A. Budd, L. Jodicke, M. A. Dammert, C. Schroeter, M. Hammer, T. Schmidt, P. Jehl, C. McGuigan, M. Dymecka, C. Chica, K. Luck, A. Via, A. Chatr-aryamontri, N. Haslam, G. Grebnev, R. J. Edwards, M. O. Steinmetz, H. Meiselbach, F. Diella, and T. J. Gibson, “ELM--the database of eukaryotic linear motifs,” *Nucleic Acids Res.*, vol. 40, no. D1, pp. D242–D251, Nov. 2011.

[111] J. Engel, P. S. Schmalhorst, and F. H. Routier, “Biosynthesis of the Fungal Cell Wall Polysaccharide Galactomannan Requires Intraluminal GDP-mannose,” *J. Biol. Chem.*, vol. 287, no. 53, pp. 44418–44424, Nov. 2012.

[112] B. Bago, “Carbon Export from Arbuscular Mycorrhizal Roots Involves the Translocation of Carbohydrate as well as Lipid,” *PLANT Physiol.*, vol. 131, no. 3, pp. 1496–1507, Feb. 2003.

[113] M. Park, E. Do, and W. H. Jung, “Lipolytic Enzymes Involved in the Virulence of Human Pathogenic Fungi,” *Mycobiology*, vol. 41, no. 2, p. 67, 2013.

[114] A. L. M. Rocha, A. Di Pietro, C. Ruiz-RoldáN, and M. I. G. Roncero, “Ctf1, a transcriptional activator of cutinase and lipase genes in Fusarium oxysporum is dispensable for virulence,” *Mol. Plant Pathol.*, vol. 9, no. 3, pp. 293–304, May 2008.

[115] C. A. Voigt, W. Schäfer, and S. Salomon, “A secreted lipase of Fusarium graminearum is a virulence factor required for infection of cereals: Lipase as a virulence factor,” *Plant J.*, vol. 42, no. 3, pp. 364–375, Feb. 2005.

[116] S. Salomon, A. Gácser, S. Frerichmann, C. Kröger, W. Schäfer, and C. A. Voigt, “The secreted lipase FGL1 is sufficient to restore the initial infection step to the apathogenic Fusarium graminearum MAP kinase disruption mutant Δgpmk1,” *Eur. J. Plant Pathol.*, vol. 134, no. 1, pp. 23–37, Jun. 2012.

[117] M. Kretschmer, J. Wang, and J. W. Kronstad, “Peroxisomal and Mitochondrial -Oxidation Pathways Influence the Virulence of the Pathogenic Fungus Cryptococcus neoformans,” *Eukaryot. Cell*, vol. 11, no. 8, pp. 1042–1054, Jun. 2012.

[118] H. Singh, *Mycoremediation: fungal bioremediation*. Hoboken, N.J: Wiley-Interscience, 2006.

[119] A. Najjar, S. Robert, C. Guérin, M. Violet-Asther, and F. Carrière, “Quantitative study of lipase secretion, extracellular lipolysis, and lipid storage in the yeast Yarrowia lipolytica grown in the presence of olive oil: analogies with lipolysis in humans,” *Appl. Microbiol. Biotechnol.*, vol. 89, no. 6, pp. 1947–1962, Nov. 2010.

[120] Z. Zou, “Fatty Acid Transport in Saccharomyces cerevisiae. DIRECTED MUTAGENESIS OF FAT1 DISTINGUISHES THE BIOCHEMICAL ACTIVITIES ASSOCIATED WITH Fat1p,” *J. Biol. Chem.*, vol. 277, no. 34, pp. 31062–31071, Jun. 2002.

[121] W. F. Visser, C. W. T. van Roermund, L. Ijlst, H. R. Waterham, and R. J. A. Wanders, “Metabolite transport across the peroxisomal membrane,” *Biochem. J.*, vol. 401, no. 2, p. 365, Jan. 2007.

[122] J. Knudsen, M. V. Jensen, J. F. Nils, T. B. Neergaard, and B. Gaigg, “Role of acylCoA binding protein in acylCoA transport, metabolism and cell signaling,” *Mol. Cell. Biochem.*, vol. 192, no. 1–2, pp. 95–103, 1999.

[123] D. Murphy, “The biogenesis and functions of lipid bodies in animals, plants and microorganisms,” *Prog. Lipid Res.*, vol. 40, no. 5, pp. 325–438, Sep. 2001.

[124] M. Trepanier, G. Becard, P. Moutoglis, C. Willemot, S. Gagne, T. J. Avis, and J.-A. Rioux, “Dependence of Arbuscular-Mycorrhizal Fungi on Their Plant Host for Palmitic Acid Synthesis,” *Appl. Environ. Microbiol.*, vol. 71, no. 9, pp. 5341–5347, Sep. 2005.

[125] P. L. Lakin-Thomas and S. Brody, “Circadian rhythms in Neurospora crassa: lipid deficiencies restore robust rhythmicity to null frequency and white-collar mutants,” *Proc. Natl. Acad. Sci. U. S. A.*, vol. 97, no. 1, pp. 256–261, Jan. 2000.

[126] M. Goodrich-Tanrikulu, D. J. Jacobson, A. E. Stafford, J.-T. Lin, and T. A. McKeon, “Characterization of Neurospora crassa mutants isolated following repeat-induced point mutation of the beta subunit of fatty acid synthase,” *Curr. Genet.*, vol. 36, no. 3, pp. 147–152, 1999.

[127] L. A. Maggio-Hall and N. P. Keller, “Mitochondrial β-oxidation in Aspergillus nidulans,” *Mol. Microbiol.*, vol. 54, no. 5, pp. 1173–1185, Oct. 2004.

[128] K. Strijbis and B. Distel, “Intracellular Acetyl Unit Transport in Fungal Carbon Metabolism,” *Eukaryot. Cell*, vol. 9, no. 12, pp. 1809–1815, Oct. 2010.

[129] Y.-Q. Shen and G. Burger, “Plasticity of a key metabolic pathway in fungi,” *Funct. Integr. Genomics*, vol. 9, no. 2, pp. 145–151, Sep. 2008.

[130] M. Kunze, I. Pracharoenwattana, S. M. Smith, and A. Hartig, “A central role for the peroxisomal membrane in glyoxylate cycle function,” *Biochim. Biophys. Acta BBA - Mol. Cell Res.*, vol. 1763, no. 12, pp. 1441–1452, Dec. 2006.

[131] O. Tehlivets, K. Scheuringer, and S. D. Kohlwein, “Fatty acid synthesis and elongation in yeast,” *Biochim. Biophys. Acta*, vol. 1771, no. 3, pp. 255–270, Mar. 2007.

[132] O. Käppeli, M. Müller, and A. Fiechter, “Chemical and structural alterations at the cell surface of Candida tropicalis, induced by hydrocarbon substrate,” *J. Bacteriol.*, vol. 133, no. 2, pp. 952–958, Feb. 1978.

[133] C. M. Roche, H. W. Blanch, D. S. Clark, and N. L. Glass, “Physiological Role of Acyl Coenzyme A Synthetase Homologs in Lipid Metabolism in Neurospora crassa,” *Eukaryot. Cell*, vol. 12, no. 9, pp. 1244–1257, Jul. 2013.

[134] M. Blatzer, M. Schrettl, B. Sarg, H. H. Lindner, K. Pfaller, and H. Haas, “SidL, an Aspergillus fumigatus Transacetylase Involved in Biosynthesis of the Siderophores Ferricrocin and Hydroxyferricrocin,” *Appl. Environ. Microbiol.*, vol. 77, no. 14, pp. 4959–4966, May 2011.

[135] G. Winkelmann, “Ecology of siderophores with special reference to the fungi,” *BioMetals*, vol. 20, no. 3–4, pp. 379–392, Jun. 2007.

[136] C. C. Philpott, S. Leidgens, and A. G. Frey, “Metabolic remodeling in iron-deficient fungi,” *Biochim. Biophys. Acta BBA - Mol. Cell Res.*, vol. 1823, no. 9, pp. 1509–1520, Sep. 2012.

[137] T. Vorapreeda, C. Thammarongtham, S. Cheevadhanarak, and K. Laoteng, “Alternative routes of acetyl-CoA synthesis identified by comparative genomic analysis: involvement in the lipid production of oleaginous yeast and fungi,” *Microbiology*, vol. 158, no. 1, pp. 217–228, Oct. 2011.

[138] N. Morin, J. Cescut, A. Beopoulos, G. Lelandais, V. Le Berre, J.-L. Uribelarrea, C. Molina-Jouve, and J.-M. Nicaud, “Transcriptomic Analyses during the Transition from Biomass Production to Lipid Accumulation in the Oleaginous Yeast Yarrowia lipolytica,” *PLoS ONE*, vol. 6, no. 11, p. e27966, Nov. 2011.

[139] J. A. K. W. Kiel, M. Veenhuis, and I. J. van der Klei, “PEX Genes in Fungal Genomes: Common, Rare or Redundant,” *Traffic*, vol. 7, no. 10, pp. 1291–1303, Oct. 2006.

[140] L. Pieuchot and G. Jedd, “Peroxisome Assembly and Functional Diversity in Eukaryotic Microorganisms,” *Annu. Rev. Microbiol.*, vol. 66, no. 1, pp. 237–263, Oct. 2012.

[141] D. Managadze, C. Würtz, S. Wiese, H. E. Meyer, G. Niehaus, R. Erdmann, B. Warscheid, and H. Rottensteiner, “A proteomic approach towards the identification of the matrix protein content of the two types of microbodies in Neurospora crassa,” *PROTEOMICS*, vol. 10, no. 18, pp. 3222–3234, Sep. 2010.

[142] T. Ohdate and Y. Inoue, “Involvement of glutathione peroxidase 1 in growth and peroxisome formation in Saccharomyces cerevisiae in oleic acid medium,” *Biochim. Biophys. Acta BBA - Mol. Cell Biol. Lipids*, vol. 1821, no. 9, pp. 1295–1305, Sep. 2012.

[143] J. A. Heyman, E. Monosov, and S. Subramani, “Role of the PAS1 gene of Pichia pastoris in peroxisome biogenesis.,” *J. Cell Biol.*, vol. 127, no. 5, pp. 1259–1273, Dec. 1994.

[144] H. R. Waterham and J. M. Cregg, “Peroxisome biogenesis,” *BioEssays*, vol. 19, no. 1, pp. 57–66, Jan. 1997.

[145] G. M. Cooper, *The Cell: A Molecular Approach*, 2nd ed. Sunderland (MA): Sinauer Associates, 2000.

[146] T. Gabaldon, “Peroxisome diversity and evolution,” *Philos. Trans. R. Soc. B Biol. Sci.*, vol. 365, no. 1541, pp. 765–773, Feb. 2010.

[147] M. Schmoll, C. Tian, J. Sun, D. Tisch, and N. L. Glass, “Unravelling the molecular basis for light modulated cellulase gene expression - the role of photoreceptors in Neurospora crassa,” *BMC Genomics*, vol. 13, no. 1, p. 127, 2012.

[148] J. C. Dunlap and J. J. Loros, “How fungi keep time: circadian system in Neurospora and other fungi,” *Curr. Opin. Microbiol.*, vol. 9, no. 6, pp. 579–587, Dec. 2006.

[149] K. Tamura, D. Peterson, N. Peterson, G. Stecher, M. Nei, and S. Kumar, “MEGA5: molecular evolutionary genetics analysis using maximum likelihood, evolutionary distance, and maximum parsimony methods,” *Mol. Biol. Evol.*, vol. 28, no. 10, pp. 2731–2739, Oct. 2011.

[150] N. Saitou and M. Nei, “The neighbor-joining method: a new method for reconstructing phylogenetic trees,” *Mol. Biol. Evol.*, vol. 4, no. 4, pp. 406–425, Jul. 1987.

[151] E. Zuckerkandl and L. Pauling, “Evolutionary divergence and convergence in proteins,” in *Evolving Genes and Proteins*, V. Bryson and H. Vogel, Eds. New York: Academic Press, 1965, pp. 97–166.

[152] C. L. Schoch, G.-H. Sung, F. Lopez-Giraldez, J. P. Townsend, J. Miadlikowska, V. Hofstetter, B. Robbertse, P. B. Matheny, F. Kauff, Z. Wang, C. Gueidan, R. M. Andrie, K. Trippe, L. M. Ciufetti, A. Wynns, E. Fraker, B. P. Hodkinson, G. Bonito, J. Z. Groenewald, M. Arzanlou, G. Sybren de Hoog, P. W. Crous, D. Hewitt, D. H. Pfister, K. Peterson, M. Gryzenhout, M. J. Wingfield, A. Aptroot, S.-O. Suh, M. Blackwell, D. M. Hillis, G. W. Griffith, L. A. Castlebury, A. Y. Rossman, H. T. Lumbsch, R. Lucking, B. Budel, A. Rauhut, P. Diederich, D. Ertz, D. M. Geiser, K. Hosaka, P. Inderbitzin, J. Kohlmeyer, B. Volkmann-Kohlmeyer, L. Mostert, K. O’Donnell, H. Sipman, J. D. Rogers, R. A. Shoemaker, J. Sugiyama, R. C. Summerbell, W. Untereiner, P. R. Johnston, S. Stenroos, A. Zuccaro, P. S. Dyer, P. D. Crittenden, M. S. Cole, K. Hansen, J. M. Trappe, R. Yahr, F. Lutzoni, and J. W. Spatafora, “The Ascomycota Tree of Life: A Phylum-wide Phylogeny Clarifies the Origin and

Evolution of Fundamental Reproductive and Ecological Traits," *Syst. Biol.*, vol. 58, no. 2, pp. 224–239, Jun. 2009.

[153] R. H. Davis, *Neurospora: contributions of a model organism*. New York: Oxford University Press, 2000.

[154] Westergaard, M and H.K. Mitchell, "A synthetic medium favoring sexual reporduction," *Am J Bot*, vol. 34, pp. 573–577, 1947.

[155] Y. Ninomiya, K. Suzuki, C. Ishii, and H. Inoue, "Highly efficient gene replacements in Neurospora strains deficient for nonhomologous end-joining," *Proc. Natl. Acad. Sci.*, vol. 101, no. 33, pp. 12248–12253, Aug. 2004.

[156] H. Vogel, "A convenient growth medium for Neurospora (medium N).," *Microb. Genet. Bull.*, vol. 13, pp. 42–43, 1956.

[157] S. Honda and E. U. Selker, "Tools for Fungal Proteomics: Multifunctional Neurospora Vectors for Gene Replacement, Protein Expression and Protein Purification," *Genetics*, vol. 182, no. 1, pp. 11–23, Jan. 2009.

[158] K. M. Smith, P. A. Phatale, C. M. Sullivan, K. R. Pomraning, and M. Freitag, "Heterochromatin is required for normal distribution of Neurospora crassa CenH3," *Mol. Cell. Biol.*, vol. 31, no. 12, pp. 2528–2542, Jun. 2011.

[159] H. V. Colot, "A high-throughput gene knockout procedure for Neurospora reveals functions for multiple transcription factors," *Proc. Natl. Acad. Sci.*, vol. 103, no. 27, pp. 10352–10357, Jul. 2006.

[160] J., Fritsch, Edward F Sambrook, T., Sambrook-Fritsch-Maniatis, Maniatis, and Cold Spring Harbor Laboratory, *Molecular cloning: a laboratory manual; [prepared for use in the CSH courses on the molecular cloning of eukaryotic genes] 1 1*. Plainview, NY: Cold Spring Harbor Laboratory Press, 1989.

[161] H. Towbin, T. Staehelin, and J. Gordon, "Electrophoretic transfer of proteins from polyacrylamide gels to nitrocellulose sheets: procedure and some applications," *Proc. Natl. Acad. Sci. U. S. A.*, vol. 76, no. 9, pp. 4350–4354, Sep. 1979.

[162] H. Tamaru, X. Zhang, D. McMillen, P. B. Singh, J. Nakayama, S. I. Grewal, C. D. Allis, X. Cheng, and E. U. Selker, "Trimethylated lysine 9 of histone H3 is a mark for DNA methylation in Neurospora crassa," *Nat. Genet.*, vol. 34, no. 1, pp. 75–79, May 2003.

[163] K. R. Pomraning, K. M. Smith, and M. Freitag, "Genome-wide high throughput analysis of DNA methylation in eukaryotes," *Methods San Diego Calif*, vol. 47, no. 3, pp. 142–150, Mar. 2009.

[164] Y. Zhang, T. Liu, C. A. Meyer, J. Eeckhoute, D. S. Johnson, B. E. Bernstein, C. Nusbaum, R. M. Myers, M. Brown, W. Li, and X. S. Liu, "Model-based analysis of ChIP-Seq (MACS)," *Genome Biol.*, vol. 9, no. 9, p. R137, 2008.

[165] Q. Li, J. B. Brown, H. Huang, and P. J. Bickel, "Measuring reproducibility of high-throughput experiments," *Ann. Appl. Stat.*, vol. 5, no. 3, pp. 1752–1779, Sep. 2011.

[166] A. Ruepp, A. Zollner, D. Maier, K. Albermann, J. Hani, M. Mokrejs, I. Tetko, U. Güldener, G. Mannhaupt, M. Münsterkötter, and H. W. Mewes, "The FunCat, a functional annotation scheme for systematic classification of proteins from whole genomes," *Nucleic Acids Res.*, vol. 32, no. 18, pp. 5539–5545, 2004.

[167] M. E. Smoot, K. Ono, J. Ruscheinski, P.-L. Wang, and T. Ideker, "Cytoscape 2.8: new features for data integration and network visualization," *Bioinforma. Oxf. Engl.*, vol. 27, no. 3, pp. 431–432, Feb. 2011.

[168] D. Merico, R. Isserlin, O. Stueker, A. Emili, and G. D. Bader, "Enrichment map: a network-based method for gene-set enrichment visualization and interpretation," *PloS One*, vol. 5, no. 11, p. e13984, 2010.

[169] V. Sokolovsky, R. Kaldenhoff, M. Ricci, and V. E. A. Russo, "Fast and reliable mini-prep RNA extraction from Neurospora crassa," *Fungal Genet. Newsl.*, vol. 37, 1990.

[170] C. Trapnell, B. A. Williams, G. Pertea, A. Mortazavi, G. Kwan, M. J. van Baren, S. L. Salzberg, B. J. Wold, and L. Pachter, "Transcript assembly and quantification by RNA-Seq reveals unannotated transcripts and isoform switching during cell differentiation," *Nat. Biotechnol.*, vol. 28, no. 5, pp. 511–515, May 2010.

[171] Raivo Kolde, *pheatmap: Pretty Heatmaps*. 2013.

[172] A. Maddi, A. Dettman, C. Fu, S. Seiler, and S. J. Free, "WSC-1 and HAM-7 Are MAK-1 MAP Kinase Pathway Sensors Required for Cell Wall Integrity and Hyphal Fusion in Neurospora crassa," *PLoS ONE*, vol. 7, no. 8, p. e42374, Aug. 2012.

[173] F. Sievers, A. Wilm, D. Dineen, T. J. Gibson, K. Karplus, W. Li, R. Lopez, H. McWilliam, M. Remmert, J. Söding, J. D. Thompson, and D. G. Higgins, "Fast, scalable generation of high-quality protein multiple sequence alignments using Clustal Omega," *Mol. Syst. Biol.*, vol. 7, Oct. 2011.

[174] T. Pan and J. E. Coleman, "GAL4 transcription factor is not a 'zinc finger' but forms a Zn(II)2Cys6 binuclear cluster," *Proc. Natl. Acad. Sci. U. S. A.*, vol. 87, no. 6, pp. 2077–2081, Mar. 1990.

[175] P. Schjerling and S. Holmberg, "Comparative amino acid sequence analysis of the C6 zinc cluster family of transcriptional regulators," *Nucleic Acids Res.*, vol. 24, no. 23, pp. 4599–4607, Dec. 1996.

[176] J. M. Carlson, A. Chakravarty, C. E. DeZiel, and R. H. Gross, “SCOPE: a web server for practical de novo motif discovery,” *Nucleic Acids Res.*, vol. 35, no. Web Server, pp. W259–W264, May 2007.

[177] G. Pavesi, P. Mereghetti, G. Mauri, and G. Pesole, “Weeder Web: discovery of transcription factor binding sites in a set of sequences from co-regulated genes,” *Nucleic Acids Res.*, vol. 32, no. Web Server, pp. W199–W203, Jul. 2004.

[178] X. Liu, D. L. Brutlag, and J. S. Liu, “BioProspector: discovering conserved DNA motifs in upstream regulatory regions of co-expressed genes,” *Pac. Symp. Biocomput. Pac. Symp. Biocomput.*, pp. 127–138, 2001.

[179] G. E. Crooks, “WebLogo: A Sequence Logo Generator,” *Genome Res.*, vol. 14, no. 6, pp. 1188–1190, May 2004.

[180] N. H. Giles, M. E. Case, J. Baum, R. Geever, L. Huiet, V. Patel, and B. Tyler, “Gene organization and regulation in the qa (quinic acid) gene cluster of Neurospora crassa,” *Microbiol. Rev.*, vol. 49, no. 3, pp. 338–358, Sep. 1985.

[181] D. W. Huang, B. T. Sherman, and R. A. Lempicki, “Systematic and integrative analysis of large gene lists using DAVID bioinformatics resources,” *Nat. Protoc.*, vol. 4, no. 1, pp. 44–57, 2009.

[182] Q. Xiang and N. L. Glass, “Identification of vib-1, a locus involved in vegetative incompatibility mediated by het-c in Neurospora crassa,” *Genetics*, vol. 162, no. 1, pp. 89–101, Sep. 2002.

[183] F. Liu, Y. Lu, L. Pieuchot, T. Dhavale, and G. Jedd, “Import Oligomers Induce Positive Feedback to Promote Peroxisome Differentiation and Control Organelle Abundance,” *Dev. Cell*, vol. 21, no. 3, pp. 457–468, Sep. 2011.

[184] W. Schliebs, C. Würtz, W.-H. Kunau, M. Veenhuis, and H. Rottensteiner, “A eukaryote without catalase-containing microbodies: Neurospora crassa exhibits a unique cellular distribution of its four catalases,” *Eukaryot. Cell*, vol. 5, no. 9, pp. 1490–1502, Sep. 2006.

[185] M. Sichting, A. Schell-Steven, H. Prokisch, R. Erdmann, and H. Rottensteiner, “Pex7p and Pex20p of Neurospora crassa function together in PTS2-dependent protein import into peroxisomes,” *Mol. Biol. Cell*, vol. 14, no. 2, pp. 810–821, Feb. 2003.

[186] I. F. Connerton, W. McCullough, and J. R. Fincham, “An acetate-sensitive mutant of Neurospora crassa deficient in acetyl-CoA hydrolase,” *J. Gen. Microbiol.*, vol. 138, no. 9, pp. 1797–1800, Sep. 1992.

[187] A. Keeping, D. Deabreu, M. Dibernardo, and R. A. Collins, “Gel-based mass spectrometric and computational approaches to the mitochondrial proteome of Neurospora,” *Fungal Genet. Biol. FG B*, vol. 48, no. 5, pp. 526–536, May 2011.

[188] K. Francis, S. F. Nishino, J. C. Spain, and G. Gadda, “A novel activity for fungal nitronate monooxygenase: detoxification of the metabolic inhibitor propionate-3-nitronate,” *Arch. Biochem. Biophys.*, vol. 521, no. 1–2, pp. 84–89, May 2012.

[189] Babu, Madan M., “An Introduction fo Microarray Data Analysis,” in *Computational genomics: theory and application*, R. P. Grant, Ed. Wymondham: Horizon Bioscience, 2004.

[190] C. Tian, T. Kasuga, M. S. Sachs, and N. L. Glass, “Transcriptional Profiling of Cross Pathway Control in Neurospora crassa and Comparative Analysis of the Gcn4 and CPC1 Regulons,” *Eukaryot. Cell*, vol. 6, no. 6, pp. 1018–1029, Apr. 2007.

[191] G. Abate, E. Bastonini, K. A. Braun, L. Verdone, E. T. Young, and M. Caserta, “Snf1/AMPK regulates Gcn5 occupancy, H3 acetylation and chromatin remodelling at S. cerevisiae ADY2 promoter,” *Biochim. Biophys. Acta*, vol. 1819, no. 5, pp. 419–427, May 2012.

[192] M. L. Springer, “Tergitol-induced colonial growth without inhibition of conidiation,” *Fungal Genet. Newsl.*, no. 38, p. 92, 1991.

[193] M. S. Aldabbous, M. G. Roca, A. Stout, I.-C. Huang, N. D. Read, and S. J. Free, “The ham-5, rcm-1 and rco-1 genes regulate hyphal fusion in Neurospora crassa,” *Microbiology*, vol. 156, no. 9, pp. 2621–2629, Jun. 2010.

[194] B. Matzanke, E. Bill, A. Trautwein, and G. Winkelmann, “Ferricrocin functions as the main intracellular iron-storage compound in mycelia ofNeurospora crassa,” *Biol. Met.*, vol. 1, no. 1, pp. 18–25, Mar. 1988.

[195] A. Machuca and A. M. F. Milagres, “Use of CAS-agar plate modified to study the effect of different variables on the siderophore production by Aspergillus,” *Lett. Appl. Microbiol.*, vol. 36, no. 3, pp. 177–181, 2003.

[196] H. Thorvaldsdottir, J. T. Robinson, and J. P. Mesirov, “Integrative Genomics Viewer (IGV): high-performance genomics data visualization and exploration,” *Brief. Bioinform.*, vol. 14, no. 2, pp. 178–192, Apr. 2012.

[197] D. Managadze, C. Würtz, S. Wiese, M. Schneider, W. Girzalsky, H. E. Meyer, R. Erdmann, B. Warscheid, and H. Rottensteiner, “Identification of PEX33, a novel component of the peroxisomal docking complex in the filamentous fungus Neurospora crassa,” *Eur. J. Cell Biol.*, vol. 89, no. 12, pp. 955–964, Dec. 2010.

[198] H. W. Platta, S. Hagen, and R. Erdmann, “The exportomer: the peroxisomal receptor export machinery,” *Cell. Mol. Life Sci.*, vol. 70, no. 8, pp. 1393–1411, Sep. 2012.

[199] S. M. Garrido, N. Kitamoto, A. Watanabe, T. Shintani, and K. Gomi, “Functional analysis of FarA transcription factor in the regulation of the genes encoding lipolytic enzymes and hydrophobic surface binding protein for the degradation of biodegradable plastics in Aspergillus oryzae,” *J. Biosci. Bioeng.*, vol. 113, no. 5, pp. 549–555, May 2012.

[200] K. Piekarska, G. Hardy, E. Mol, J. van den Burg, K. Strijbis, C. van Roermund, M. van den Berg, and B. Distel, “The activity of the glyoxylate cycle in peroxisomes of Candida albicans depends on a functional -oxidation pathway: evidence for reduced metabolite transport across the peroxisomal membrane,” *Microbiology*, vol. 154, no. 10, pp. 3061–3072, Oct. 2008.

[201] G. Jedd and N. H. Chua, “A new self-assembled peroxisomal vesicle required for efficient resealing of the plasma membrane,” *Nat. Cell Biol.*, vol. 2, no. 4, pp. 226–231, Apr. 2000.

[202] R. Caspi, T. Altman, K. Dreher, C. A. Fulcher, P. Subhraveti, I. M. Keseler, A. Kothari, M. Krummenacker, M. Latendresse, L. A. Mueller, Q. Ong, S. Paley, A. Pujar, A. G. Shearer, M. Travers, D. Weerasinghe, P. Zhang, and P. D. Karp, “The MetaCyc database of metabolic pathways and enzymes and the BioCyc collection of pathway/genome databases,” *Nucleic Acids Res.*, vol. 40, no. D1, pp. D742–D753, Nov. 2011.

[203] T. Nakagawa, “Peroxisomal Membrane Protein Pmp47 Is Essential in the Metabolism of Middle-chain Fatty Acid in Yeast Peroxisomes and Is Associated with Peroxisome Proliferation,” *J. Biol. Chem.*, vol. 275, no. 5, pp. 3455–3461, Feb. 2000.

[204] E. H. Hettema, C. W. van Roermund, B. Distel, M. van den Berg, C. Vilela, C. Rodrigues-Pousada, R. J. Wanders, and H. F. Tabak, “The ABC transporter proteins Pat1 and Pat2 are required for import of long-chain fatty acids into peroxisomes of Saccharomyces cerevisiae,” *EMBO J.*, vol. 15, no. 15, pp. 3813–3822, Aug. 1996.

[205] A. Méndez-Vilas, *Science against microbial pathogens: communicating current research and technological advances*. Badajoz: Formatex Research Center, 2011.

[206] C. H. Pohl, J. L. Kock, and V. S. Thibane, “Antifungal free fatty acids: a review.”

[207] F. Abe and T. Hiraki, “Mechanistic role of ergosterol in membrane rigidity and cycloheximide resistance in Saccharomyces cerevisiae,” *Biochim. Biophys. Acta BBA - Biomembr.*, vol. 1788, no. 3, pp. 743–752, Mar. 2009.

[208] L. W. Parks and W. M. Casey, “Physiological Implications of Sterol Biosynthesis in Yeast,” *Annu. Rev. Microbiol.*, vol. 49, no. 1, pp. 95–116, Oct. 1995.

[209] C. Kionka and W. H. Kunau, “Inducible beta-oxidation pathway in Neurospora crassa,” *J. Bacteriol.*, vol. 161, no. 1, pp. 153–157, Jan. 1985.

[210] J. Freitag, J. Ast, and M. Bölker, “Cryptic peroxisomal targeting via alternative splicing and stop codon read-through in fungi,” *Nature*, vol. 485, no. 7399, pp. 522–525, May 2012.

[211] C. C. C. R. de Carvalho, M. P. C. Marques, and P. Fernandes, “Recent achievements on siderophore production and application,” *Recent Pat. Biotechnol.*, vol. 5, no. 3, pp. 183–198, Dec. 2011.

[212] B. F. Matzanke, E. Bill, A. X. Trautwein, and G. Winkelmann, “Role of siderophores in iron storage in spores of Neurospora crassa and Aspergillus ochraceus,” *J. Bacteriol.*, vol. 169, no. 12, pp. 5873–5876, Dec. 1987.

[213] M. Gründlinger, S. Yasmin, B. E. Lechner, S. Geley, M. Schrettl, M. Hynes, and H. Haas, “Fungal siderophore biosynthesis is partially localized in peroxisomes,” *Mol. Microbiol.*, vol. 88, no. 5, pp. 862–875, Jun. 2013.

[214] M. Eisendle, H. Oberegger, R. Buttinger, P. Illmer, and H. Haas, “Biosynthesis and Uptake of Siderophores Is Controlled by the PacC-Mediated Ambient-pH Regulatory System in Aspergillus nidulans,” *Eukaryot. Cell*, vol. 3, no. 2, pp. 561–563, Apr. 2004.

[215] L. Peraza-Reyes and V. Berteaux-Lecellier, “Peroxisomes and sexual development in fungi,” *Front. Physiol.*, vol. 4, 2013.

[216] V. Berteaux-Lecellier, M. Picard, C. Thompson-Coffe, D. Zickler, A. Panvier-Adoutte, and J.-M. Simonet, “A nonmammalian homolog of the PAF7 gene(Zellweger syndrome) discovered as a gene involved in caryogamy in the fungus Podospora anserina,” *Cell*, vol. 81, no. 7, pp. 1043–1051, Jun. 1995.

[217] T. Umemoto and Y. Fujiki, “Ligand-dependent nucleo-cytoplasmic shuttling of peroxisome proliferator-activated receptors, PPARα and PPARγ,” *Genes Cells Devoted Mol. Cell. Mech.*, vol. 17, no. 7, pp. 576–596, Jul. 2012.

[218] T. Schafmeier, A. Diernfellner, A. Schäfer, O. Dintsis, A. Neiss, and M. Brunner, “Circadian activity and abundance rhythms of the Neurospora clock transcription factor WCC associated with rapid nucleo-cytoplasmic shuttling,” *Genes Dev.*, vol. 22, no. 24, pp. 3397–3402, Dec. 2008.

Appendix

1. Publications

Meritxell Riquelme, **Erin L. Bredeweg**, Olga Callejas-Negrete, Robert W. Roberson, Sarah Ludwig, Alejandro Beltrán-Aguilar, Stephan Seiler, and Michael Freitag. "The *Neurospora crassa* exocyst complex tethers Spitzenkörper macrovesicles to the apical plasma membrane. Published online before print, doi: 10.1091/mbc.E13-06-0299, 2014.

Kristina M. Smith, Pallavi A. Phatale, **Erin L. Bredeweg**, Lanelle R. Connolly, Kyle R. Pomraning, Michael Freitag. Epigeneticsof filamentous fungi in Epigenetic Regulation and Epigenomics. Encyclopedia of Molecular Biology and Molecular Medicine, Wiley-Blackwell. 2012.

Kyle R. Pomraning, Kristina M. Smith, **Erin L. Bredeweg,** Lanelle R. Connolly, Pallavi A. Phatale, Michael Freitag. "Library Preparation and Data Analysis Packages for Rapid Genome Sequencing." In: Nancy P. Keller and Geoffrey Turner (eds.), Fungal Secondary Metabolism: Methods and Protocols, Methods in Molecular Biology, vol. 944, Springer Science and Business Media, LLC. 2012. p. 1-22.

Kristina M. Smith, Gencer Sancar, Rigzin Dekhang, Christopher M. Sullivan, Shaojie Li, Andrew G. Tag, Cigdem Sancar, **Erin L. Bredeweg**, Henry D. Priest, Ryan F. McCormick, Terry L. Thomas, James C. Carrington, Jason E. Stajich, Deborah Bell-Pedersen, Michael Brunner, and Michael Freitag. Transcription Factors in Light and Circadian Clock Signaling Networks Revealed by Genomewide Mapping of Direct Targets for Neurospora White Collar Complex. Eukaryotic Cell, 2010. 9(10): p. 1549-56.

Patrick E. Chappell, Cheri P. Goodall, Karen J. Tonsfeldt, Rachel S. White, **Erin Bredeweg,** and Kristin L. Latham. Modulation of Gonadotrophin-Releasing Hormone Secretion by an Endogenous Circadian Clock. Journal of Neuroendocrinology, 2009. 21(4): p. 339-345.

2. Projects with publications in preparation

1. **Erin L. Bredeweg**, Kristina M. Smith, Rigzin Dekhang, Fei Yang, Jillian M. Emerson, Jay C. Dunlap, Deborah Bell-Pedersen, Matthew S. Sachs and Michael Freitag. "Two Fatty Acid Regulators in *Neurospora crassa*."
   (This work, in preparation for submission to "G3")
   Samples collected in recent months await analysis by mass spectrometry. A manuscript is in preparation for work on FAR-1 and FAR-2.

2. Zhigang Qi, **Erin L. Bredeweg**, Kristina Smith, Michael Freitag, and Frank E. Nargang. "Function of the AOD2 and AOD5 transcription factors in the expression of AOX and gluconeogenesis genes in *Neurospora crassa*"
   (in preparation for submission to "Eukaryotic Cell")
   I have done mapping, ChIP peak analysis and extensive annotation using self-authored programs for this project.

3. Rigzin Dekhang, **Erin L. Bredeweg**, Jillian M. Emerson, Jay C. Dunlap, Matthew S. Sachs,' Michael Freitag, Deborah Bell-Pedersen. "Characterization of circadian output pathways mediated by transcription factor ADV-1 in *N. crassa.*"
   (in prepraration)
   I performed ChIP-library preparation, read mapping, and peak analysis and annotation for this project.

4. Cheng Wu, Matthew Peterson, Fei Yang, Rigzin Dekhang, Ying Zhang, **Erin L. Bredeweg**, Kristina M. Smith, Chandrashekara Mallappa, Jeremy Zucker, Jay C. Dunlap, Michael Freitag, Deborah Bell-Pedersen, James Galagan, Matthew S, Sachs. "Genome-wide characterization of light-regulated genes in *Neurospora crassa*"
   (in preparation for submission to "G3")
   I performed ChIP-library preparation, read mapping, and peak analysis and annotation for this project.

5. Chandrashekara Mallappa, Nicole Kent, Jillian M. Emerson, **Erin L. Bredeweg**, Matt Sachs, Michael Freiag, Jay C. Dunlap. CSP-1 binding in *Neurospora crassa*.
   I have done ChIP-library preparation for this project.

6. Rodrigo Gonçalves, **Erin L. Bredeweg**, Michael Freitag and Maria-Celia Bertolini. "Characterization of genomic targets for the *Neurospora crassa* hypothetical transcription factor NCU04390 by ChIP-sequencing."
   (in preparation)
   I performed and taught ChIP-sequencing peak analysis for this project to a visiting graduate student.

7. John B. Hays, Kyle R. Pomraning, Buck W. Wilcox, **Erin L. Bredeweg**, Shannon Dealy and Michael Freitag. "Mutation accumulation in *msh2* and wildtype *Arabidopsis thaliana*."
   (in preparation)
   I have done genomic DNA library preparation for this project.